3834

NATIONAL LIBRARY

OTTAWA

CANADA

BIBLIOTHÈQUE NATIONALE

OTTAWA

NAME OF AUTHOR....Miksa...de...Sorgo........

TITLE OF THESIS....THE...Flash...Photolysis...of..
....Sulfur...Systems..............

....

UNIVERSITY.........U.of.A.................

DEGREE....Ph.D...........YEAR GRANTED......1969....

Permission is hereby granted to THE NATIONAL

LIBRARY OF CANADA to microfilm this thesis and to

lend or sell copies of the film.

The author reserves other publication rights,

and neither the thesis nor extensive extracts from

it may be printed or otherwise reproduced without

the author's written permission.

(Signed)...............

PERMANENT ADDRESS:

....11527-72 AVE

....Edmonton

....

DATED.Dec...17......1968

NL-91

THE UNIVERSITY OF ALBERTA

THE FLASH PHOTOLYSIS OF SULFUR SYSTEMS

by

(C) MIKSA de SORGO

A THESIS

SUBMITTED TO THE FACULTY OF GRADUATE STUDIES

IN PARTIAL FULFILMENT OF THE REQUIREMENTS

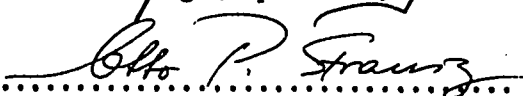FOR THE DEGREE OF DOCTOR OF PHILOSOPHY

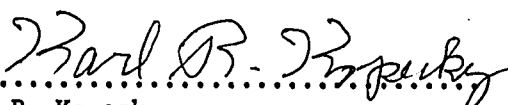DEPARTMENT OF CHEMISTRY

EDMONTON, ALBERTA

December, 1968

UNIVERSITY OF ALBERTA

FACULTY OF GRADUATE STUDIES

The undersigned certify that they have read, and recommend to the Faculty of Graduate Studies for acceptance, a thesis entitled THE FLASH PHOTOLYSIS OF SULFUR SYSTEMS submitted by Miksa de Sorgo in partial fulfilment of the requirements for the degree of Doctor of Philosophy.

....
H. E. Gunning (Supervisor)

....
O. P. Strausz

....
K. R. Kopecky

....
P. Kebarle

....
H. R. Krouse (Physics)

....
P. A. Leermakers (Wesleyan University)

December 13, 1968

ABSTRACT

The reactions of S (^3P) and S (^1D) atoms as well as the reactions of the sulfur radicals S_2, S_3, HS, and HS_2 have been investigated with the technique of flash photolysis kinetic spectroscopy.

S (^3P) atoms were formed in the short wavelength photolysis of CS_2, in the relaxation of S (^1D) by CO_2, and in the disproportionation of HS radicals. S (^3P) atoms were shown to combine to form S_2 in all three low lying electronic states.

S (^1D) atoms, formed in the photolysis of COS, abstracted a sulfur atom from COS. The abstraction reaction most likely proceeds through the intermediate COS_2. S (^1D) atoms were found to insert into H_2 and CH_4 forming hot products which underwent considerable secondary cracking reactions.

S_2 $(^1\Delta_g)$ was formed in the abstraction from COS by S (^1D), in the combination of S (^3P) atoms, the cross disproportionation of HS and HS_2, and in the disproportionation of HS_2. S_2 $(^1\Delta_g)$ suffered collisional relaxation to the ground state and in the presence of H_2, the process is very rapid due to the near resonance condition between the donor and acceptor.

S_2 $(^3\Sigma_g^-)$ was formed in the combination of S (^3P) atoms and in the disproportionation of HS and HS_2 radicals. Ground state S_2 is

also formed in the reactions:

$$CS_2^* \; + \; CS_2 \qquad\qquad 2\;CS \; + \; S_2$$

$$C_2H_4S^* \; + \; C_2H_4S \qquad\qquad 2\;C_2H_4 \; + \; S_2$$

S_2 ($^3\Sigma_g^-$) decays by third body combination forming S_4 and ultimately polymeric sulfur. Rate constants for the combination have been calculated with several third bodies. The efficiency of the third body increases as its complexity increases. Ethylene episulfide is about 50 times as efficient as H_2.

HS was formed in the photolysis of H_2S and H_2S_2 as well as in the reaction of S (^1D) atoms with H_2 and CH_4. HS was found to undergo disproportionation with itself and with HS_2 as well as combination reactions. The disproportionation into H_2 + S_2 was shown to be unimportant. The extinction coefficient of the 3060 Å line was determined and absolute rate constants for HS decay were obtained.

HS_2 was formed in the photolysis of H_2S_2 and also in the recation between HS and S (^3P). HS_2 was found to undergo disproportionation with itself and HS and combination with itself and with HS.

The triplet excited state of CS_2 formed in the long wavelength photolysis of carbon disulfide underwent luminescence as well as chemical reaction with another CS_2 and with O_2.

Rate constants of several radical reactions are listed.
Spectra of the intermediate radicals are shown in the Plates.

ACKNOWLEDGEMENTS

TABLE OF CONTENTS

LIST OF TABLES

LIST OF PLATES

LIST OF ILLUSTRATIONS

CHAPTER I

INTRODUCTION

The subject of photochemistry is concerned with the
processes resulting from the interaction of radiation with matter[1,2].
The radiation of photochemical importance almost exclusively lie
in the visible, ultra violet and the vacuum ultra violet regions
of the spectrum. The photon, once absorbed by the molecule, causes
a change in the electronic configuration in the molecule with the
result that the new molecule is higher in energy and has different
reactivity and characteristics. In general there are more than one
energy levels and corresponding excited states and a molecule may
absorb in different regions of the spectrum giving rise to different
modes of reaction subsequent to photoexcitation.

A photochemical reaction can be separated into three
stages:

a) light absorption. According to the Einstein Law
of Chemical Equivalence, in the primary process each molecule is
activated by the absorption of one photon.

b) the primary reaction - the immediate chemical
change that occurs in the excited molecule. Some of these are:

1, Unimolecular reaction, dissociation or
isomerization of the excited molecule.

2, Bimolecular reaction, reaction involving a second molecule.

3, Luminescence, light emission with simultaneous transition to a lower state of the same or different multiplicity.

4, Internal conversion, nonradiative transition to a lower state of the same multiplicity.

5, Intersystem crossing, nonradiative conversion to a state of different multiplicity.

c) secondary reactions – the reactions of the product of the primary reaction.

Sometimes, instead of reacting or losing its energy, an excited molecule may collide with another molecule and transfer its energy causing the other molecule to be excited. This process is called photosensitization. Mercury photosensitization is a common example of such an energy transfer[3].

Except in a few simple cases, the course of a photochemical reaction between the initial excitation and the formation of the stable products is quite complex and often involves the participation of atoms, radicals, excited states and even ions. The short lifetimes and the low steady state concentrations of these reactive intermediates prevented their detection by physical methods. Therefore, the postulated mechanisms were derived from circumstantial evidence provided by spectroscopic observations and quantitative measurements of the end products. In most cases the proposed

mechanisms were satisfactory but the lack of physical evidence for the proposed intermediates often led to undue criticism.

It was for this reason that Norrish and Porter in 1946 tried to obtain spectroscopic evidence of the presence of these short lived intermediates in a photochemical reaction. They found that very large measures of photolysis could easily be achieved by applying a very intense light flash to suitable reactants[4]. These early flashes were produced by discharging a bank of condensers through argon and were of 1 - 2 msec duration and dissipated up to 10,000 joules energy. It seemed obvious that if free radicals were produced, they would be of such high concentration that they could be detected through their absorption spectra. This was first achieved by Porter[5] by using a second flash as a photographic source triggered mechanically at short intervals after the first flash. He was able to demonstrate the decomposition of chlorine and to obtain the absorption spectrum of CS from the photodecomposition of carbon disulfide.

This early success was followed by the development of the technique. Shorter flash durations were achieved by the use of improved very low inductance capacitors. Short, very precise delays were achieved by using electronic delay devices which were capable of timing to within a microsecond. The basic device[6] still in use today, though much more refined, was developed in 1953 and is described in Chapter 2 of this thesis.

It became apparent that many of the early results were invalidated by the great rise in temperature which resulted in thermal as well as photochemical dissociation. This temperature rise comes from the fact that when the intense flash is applied, the light energy absorbed is rapidly degraded to heat and when only a few torr of reactant are present, this temperature rise may exceed a thousand degrees. If a large excess of inert gas, e.g., 500 torr nitrogen, is present, the temperature rise can be limited to a few degrees. Thus under adiabatic conditions resulting from lack of temperature control, thermal cracking as well as explosive reactions may be initiated.

Carbon Disulfide

Porter[5] first demonstrated the great significance of the technique of flash photolysis-kinetic spectroscopy in ellucidating the mechanism of the photodecomposition of carbon disulfide. Since the final products are sulfur and a polymer, little was known about the photochemistry of this compound. Porter detected the transients CS and S_2 ($^3\Sigma_g^-$) when he flashed carbon disulfide in a quartz vessel and proposed the mechanism:

$$CS_2 + h\nu \rightarrow CS + S \tag{1}$$

$$S + CS_2 \rightarrow CS + S_2 \, (^3\Sigma_g^-) \tag{2}$$

$$n \, S_2 \rightarrow S_{2n} \tag{3}$$

$$n \ CS \quad \rightarrow \quad (CS)_n \qquad \{4\}$$
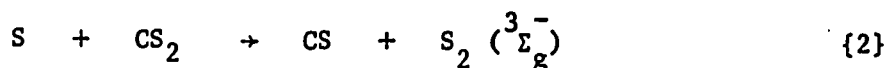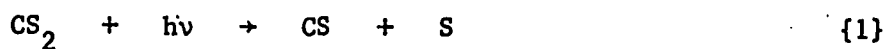
Arguing on the grounds of spin conservation, he stated that the S atom formed in {1} must be in the singlet state.

If a singlet sulfur atom is produced in {1}, then from the same rules the S_2 produced in {2} should also be in a singlet state. This singlet state was not observed.

Wright[7] repeated Porter's experiments and obtained similar results. He concluded that CS decay was a heterogeneous process and that no condensation or reaction with sulfur occurred in the gas phase.

Owing to limitations of his apparatus, he was unable to study the formation of S_2. He did conclude that two processes could form S_2, namely,

$$S \ + \ CS_2 \quad \rightarrow \quad CS \ + \ S_2 \qquad \{2\}$$

$$S \ + \ S \ + \ M \quad \rightarrow \quad S_2 \ + \ M* \qquad \{5\}$$
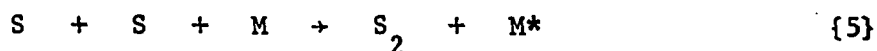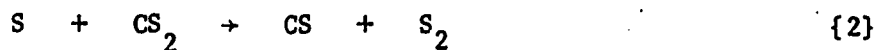
although reaction {5} would only become significant at very high pressures of inert gas.

Callear[8] also studied the flash photolysis of carbon disulfide using much lower pressures, 0.03 torr, and a much more refined apparatus. He was able to detect the formation of S (^{3}P) atoms but neither the (^{1}S) nor the (^{1}D) could be observed. Therefore he concluded that the initial step in the photolysis was absorption

to a singlet state, followed by intersystem crossing to one of the nearby triplet states[10,11] and decomposition from this triplet state. This scheme can be summed up in the equation

$$CS_2 + h\nu \rightarrow CS \ (^1\Sigma^+) + S \ (^3P) \qquad \{6\}$$
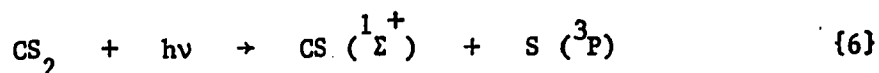
He attributed the formation of S_2 to recombination via reaction {5} rather than to the abstraction reaction {2} proposed by Wright and by Porter.

Callear proposed that the fate of S_2 is a third order recombination via

$$2 \ S_2 + M \rightarrow S_4 + M^* \qquad \{7\}$$
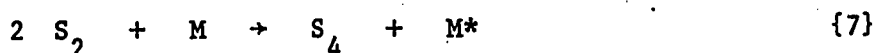
although this mechanism failed to explain the observed pressure dependence of S_2 formation and decay.

A thorough investigation of the flash photolysis of carbon disulfide was carried out by Basco and Pearson[9]. They found that their results were best explained by the following mechanism:

$$CS_2 + h\nu \rightarrow CS + S \qquad \{6\}$$

$$CS_2 + S \rightleftarrows CS_3 \qquad \{8\}$$

$$CS_3 + S \rightarrow CS_2 + S_2 \ (^3\Sigma_g^-) \qquad \{9\}$$

$$2 \ S_2 + M \rightarrow S_4 + M^* \qquad \{10\}$$
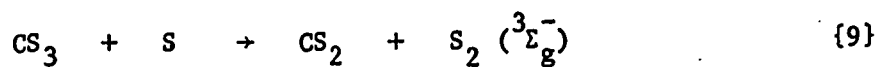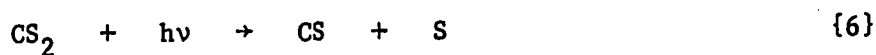
They based this mechanism on the observations that the rate of S_2 formation is dependent on carbon disulfide pressure, that the activation energy of S_2 formation is negative, and that the addition of a large excess of inert gas has little effect on the rate of S_2 production.

They also carried out the flash photolysis of carbon disulfide in the presence of small amounts of nitric oxide. The marked increase in the rate of formation of S_2 was attributed to the reaction scheme

$$S \ + \ NO \ \rightleftarrows \ SNO \qquad\qquad \{11\}$$

$$SNO \ + \ S \ \rightarrow \ NO \ + \ S_2 \qquad\qquad \{12\}$$
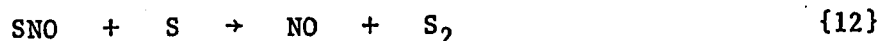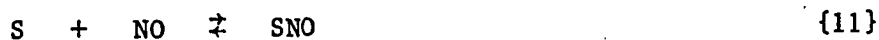
In the presence of nitric oxide, a new transient spectrum was observed in the spectral region of λ = 3500 - 4300 Å. No attempt was made to assign the spectrum but they suggested that it resembled the spectrum of NO_2.

They were able to obtain values for the rate constant k_8, the ratio k_9 / k_{-8}, and for the equilibrium constant $K = k_8/k_{-8}$. These values are $3\pm1 \times 10^{11}$ $M^{-2}sec^{-1}$, $1.2\pm0.5 \times 10^4$ and $\sim 10^5$ respectively.

Heicklen[12] has observed luminescence from carbon disulfide vapor irradiated with light between 2800 Å and 3600 Å. He was able to show that the excited molecule formed in the primary process

$$CS_2 + h\nu \rightarrow CS_2^* \qquad \{13\}$$

is long lived, $\tau = 3.3 \times 10^{-6}$ sec., and emission from the excited

state occurs before vibrational relaxation can take place

$$CS_2^* \rightarrow CS_2 + h\nu \qquad \{14\}$$

He proposed that luminescence quenching in carbon disulfide vapor

takes place via the self quenching process

$$CS_2^* + CS_2 \rightarrow 2\ CS_2 \qquad \{15\}$$
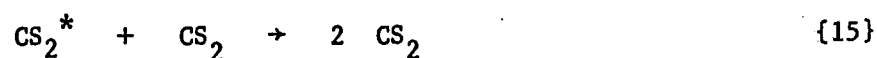
With the exception of Heicklen's work, all of the above

mentioned investigations were carried out in quartz vessels and

consequently carbon disulfide was photolyzed in its short wavelength

region, leaving the much weaker long wavelength region unexplored.

The object of this investigation was to examine the

mechanism of luminescence quenching and to establish whether

chemical reaction can occur from the luminescent state. A secondary

objective was to examine the recombination of S (^{3}P) atoms.

Carbonyl Sulfide and the Reactions of S (^{1}D) and (^{3}P) Atoms

The ultra violet absorption spectrum of gaseous carbonyl

sulfide consists of a series of weak vibrational bands superimposed

on a strong continuum in the region of 2000 Å to 2600 Å. Sidhu et al[13]

have calculated the lifetime of the excited state to be 10^{-9} sec.

They also found that the first absorption corresponds to transition $\pi^* \leftarrow \pi$.

As early as 1932, it was suggested that the photochemical decomposition of carbonyl sulfide may form S (^{1}D) atoms[14]. Forbes and Kline[15] found that the quantum yield of CO was close to unity and assumed that S atoms are incapable of secondary reactions.

Strausz and Gunning[16] studied the photolysis of COS and showed that it was a clean source of sulfur atoms with the carbon monoxide being a good monitor of the amount of S atoms produced.

Taking the heat of formation of S (^{3}P) atoms as 66 Kcal/mole[17] and ΔH_f COS = -33.8 Kcal/mole[18], then D(OC=S) = 72.4 Kcal/mole. The first two excited states of sulfur are ^{1}D and ^{1}S and are 26.4 and 63.4 Kcal/mole above ground state respectively[19]. Therefore the two primary processes

$$COS \;+\; h\nu \;\rightarrow\; CO \;+\; S\;(^1D) \qquad\qquad \{1\}$$

$$COS \;+\; h\nu \;\rightarrow\; CO \;+\; S\cdot(^1S) \qquad\qquad \{2\}$$
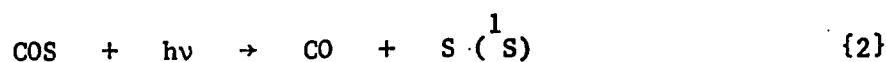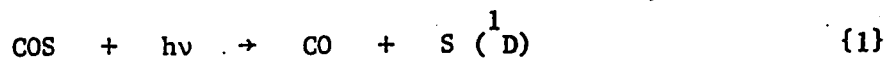
can commence at 2895 Å and at 2105 Å respectively.

The mechanism proposed for the decomposition of carbonyl sulfide is

$$COS \;+\; h\nu \;\rightarrow\; CO \;+\; S\;(^1D) \qquad\qquad \{1\}$$

$$S\;(^1D) \;+\; COS \;\rightarrow\; CO \;+\; S_2 \qquad\qquad \{3\}$$

$$COS \;+\; S\;(^1D) \;\rightarrow\; COS* \;+\; S\;(^3P) \qquad\qquad \{4\}$$

$$COS + S\ (^3P) \rightarrow CO + S_2 \qquad\qquad \{5\}$$

$$2\ S\ (^3P) + M \rightarrow S_2 + M^* \qquad\qquad \{6\}$$
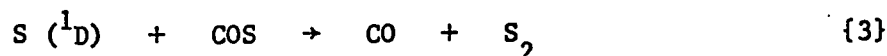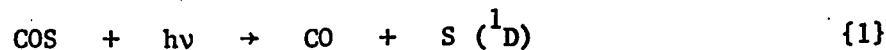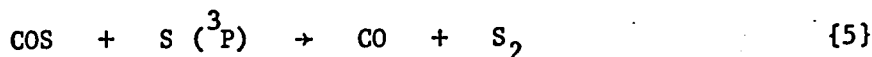
Carbonyl sulfide was shown to bring about the relaxation of S (^{1}D) to the ground state via reaction {4}[20]. Reaction {6} is not important since the addition of an S atom scavenger reduces the CO yield to one half.

The quantum yield of carbon monoxide has been measured[13] under different conditions and was found to be 1.80 rather than the expected value of 2.0. However, since the quantum yield is independent of pressure, this low value is probably due to an inefficiency in the primary photolytic process[13].

The reaction between S (^{1}D) atoms and paraffinic hydrocarbons was shown to be an insertion process[21,22]. The exothermicity of the process is about 85 Kcal/mole and except with methane, the number of available degrees of freedom are sufficient to prevent decomposition of the hot mercaptan.

The rate of reaction of S (^{1}D) with the C – H was found to be independent of the bond type. The mercaptan distribution with propane was n-PrSH/iso-PrSH = 2.85 ± 0.05 and with isobutane, i-BuSH/t-BuSH = 8.8 ± 0.1. This indicates that the attack is indiscriminate and hence of high efficiency.

The addition of carbon dioxide reduces the mercaptan yield to zero indicating that S (^{3}P) atoms do not insert or abstract[22]. The fact that the CO yield can not be reduced to exactly one half

was attributed to the formation of S (^{3}P) atoms in the primary process. From the rate of mercaptan formation, it was concluded that this process may occur to the extent of 26%[22].

$$COS \quad + \quad h\nu \quad \rightarrow \quad CO \quad + \quad S\ (^3P) \qquad \{7\}$$
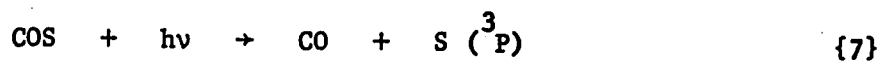
The following mechanism was proposed for the reaction of S (^{1}D) atoms with paraffinic hydrocarbons:

$$COS \quad + \quad h\nu \quad \rightarrow \quad CO \quad + \quad S\ (^1D) \qquad \{1\}$$

$$S\ (^1D) \quad + \quad RH \quad \rightarrow \quad RSH \qquad \{8\}$$

$$S\ (^1D) \quad + \quad RH \quad \rightarrow \quad RH^* \quad + \quad S\ (^3P) \qquad \{9\}$$

$$S\ (^1D) \quad + \quad COS \quad \rightarrow \quad CO \quad + \quad S_2 \qquad \{3\}$$

$$S\ (^3P) \quad + \quad COS \quad \rightarrow \quad CO \quad + \quad S_2 \qquad \{5\}$$

$$2\ S\ (^3P) \quad + \quad M \quad \rightarrow \quad S_2 \quad + \quad M^* \qquad \{6\}$$
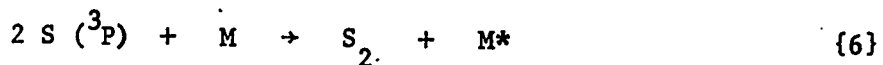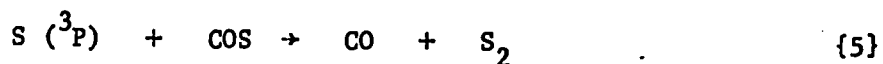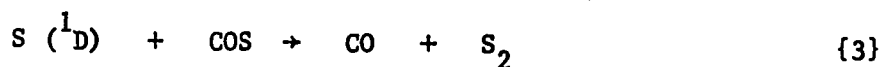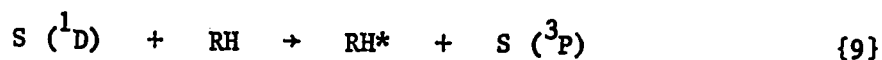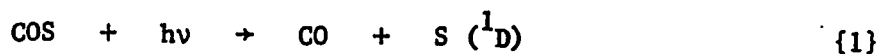
The rate of reaction {3} was shown to be about twice as fast as {8}.

In the case of methane, considerable cracking of the hot mercaptan occurred since the number of dergrees of freedom was less than in the higher paraffins. The following mechanism based on the secondary products was offered:

$$CH_4 \quad + \quad S\ (^1D) \quad \rightarrow \quad CH_3SH^* \qquad \{10\}$$

$$CH_3SH^* \; + \; M \; \rightarrow \; CH_3SH \; + \; M^* \qquad \{11\}$$

$$CH_3SH \; \rightarrow \; CH_3S \; + \; H \qquad \{12\}$$

$$H \; + \; CH_4 \; \rightarrow \; H_2 \; + \; CH_3 \qquad \{13\}$$

$$2 \; CH_3S \; \rightarrow \; CH_3SSCH_3 \qquad \{14\}$$

$$CH_3S \; + \; CH_3 \; \rightarrow \; CH_3SCH_3 \qquad \{15\}$$

$$CH_3S \; + \; CH_3 \; \rightarrow \; CH_2S \; + \; CH_4 \qquad \{16\}$$

$$2 \; CH_3 \; \rightarrow \; C_2H_6 \qquad \{17\}$$
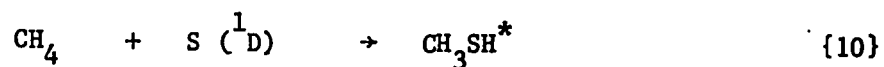
The ratio $CH_3SH/\Sigma CH_3S = 0.67$ was found to be independent of the total pressure up to 1450 torr indicating that about one third of the hot mercaptan underwent pressure independent fragmentation[21].

The products of the reaction of sulfur atoms with olefins were found to be episulfides, vinylic mercaptans, and alkenyl mercaptans[23]. The carbon monoxide yield decreased to one half indicating that complete scavenging of the sulfur atoms had been accomplished. The addition of a large excess of carbon dioxide suppressed the formation of all mercaptans indicating that they are formed from S (^{1}D) atoms only. Ground state triplet atoms react with olefins to form only an episulfide. Alkenyl and vinylic mercaptans indicate the participation of singlet sulfur atoms. The following mechanism was proposed to account for the reaction of S (^{1}D) atoms with olefins:

$$COS + h\nu \rightarrow CO + S\,(^1D) \qquad \{1\}$$

$$COS + S\,(^1D) \rightarrow CO + S_2 \qquad \{3\}$$

$$S\,(^1D) + olefin \rightarrow episulfide \qquad \{18\}$$

$$\rightarrow alkenyl\ mercaptan \qquad \{19\}$$

$$\rightarrow vinylic\ mercaptan \qquad \{20\}$$

$$\rightarrow S\,(^3P)\cdot + olefin^* \qquad \{21\}$$

$$S\,(^3P) + olefin \rightarrow episulfide \qquad \{22\}$$
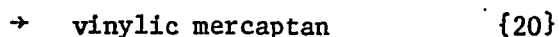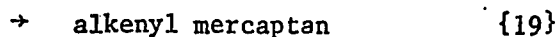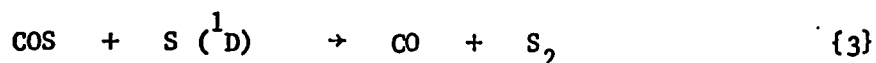
Thus a convenient method of distinguishing between singlet and triplet sulfur atoms was developed. Triplets form only episulfides while singlets form episulfides and mercaptans. Triplets do not react with paraffins while singlets insert to give the corresponding mercaptans.

Basco and Pearson investigated the flash photolysis of carbonyl sulfide and proposed that S_2 formation proceeds via the mechanism[9]:

$$COS + h\nu \rightarrow CO + S\,(^1D) \qquad \{1\}$$

$$COS + S \rightleftarrows COS_2 \qquad \{23\}$$

$$COS_2 + S \rightarrow COS + S_2 \qquad \{24\}$$

$$2\,S_2 + M \rightarrow S_4 + M^* \qquad \{25\}$$
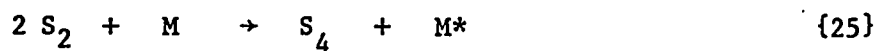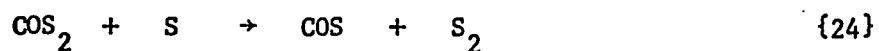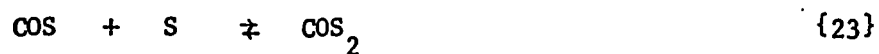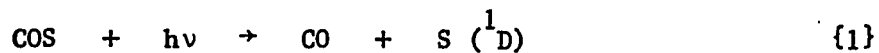
These conclusions are in disagreement with those of Strausz and Gunning[16] since they can not explain the decrease in the CO yield when an olefin or paraffin is added to the system.

McGrath et al[24] also investigated the flash photolysis of carbonyl sulfide and observed a new transient spectrum which they said may be due to an excited state of S_2. They attempted no assignment of this spectrum. They also observed that S (^{1}D) atoms react with hydrogen to give the transient HS. They did not attempt a mechanism for HS formation.

The object of the investigation of the flash photolysis of carbonyl sulfide was to examine the abstraction reaction {3} as well as to attempt to obtain rate constants for the reactions of S (^{1}D), S (^{3}P) atoms and S_2.

The reaction of S (^{1}D) with hydrogen and with methane was also examined to determine the mechanisms involved in the thermal cracking reactions.

Hydrogen Sulfide

Hydrogen sulfide begins to absorb in the ultra violet region at 2600 Å and reaches maximum absorption at 2200 Å. The absorption is continuous and shows no structure.

Forbes et al[25] investigated the photochemistry of hydrogen sulfide and found that the quantum yield for H_2S disappearance is unity. They varied the wavelength from 2080 Å to

2370 Å and the pressure from 7.5 torr to 1400 torr but the quantum

yield did not change. They also found that the intensity, which

was changed by a factor of 15, did not affect the results. From

these facts, they concluded that the most likely primary step is

$$H_2S \quad + \quad h\nu \quad \rightarrow \quad H \quad + \quad HS \qquad \{1\}$$

and that HS radicals must be stable with respect to dissociation

into atoms. They postulated that if H atoms react via

$$H \quad + \quad H_2S \quad \rightarrow \quad H_2 \quad + \quad HS \qquad \{2\}$$

then HS must undergo

$$2\,HS \quad \rightarrow \quad H_2S \quad + \quad S \qquad \{3\}$$

An alternate primary process is the reaction

$$H_2S \quad + \quad h\nu \quad \rightarrow \quad H_2 \quad + \quad S \qquad \{4\}$$
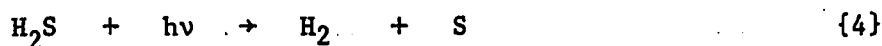
However, the work of Avery and Forbes[26] ruled out this step. They

found that the photolysis of hydrogen sulfide in carbon tetrachloride

solution resulted in the formation of sulfur, hexachloroethane, and

trichloromethyl marcaptan. These products can only be explained

in terms of reaction {1} being the primary process.

Porter[27] carried out the flash photolysis of hydrogen

sulfide and was able to show that the primary photochemical step

is reaction {1} by observing the spectrum of HS at the shortest delay.

He proposed the following reaction scheme for the decomposition of hydrogen sulfide

$$H_2S + h\nu \rightarrow H + HS \tag{1}$$

$$H + H_2S \rightarrow H_2 + HS \tag{2}$$

$$2 HS \rightarrow H_2 + S_2 \, (^3\Sigma_g^-) \tag{5}$$

$$2 S_2 \, (^3\Sigma_g^-) + M \rightarrow S_4 + M* \tag{6}$$
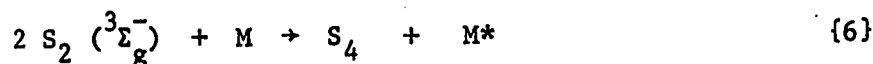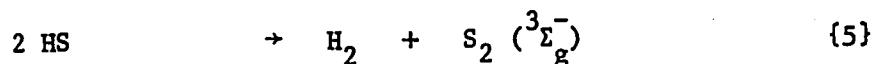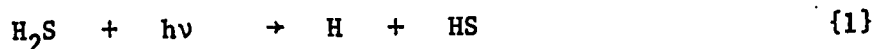
Porter also detected a new transient spectrum in the region of 3100 Å to 3770 Å and attributed it to the species HS_2. He did not propose a mechanism for its formation.

Darwent and Roberts[28] also investigated the photolysis of hydrogen sulfide by measuring the quantum yield of hydrogen at a variety of conditions. They found that the quantum yield of H_2 was 1.09 at 30 torr and 1.26 at 400 torr. They attributed this increase to the reaction

$$2 HS \rightarrow H_2 + S_2 \tag{7}$$

They found that at 400 torr pressure, about 13% of the HS reaction proceeded via {7}, the rest via {3}.

Darwent and Krasnansky have been able to show that the rate of reaction {2} is fast[29] although its absolute rate constant is not known with any certainty since the H atom is translationally hot when formed and depending on the total pressure, will influence

the reaction rate.

In a recent study, Darwent et al[30] have been able to show that the rate of reaction {7} is much slower than the rate of {5} at low pressures. They reacted methyl with hydrogen sulfide via

$$CH_3 + H_2S \rightarrow CH_4 + HS \qquad \{8\}$$
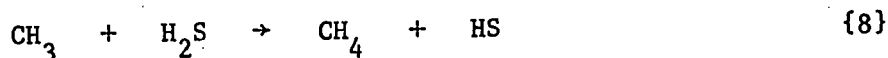
and noted that H_2 was not formed. Therefore, reaction {7} must not be important.

Stiles et al[31] however were able to show that the electron spin resonance spectrum obtained from the photolysis of hydrogen sulfide was that of S_2 ($^3\Sigma_g^-$) and most probably came from the reaction of HS via {7}.

Since there is some disagreement in the literature about the reactions of HS, the photochemistry of hydrogen sulfide was reinvestigated to clarify this situation.

Hydrogen Disulfide

The only study on the reactions of hydrogen disulfide was made by Dolgoplosk and coworkers[32]. They reacted hydrogen disulfide in liquid pentenes at 70°C. From the products found, they proposed that H_2S_2 decomposes via

$$H_2S_2 \rightarrow 2 HS \qquad \{1\}$$

followed by

$$HS + H_2S_2 \rightarrow H_2S + HS_2 \qquad \{2\}$$

They also discussed some of the addition reaction of HS and HS_2 with the various olefins to produce mercaptans and disulfides.

Except for this one investigation, no attention has been paid to the photochemistry of hydrogen sulfide. The investigation of the photochemistry of this compound was undertaken for this very reason. Also, it seemed reasonable that if the transient spectrum was correctly assigned by Porter to HS_2, then hydrogen disulfide would be a good source of this species.

Ethylene Episulfide

Low intensity studies of the photolysis of ethylene episulfide,[E], have shown that the major product is ethylene and sulfur. The quantum yield of ethylene was found to be about 1.67 at 7.3 torr and 1.57 at 16.0 torr[33]. The mechanism suggested for the formation of this product is

$$C_2H_4S + h\nu \rightarrow {}^1E^* \qquad \{1\}$$

$${}^1E^* \rightarrow {}^3E^* \qquad \{2\}$$

$${}^3E^* \rightarrow C_2H_4 + S\,({}^3P) \qquad \{3\}$$

$$E + S\,({}^3P) \rightarrow C_2H_4 + S_2 \qquad \{4\}$$
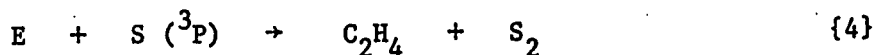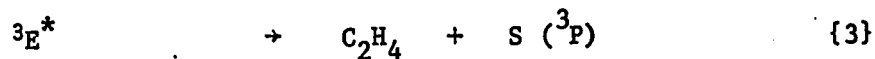
The sulfur atoms are formed in the triplet ground state since

mercaptans could not be found among the products on addition of paraffins or olefins, although the episulfide of the added olefin was readily detected.
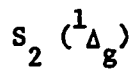
S_2 $(^1\Delta_g)$

The emission spectrum of S_2 $(^1\Delta_g)$ has been observed by several workers[55,56,57]. Barrow et al.[56] have attributed the spectrum to the transition $b^1\Delta_u \rightarrow x^1\Delta_g$. The vibrational assignment has recently been reassigned[58] based on the rotational analysis of $^{34}S_2$ enriched samples.

McGrath et al.[24] observed several lines of this spectrum in the flash photolysis of carbonyl sulfide although they did not assign the spectrum to the S_2 $(^1\Delta_g)$ species. Strausz et al.[59] have observed the spectrum from a variety of substrates and also detected five short wavelength bands that were not seen in emission. The following bands were observed in absorption:

2343 (15,0)	2426.0 (11,0)	2520.7 (7,0)*
2364 (14,0)	2448.4 (10,0)	
2384.1 (13,0)	2471.7 (9,0)	
2404.7 (12,0)	2495.8 (8,0)	

* Partially obscured by Si emission line.

CHAPTER II

EXPERIMENTAL

APPARATUS

1, High – vacuum system

A conventional high – vacuum system was used consisting
of pumping, distillation, storage, metering and product analysis
stages. The system was completely grease free employing only
Delmar mercury float valves and helium tested Hoke valves.

The pumping stage consisted of a Welch Duoseal Model 1405
mechanical pump and a two stage mercury diffusion pump. Typical
pressures attained were 10^{-6} torr. The distillation stage (Fig. 1)
served the dual purpose of reagent purification and product fractiona-
tion. It consisted of three traps isolated by mercury float valves.
The storage stage consisted of five 2 liter pyrex bulbs where the
purified reagents were stored behind mercury float valves. The
metering stage (Fig. 1) consisted of a mercury manometer and a McLeod
gauge. The manometer was used for measuring pressures in excess of
2 torr while the McLeod gauge was used for lower pressures. The
reactants were measured directly into either the flash cell or into
the static cell. The product analysis stage (Fig. 2) consisted of a
Toepler pump in conjunction with a set of calibrated bulbs for
quantitative measurements of the fractionated products. A second

to Toepler

to vacuum

to solid N_2
trap

to vacuum

to storage

to vacuum
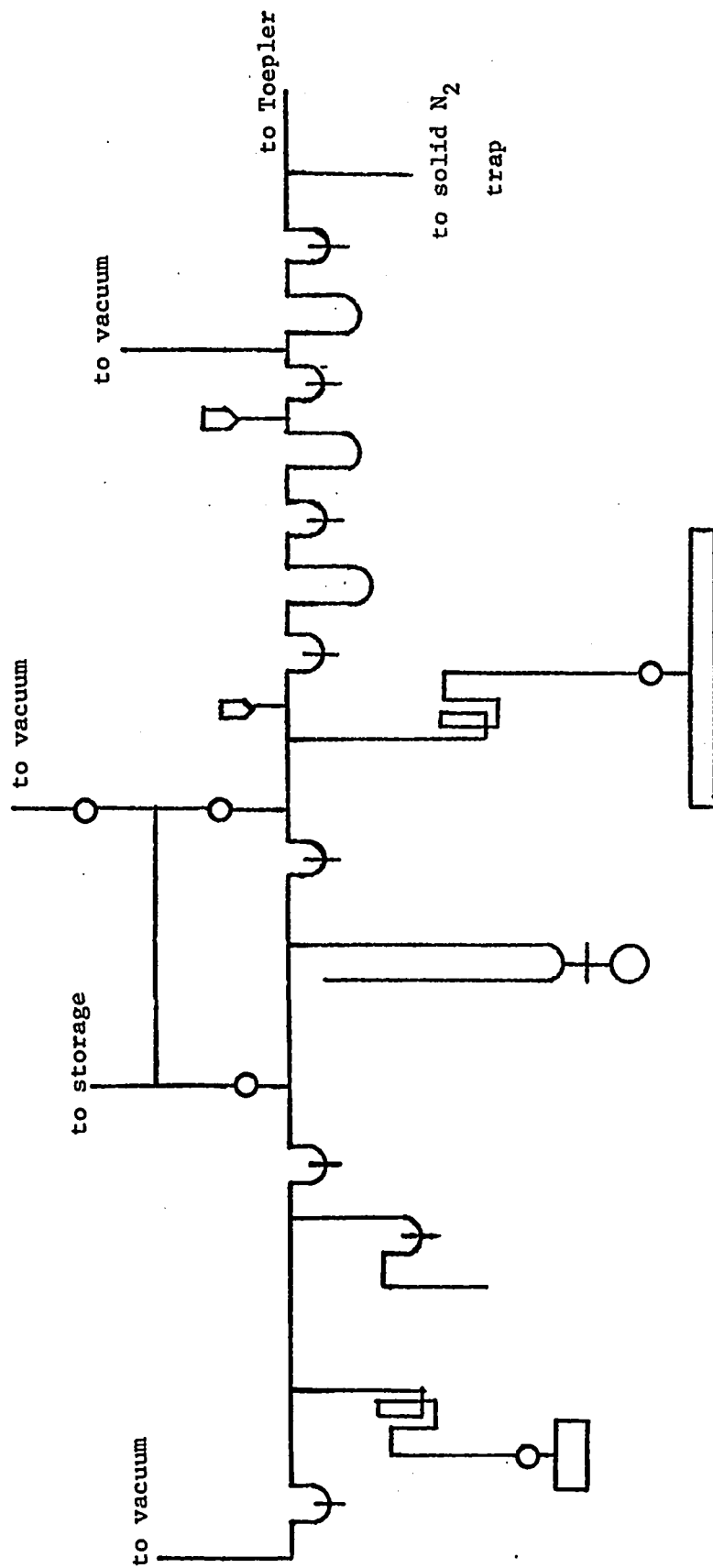
Fig. 1   Metering and Distillation Stage

to flow
meter

helium flow →

to vacuum

Fig. 2   Analytical Stage

Toepler pump was used to transfer products into the G.L.C. sampler

for chromatographic separation and analysis. The G.L.C. unit

consisted of a thermal conductivity unit, Gow - Mac Model TR IIIB,

a power supply, Gow - Mac 999-C and a Sargent recorder, Cat. No.

S - 72189. Helium at a flow rate of 60 cc/min was used as carrier.

G.L.C. columns were constructed of 6 mm ID glass coils.

2, Mercury - free system

The mercury and metal free system (Fig. 3) consisted of a

trap for hydrogen disulfide, several inlets of 12/30 standard taper

joints, a mercury manometer with N.R.C. DC 704 pump oil covering the

mercury surfaces, and storage bulbs for krypton and nitrogen. High -

vacuum was achieved by a Welch Duoseal Model 1405 mechanical pump

and an oil diffusion pump using N.R.C. DC 704 pump oil. The only

purpose for this system was to fill the flash lamps and for metering

reactants in the hydrogen disulfide experiments. Typical pressures

attained were about 10^{-5} torr.

3, Static photolysis assembly

Most static photolyses were carried out with an Hanovia

Type SH medium pressure mercury arc. A second light source, Osram Cd

resonance arc, was used in several hydrogen disulfide experiments.

The reaction vessels were either cylindrical quartz with plane

quartz windows or cylindrical pyrex (transmitted $\lambda > 2900$ Å) with

plane pyrex windows. The dimensions of all cells were 10 cm long

and 5 cm in diameter. The cell was positioned 10 cm in front of

to flash lamps

to vacuum

Hg manometer
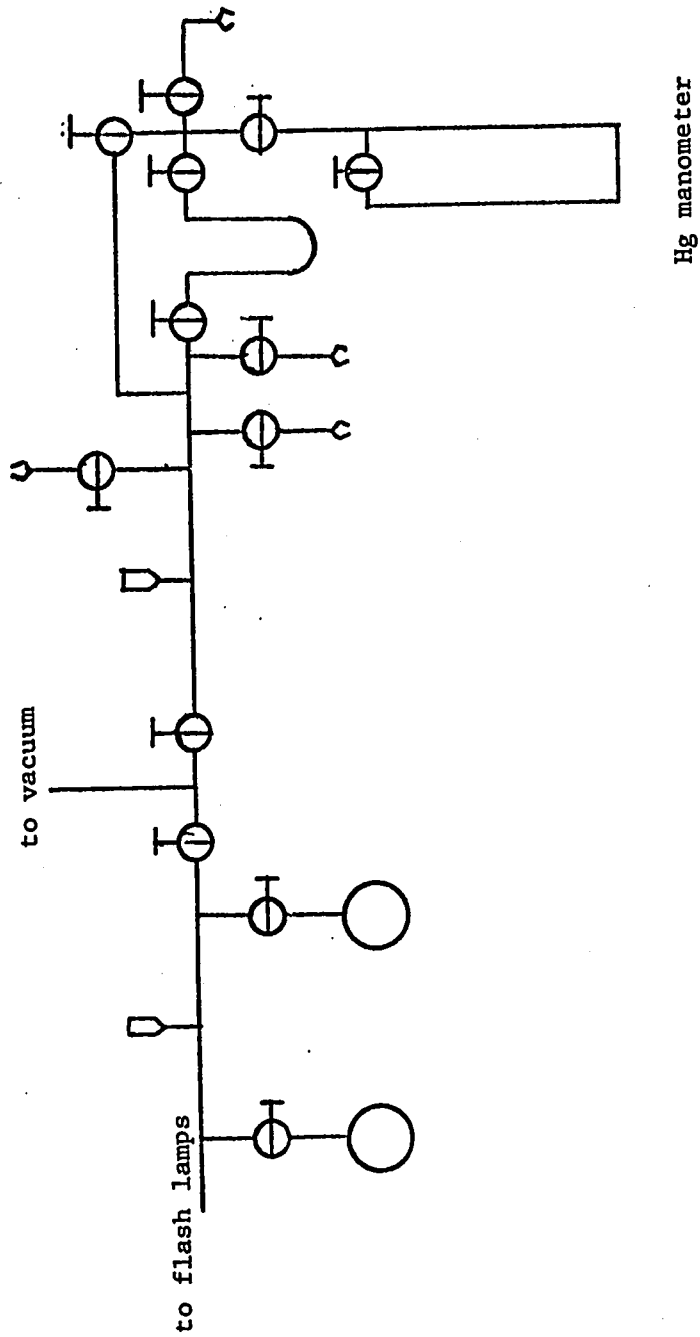
Fig. 3   Mercury Free High Vacuum System

the light source in such a manner that the cell could be removed for cleaning and be replaced into the same original position.

4. Flash apparatus

The componenets of the flash unit were: (a) reaction housing, (b) photo - flash source, (c) delay generation, (d) spectroscopic source flash, (e) delay monitoring, and (f) optical bench and spectrograph.

(a) Reaction housing. The reaction housing was a cylindrical tube 60 cm. long and 15 cm. ID. The top half of the reactor could be removed for changing the cell and the bottom half was supported on the optical bench. The bottom half contained two supports for positioning the center of the reaction vessel on the optical axis of the apparatus. The inside of the reactor was coated with either MgO or with polished aluminum to reflect the light of the photo - flash. Since MgO was a loose deposit that tended to flake off, the aluminum reflector was used unless maximum light intensity was essential.

All reaction vessels used in the course of this work were 50 cm. long and were equipped with plane quartz windows. Cell walls were constructed of quartz, Vycor 7910, or pyrex with cell diameters of 28, 47, or 50 mm. Most flashes were done in Vycor 7910 cells unless specified otherwise.

(b) Photo - flash source. The photo - flash unit (fig.4) consisted of a conventional high voltage power supply,
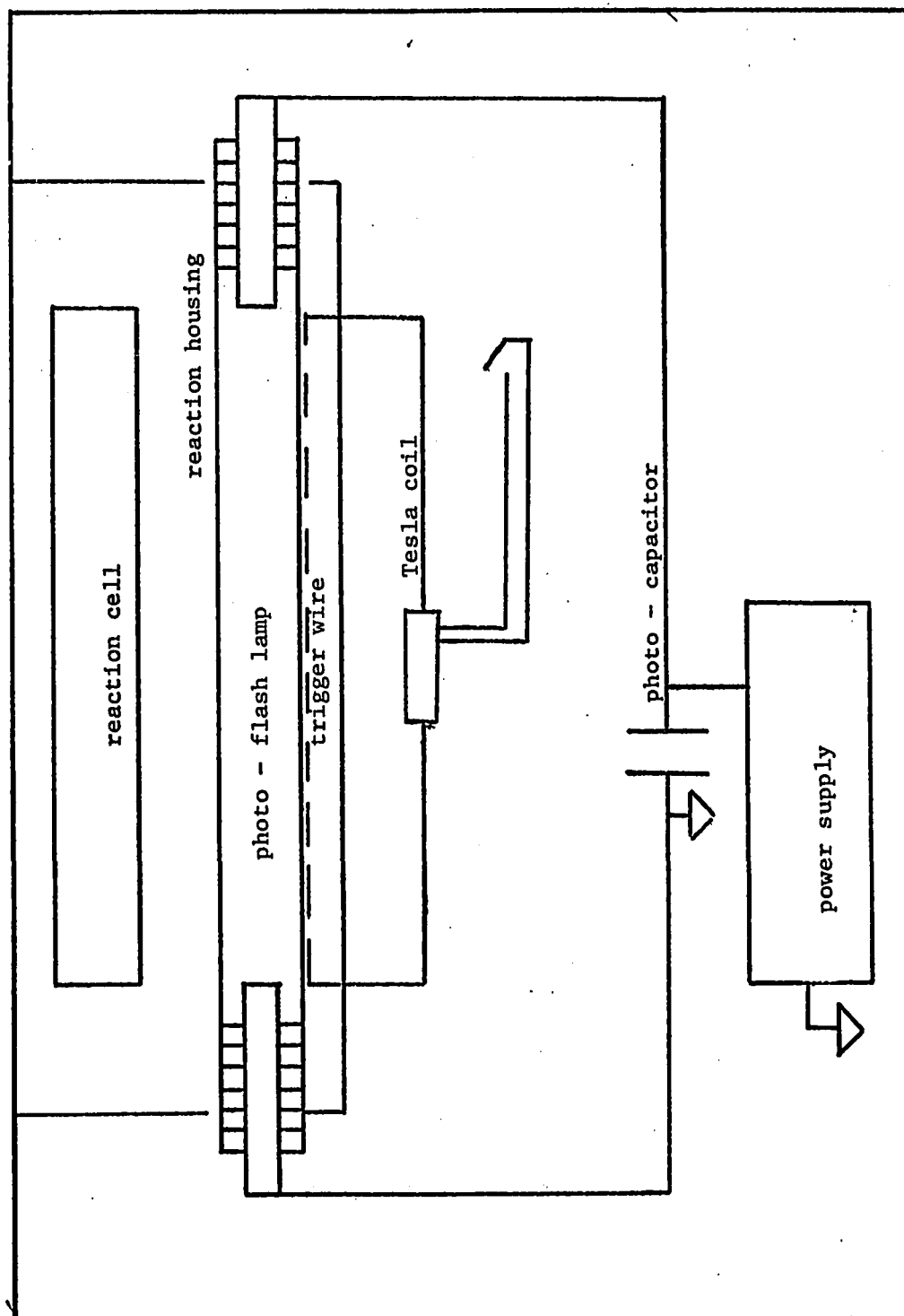
Fig. 4   Photo – flash Source

a Tobe Deutschmann Model ESC 249 E, 60 µf, 10 Kv low inductance capacitor, a quartz flash lamp of 12 mm ID with molybdenum alloy electrodes, Vitreosil Model T/E7/232, 50 cm tip to tip and a trigger wire along the outer surface of the lamp operated from a single pulse Tesla coil. The photo - flash lamp was filled with 10 torr nitrogen + 60 torr krypton. The photo - flash reached maximum intensity in 14 µsec and decayed with a half life of 25 µsec.

(c) Delay generation unit. The time delay unit, whose function was to fire the source lamp after a predetermined delay after the photo - lamp is shown in Figure 5. It consisted of a photocell, Phillips 6910 blue sensitive, an electronic delay unit and a thyrotron valve.

The electronic delay unit had a set of coarse and fine delay settings which were calibrated with an oscilloscope. The delay unit could be eliminated from the circuit by an in - out switch. Another switch selected either the photo - flash or the source flash for firing. The delay unit also served as the power supply for the photocells.

(d) Spectroscopic source flash. The source flash assembly (Fig. 5) consisted of a trigger gap, spark gap, high voltage power supply, source capacitor and a source flash lamp. The spark gap and the trigger gap are shown in Figure 6. The source flash lamp (Fig. 7) was constructed of quartz with two molybdenum alloy electrodes. The lamp was filled with 100 torr krypton and the flash
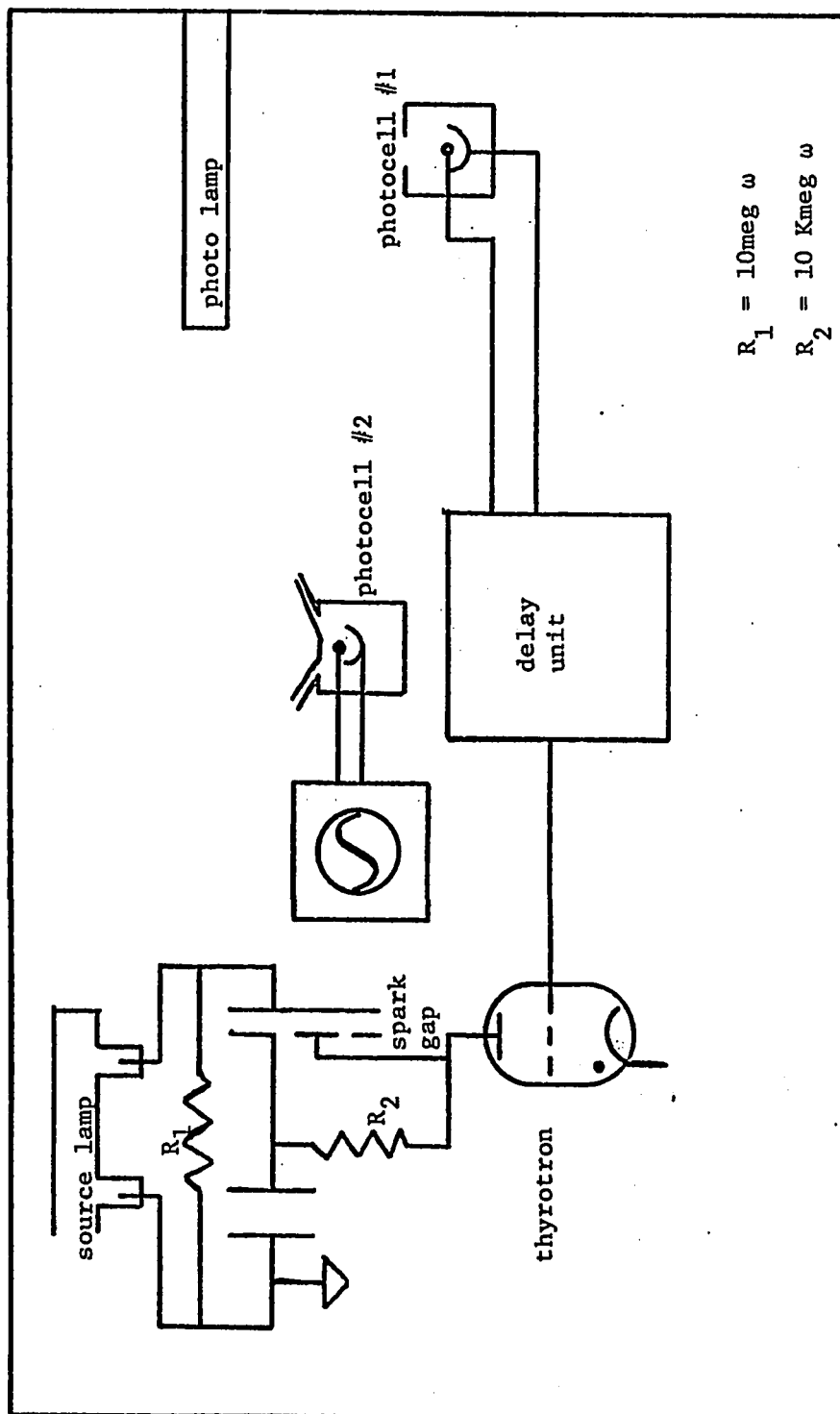
Fig. 5   Source Flash and Delay Unit

to source lamp

to thyrotron
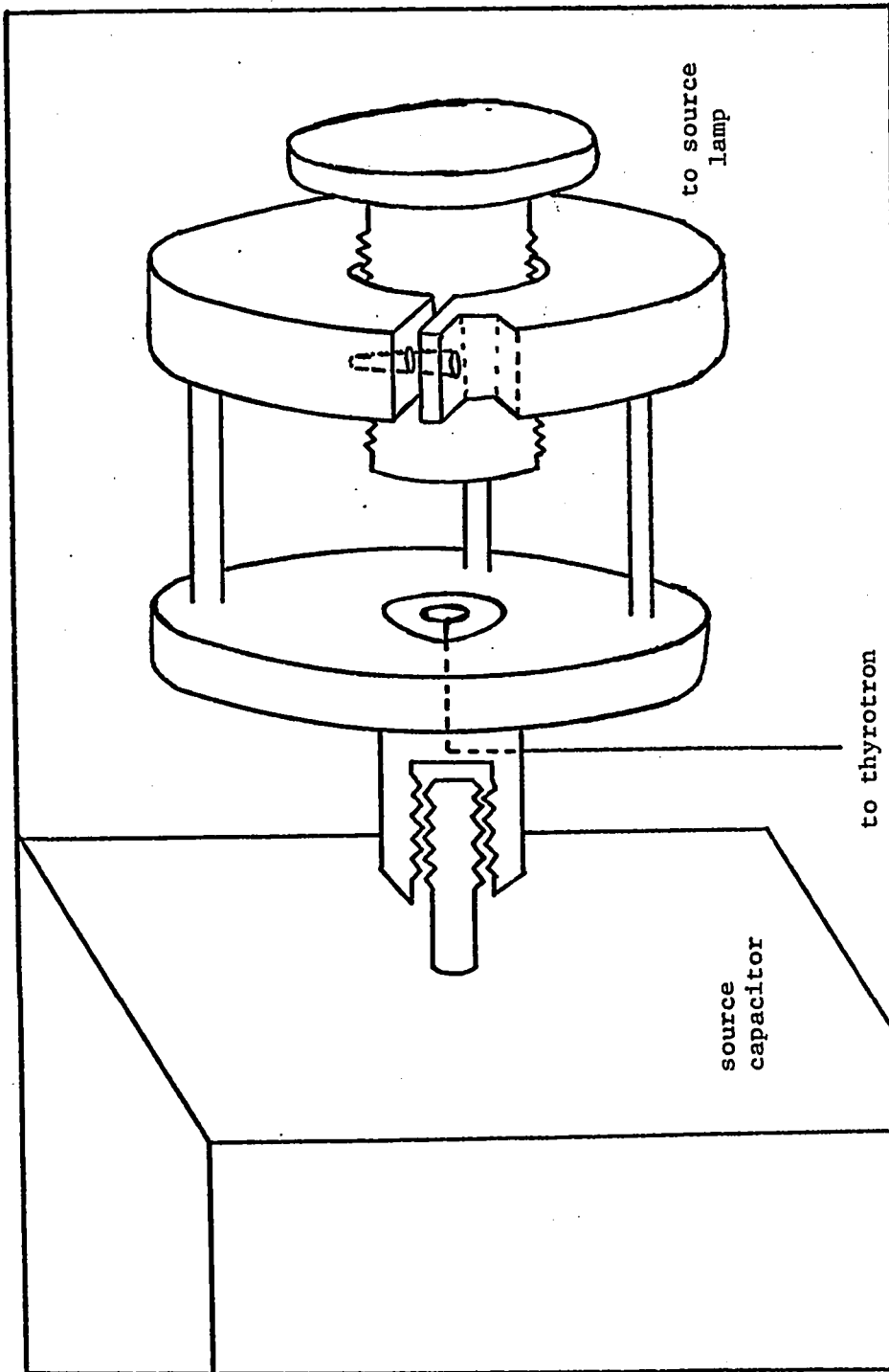
source capacitor

Fig. 6   Spark Gap and Trigger Gap

24/40

24/40

to source capacitor

200 cc pyrex
bulb

to vacuum line
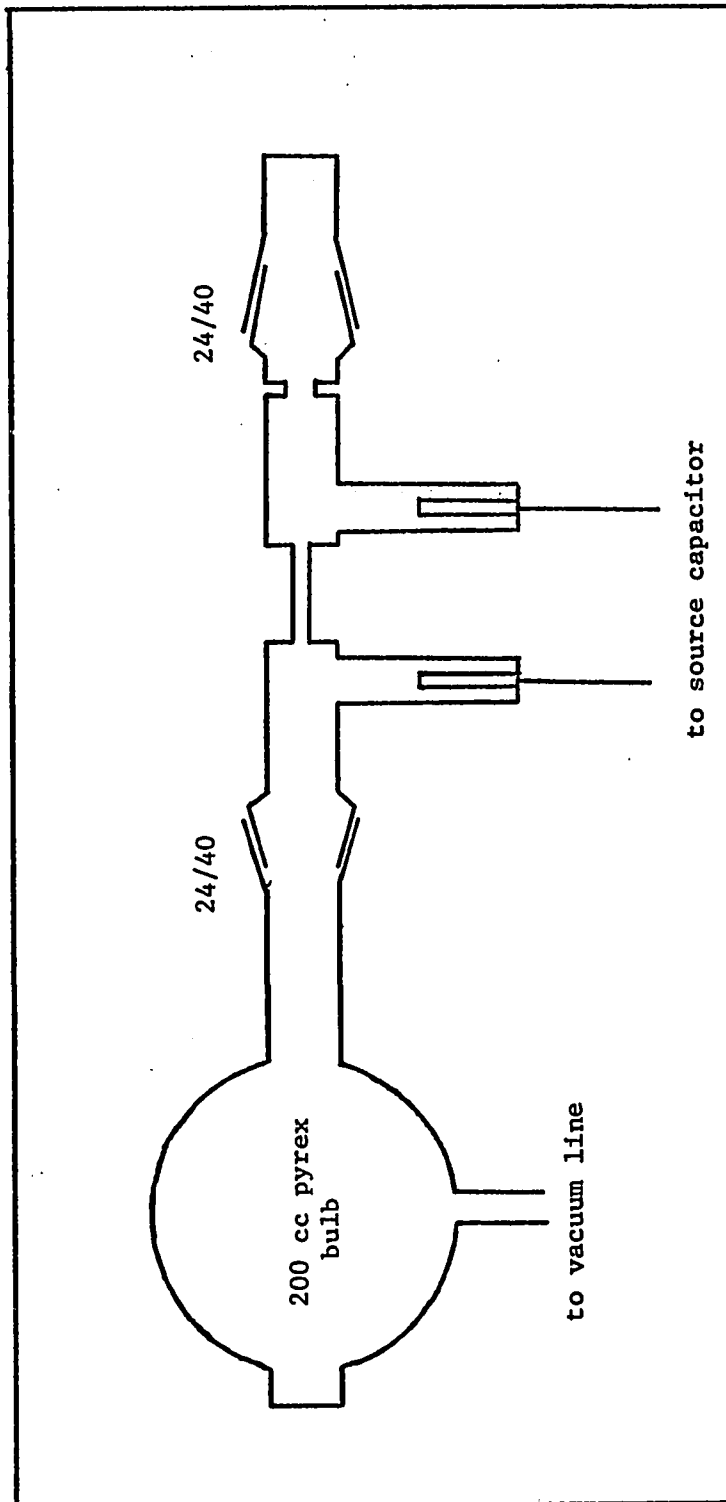
Fig. 7   Source Flash Lamp (drawn exactly to one – half scale)

reached maximum intensity in 5 μsec and decayed with a half life of 15 μsec. The source capacitor, Cornell Dubilier, NRG type 206 low inductance capacitor was 2.6 μf and was charged to 10 Kv.

(e) Delay monitoring. Delays were monitored with a photocell, No.2, and the output was displayed on a Hewlett Packard Model 130 C oscilloscope. The traces were photographed with a Hewlett Packard Polaroid camera Model 196B. A typical delay is shown in Figure 8. Delay times were measured from the onset of the photo - flash to the point where half of the source flash energy had been dissipated.

(f) Optical bench and spectrograph. The optical arrangement is shown in Figure 9. The quartz lens had a focal length of 25 cm and was used to focus the near end of the capillary onto the spectrograph slit. The collimator was of standard design and reduced the scattered light from the photo - flash to very low levels. The spectrograph was an Hilger Watts medium quartz Model E 498. Spectra were recorded on either Kodak 103a - O or Ilford HPS plates. An Hilger Watts neutral density wedge, positioned immediately in front of the entrance slit was used to calibrate the photographic plates to obtain absolute optical densities.

(g) Chain of events in one flash. When the manual switch was closed, the single pulse Tesla coil applied a high voltage pulse to the trigger wire which caused some ionization inside the photo - lamp, causing a decrease in the lamp resistance and a spontaneous discharge of the photo - capacitor through the lamp.
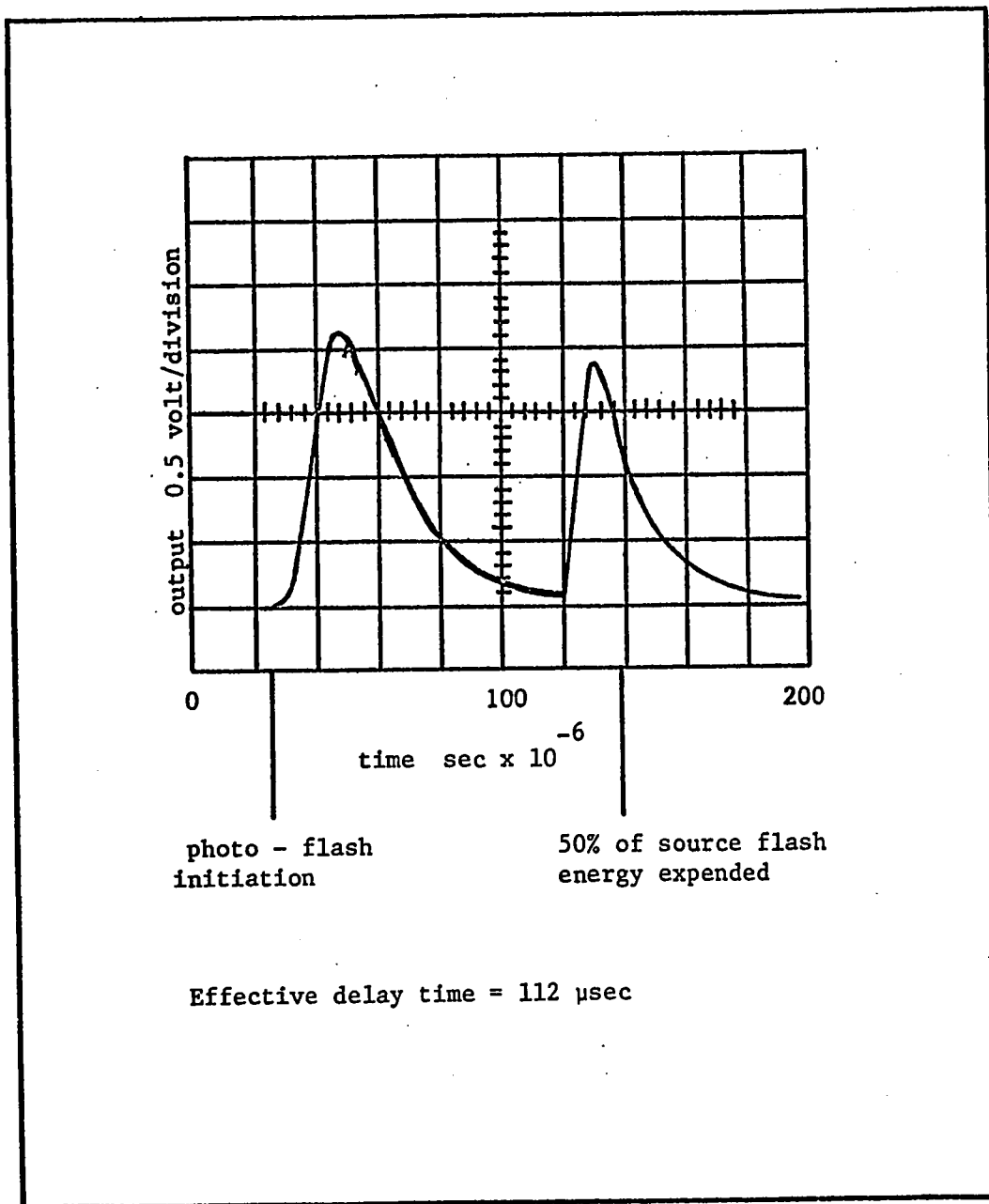
Fig. 8   Oscilloscope trace for delay setting 2/6

Neutral Density Wedges

Collimator

Source flash lamp

Quartz lens

25 cm. focal

length

Reaction cell

and housing
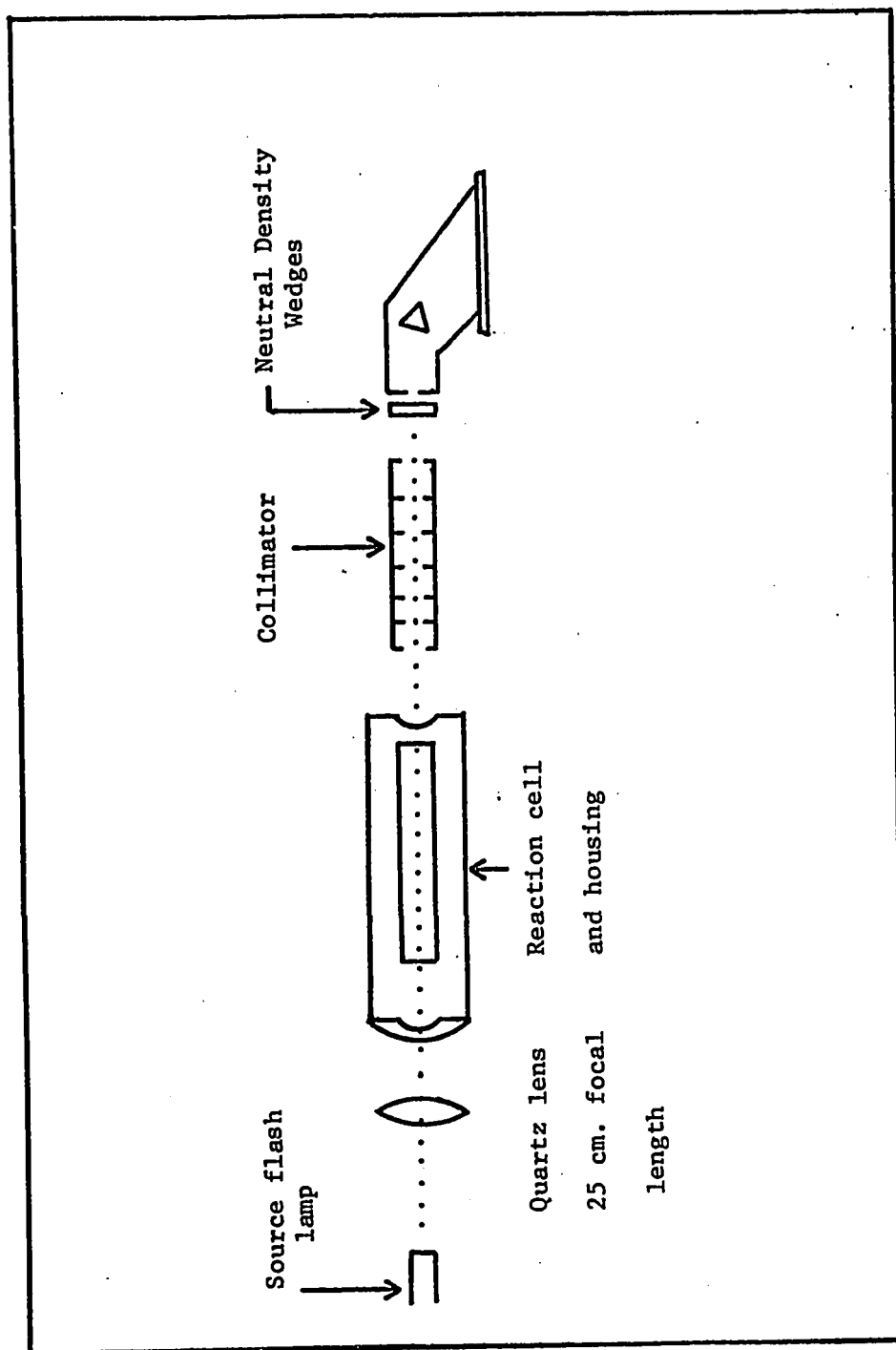
Fig. 9   Optical Bench.

Photocell #1 saw the flash and its output was fed into the delay

unit where it was delayed for the required time. After the delay the

signal passed to the grid of the thyrotron and the "valve" was open.

When the thyrotron began to conduct, the trigger gap electrode

discharged to the spark gap causing some ionization between the

spark gap electrodes. This ionization had the effect of decreasing

the effective resistance between the spark gap electrodes to such an

extent that the source capacitor was now able to discharge across

the spark gap and across the lamp in series with it. Photocell #2

saw the flashes and the output was displayed on the oscilloscope.

MATERIALS

The materials used in this work, their source, grade, and

purification are given in Table I. Hydrogen disulfide was prepared

by the method of Feher[37]. Ethylene episulfide was distilled from

a heated mixture of ethylene carbonate and KCNS[33].

EXPERIMENTAL PROCEDURE

1) Static photolyses

Reactants were measured into the reaction cell with a

mercury manometer and allowed to equilibrate for one hour. The light

source was also given a one hour warm up time. It was found that

after a one hour warm up, the 2537 Å line was completely self

reversed in the medium pressure mercury arc and consequently there

TABLE I

MATERIALS USED

Materials	Source	Grade	Purification
Acetone	Eastman Kodak	Spectro grade	Distilled from chlorobenzene slush (~45)
Acetone – $\underline{d}_6$	Merck, Sharp and Dohme	NMR grade	Distilled from chlorobenzene slush (~45)
Argon	Airco	Analyzed reagent	None
cis – 2 – Butene	Phillips	Research	Degassed
Carbon dioxide	Airco	Analyzed reagent	None
Carbon disulfide	Baker	Reagent	Distilled from chlorobenzene slush (~45)
Carbonyl sulfide	Matheson	H_2S impurity	Passed through sat'd NaOH solution. Distilled from n – pentane slush (~130)
Deuterium	Matheson	C.P. grade	None
Ethylene	Phillips	Research	Degassed

TABLE I

(continued)

Materials	Source	Grade	Purification
Ethylene episulfide	Prepared		Distilled from methanol slush (-98)
Hydrogen	Liquid Air	Tank grade	Passed through heated Ag-Pd thimble (Milton Roy Co.)
Hydrogen disulfide	Prepared		Distilled from chlorobenzene slush (-45)
Hydrogen sulfide	Matheson	C.P. grade (99.5% pure)	Degassed
Krypton	Airco	Analyzed reagent	None
Methane	Phillips	Research grade	Degassed at - 210
Nitrogen	Airco	Analyzed reagent	None
Oxygen	Airco	Analyzed reagent	None
Propane	Phillips	Research grade	Degassed
Propylene	Phillips	Research grade	Degassed

was no need to eliminate mercury from the cell.

After irradiation, the cell contents were frozen in the cold finger and any non - condensables transfered by the Toepler pump into the gas burette. The material in the cell was warmed and refrozen twice to insure complete removal of all trapped non - condensables. The contents of the cell were then transfered to the analytical stage, fractionated and analyzed.

If so desired, individual products could be trapped in the G.L.C. trapping train and transfered to break seals for mass spectral analysis. Mass spectra were obtained on a Metropolitan Vickers MS2 mass spectrometer.

2) Flash photolysis and kinetic spectroscopy

Reactant and product handling was the same as above. The capacitors were charged to the desired voltage, usually 9 Kv for the photo - capacitor, 10 Kv for the source capacitor. 15 micron slits were used throughout this work. A wavelength scale accurate to ± 2 Å was recorded on the plate. Before a time delay sequence was started, the spectrum of the empty cell and of the cell plus the reactants were recorded. Since the photographic plate response to incident light was not linear, each plate had to be calibrated with a set of neutral optical density wedges, O.D. values 0.0, 0.2, 0.4, 0.6, 0.8, 1.0, 1.2. The delay times were so chosen as to show the formation and decay of the intermediates. Two or three short delays of less than 50 μsec were used to show the growth portion and then

TABLE II

Retention Times

Compound	Column[a]	Column temp. C°	Retention time min.
Oxygen	IV	25	2:40
Nitrogen	IV	25	3:30
Carbon monoxide	IV	25	5:20
Hydrogen	IV	25	1:40
Carbon disulfide	II	25	4 : 35
Carbonyl sulfide	III	0	12 : 50
Carbon dioxide	III	0	9 : 00
Hydrogen sulfide	III	0	16 : 00
Sulfur dioxide	II	25	2 : 45
Methyl mercaptan	I	25	3 : 00
Ethyl mercaptan	I	25	4 : 15
Vinyl mercaptan	I	25	5 : 20
Ethylene episulfide	I	25	9 : 50
n - Propyl mercaptan	II	34	25 : 05
iso - Propyl mercaptan	II	34	14 : 05

a)   column I, 7 foot, 10% tricresyl phosphate on chromosorb W, 60 cc/min hydrogen flow.

TABLE   II

(continued)

column II,   10 foot, 20% tricresyl phosphate on

chromosorb W, 60 cc/min hydrogen flow.

column III,   10 foot, medium activity silica gel,

60 cc/min hydrogen flow.

column IV   10 foot, molecular sieve, 60 cc/min

helium flow.

roughly evenly spaced delays were used to show the decay. After the completion of the delay study a spectrum of the cell plus reactants plus products and one of the re-evacuated cell were recorded. Any absorption not appearing in the empty,the before and the after shots was attributed to intermediates.

The photographic plate was developed for four minutes in Kodak D-19 developer and fixed in Kodak Rapid Fixer for five minutes. The plates were washed in running water for half an hour.

Plate densitometry was carried out on either a Jarrel Ash Model 2310 recording microdensitometer or in the latter part of the work on a Joyce, Loebl Model MK III C double beam recording micro-densitometer. The calibration shots were used to obtain plots of densitometer reading against absolute optical density. From the densitometer readings for the intermediates, their absolute optical densities were determined and plotted against time. Optical density could be related to concentration by the equation

$$O.D. = \varepsilon C \ell$$

where ε is the molar decadic extinction coefficient, C is the concentration in moles per liter, and ℓ is the path length in cm.

3) Hydrogen disulfide

Hydrogen disulfide was found to be very unstable, readily decomposing in the presence of moist glass walls, metals, rough glass joints, or basic compounds. Reaction cells and the mercury free vacuum system were preconditioned with HCl by allowing about 200 torr

anhydrous HCl to stand in these parts for about two hours. This conditioning made the walls slightly acidic and prevented decomposition without affecting the reaction. Since sulfur was formed as a product of the photolysis a reaction mixture could only be used once before the remaining substrate would decompose. Therefore, for delay time studies ten identical cells were filled at the same time to insure equal pressures. Each cell was flashed only once. The cells were cleaned after every photolysis with a solution of 5% HF.

Hydrogen disulfide was found to be unstable at pressures above 4 torr at room temperature or above -20 C in the liquid phase. At -45 C the vapor pressure was approximately 1.8 torr and this pressure was used for all studies. The trap containing the hydrogen disulfide was warmed to this temperature and the substrate was allowed to expand into the reaction cells.

CHAPTER III

THE PHOTOCHEMISTRY OF CARBON DISULFIDE

A. RESULTS

    1. Short wavelength photolysis

    2. Long wavelength photolysis

B. DISCUSSION

    1. Short wavelength photolysis

    2. Long wavelength photolysis

RESULTS

1. Short wavelength (λ = 1950 - 2250 Å) photolysis.

Photolysis of carbon disulfide vapor under static conditions gave a brown polymer as the only product. When the photolysis was carried out in the presence of propane, the polymer yield was apparently not affected. In the presence of ethylene, the polymer yield decreased and ethylene episulfide was found as the only volatile product.

When 5 torr carbon disulfide was flash photolyzed in the presence of 50 torr carbon dioxide as diluent gas, the transients detected by kinetic spectroscopy were S_2 ($^1\Delta_g$), S_2 ($^3\Sigma_g^-$), and CS ($^1\Sigma^+$). The singlet and the triplet states of S_2 were observed in their respective ground vibrational states even at the shortest delay time, 20 µsec. CS was observed to be vibrationally excited up to the $v'' = 3$ level.

The series of absorption spectra, Plate 1, show the formation and decay of the intermediates. The spectrum of CS was at maximum intensity at the shortest delay and did not change over the delay range used. The CS (0,0) spectrum was visible for several minutes after the flash. The vibrationally excited states of CS are relaxed to the $v'' = 0$ level. The S_2 ($^1\Delta_g$) spectrum reaches maximum intensity at 27 µsec and decays within 70 µsec. The corresponding times for S_2 ($^3\Sigma_g^-$) are 70 and 500 µsec respectively.

CS_2

$S_2 \ (B^3\Sigma_u^- \leftarrow X^3\Sigma_g^-)$

$(2,0) \ (1,0) \ (0,0) \ (1,1) \ (2,2)$

$CS \ (A^1\Pi \leftarrow X^1\Sigma^+)$

$S_2 \ (b^1\Sigma_g^+ \leftarrow a^1\Delta_g)$

The effect of diluent gas was examined by carrying out the flash photolysis of 5 torr carbon disulfide in the presence of 50 torr argon, 50 torr carbon dioxide and 5 torr nitric oxide + 45 torr argon. The following results were observed:

a) The spectrum of S_2 ($^1\Delta_g$) appeared strongly in the presence of carbon dioxide but only weakly in the presence of argon or nitric oxide.

b) The effect of diluent gas on the formation and decay of S_2 ($^3\Sigma_g^-$) is shown in Figure 10. The rate of S_2 formation was highest in the presence of nitric oxide and slowest in the presence of argon. The rate of decay showed similar dependence on the diluent gas.

c) The vibrationally excited CS was relaxed rapidly by carbon dioxide but only slowly by argon and nitric oxide.

d) In the presence of nitric oxide, a new absorber was detected. The weak spectrum appeared in the region $\lambda = 3500 - 4300$ Å and consisted of twenty unevenly spaced bands. The spectrum reached maximum intensity within 100 μsec and decayed within 400 μsec.

The flash photolysis of 5 torr carbon disulfide in the presence of 100 torr ethylene gave ethylene episulfide as the only stable product. The spectrum of CS was observed by kinetic spectroscopy but the spectra of both the singlet and the triplet S_2 were absent.
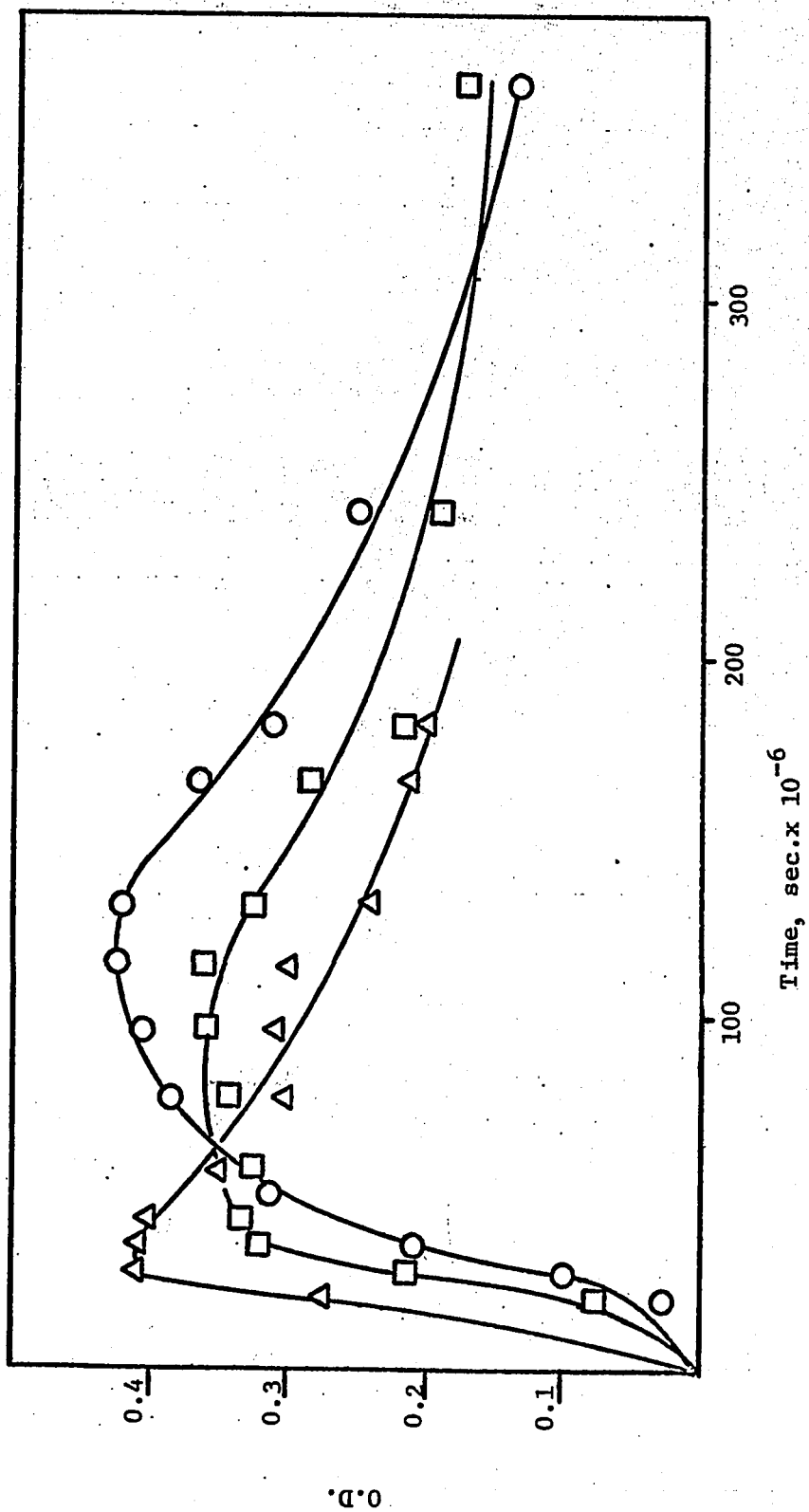
Fifure 10. Plot of O.D. against time for S_2 $(^3\Sigma_g^-)$ as a function of added inert gas.

O + 50 torr Argon;   □ + 50 torr CO_2;   △ + 5 torr NO + 45 torr Argon.

Time, sec.x 10^{-6}

O.D.

2. Long wavelength (λ = 2800 - 3600 Å) photolysis.

The long wavelength photolysis of 20 torr carbon disulfide vapor resulted in a brown polymer as the only product. The addition of 100 torr ethylene or 100 torr propane caused a decrease in the polymer yield but no volatile products could be found. However, when the photolysis of 20 torr carbon disulfide was carried out in the presence of 100 torr oxygen in a Vycor 7910 cell (transmitted λ > 2290 Å), the polymer yield decreased markedly and carbonyl sulfide and sulfur dioxide were formed in the ratio of 1:2. The photolysis of the same mixture in a pyrex cell (transmitted λ > 2900 Å) resulted in the formation of sulfur dioxide only.

In the flash photlysis of 7 torr carbon disulfide in the presence of 400 torr nitrogen as diluent gas, the transients detected by kinetic spectroscopy were S_2 ($^3\Sigma_g^-$) and CS ($^1\Sigma^+$) in the v'' = 0 and 1 vibrational levels. The S_2 spectrum reached maximum intensity within 35 μsec and lasted for about 500 μsec. The CS (0,0) band lasted for several minutes but the (1,1) band decayed within 100 μsec.

The spectra of CS and S_2 were detected in the flash photolysis of 20 torr carbon disulfide in the presence of 80 torr ethylene but the S_2 spectrum was weaker than in the presence of nitrogen. Ethylene episulfide was not found. From the flash photolysis of 3 torr COS + 30 torr CS_2 + 90 torr butene-2 + 280 torr N_2, CS and S_2 were observed and butene-2 episulfide was isolated.

However, when carbonyl sulfide was omitted from the above mixture, no episulfide was formed but S_2 and CS were still observed. Again the S_2 spectrum was weak.

The flash photolysis of 22 torr CS_2 in the presence of 90 torr oxygen and 280 torr nitrogen as diluent gas resulted in the complete suppression of the S_2 spectrum while the CS spectrum was not much affected. Sulfur dioxide was the only volatile product and its spectrum only appeared at delay times greater than 1 msec. The spectra of SO or S_2O were not observed. In the absence of diluent gas, the $CS_2 - O_2$ mixture exploded yielding carbon dioxide and sulfur dioxide in stoichiometric proportions.

Luminescence measurements.

Figures 11 and 12 show reciprocal Stern-Volmer plots for the intensity of luminescence, I, vs. pressure of carbon disulfide and oxygen respectively. The exciting wavelength was 3000 Å. The luminescence intensities were approximately corrected for absorption by dividing the measured intensity by the total percentage of light absorbed.
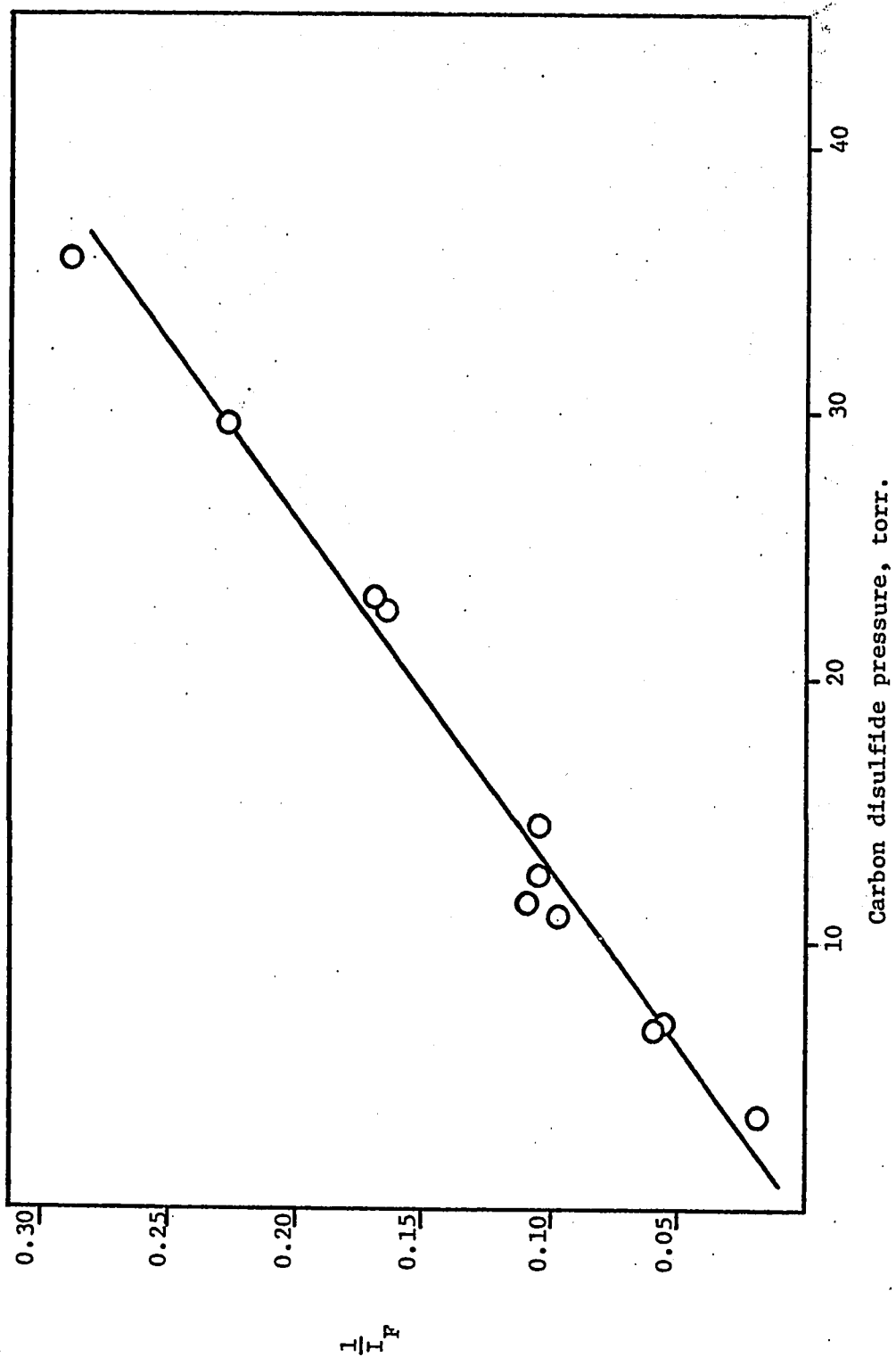
Figure 11. Reciprocal Stern – Volmer plot for the luminescence intensities vs. carbon disulfide pressure.

Oxygen pressure, torr.
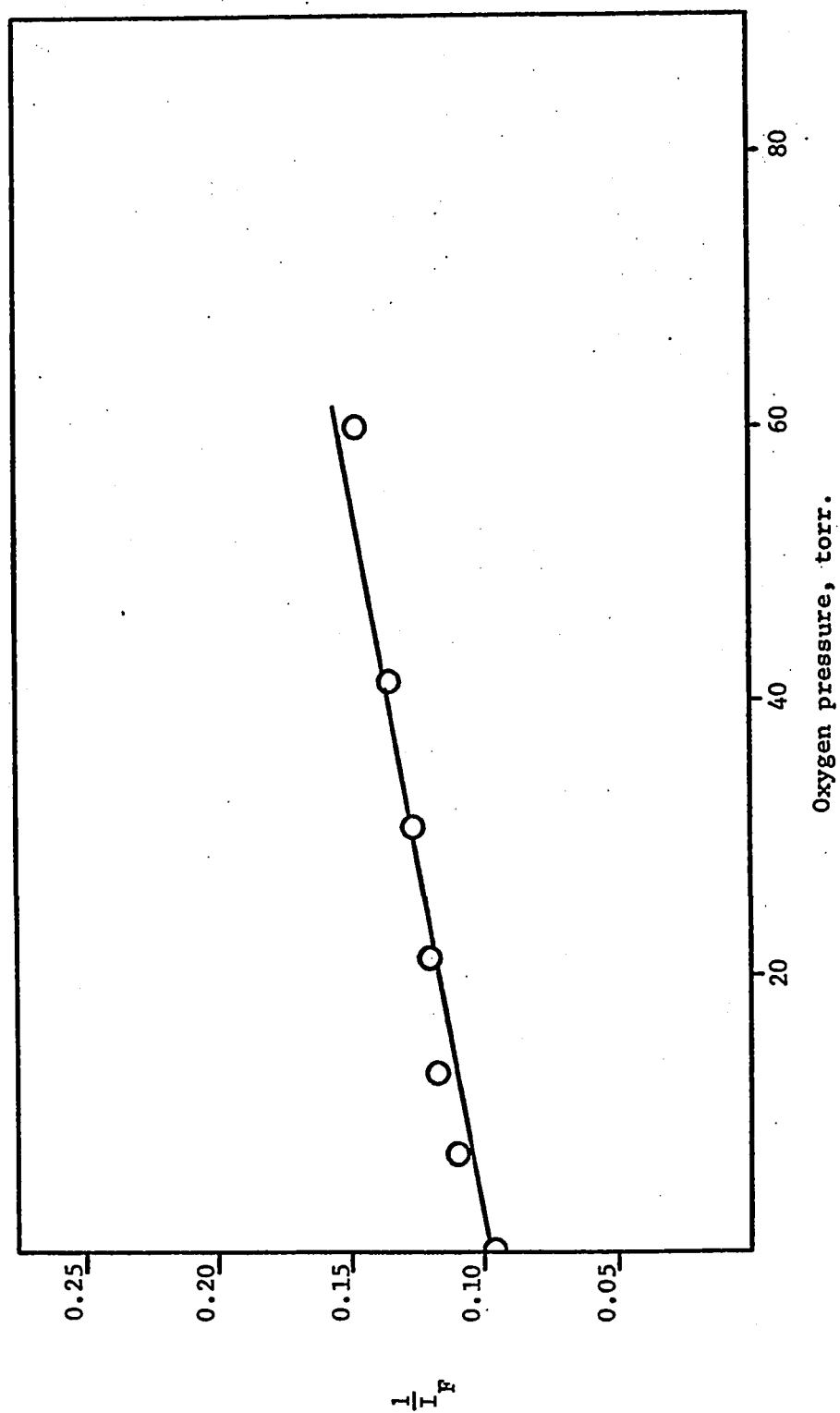
Figure 12.   Reciprocal Stern – Volmer plot for the luminescence intensities vs.

added oxygen pressure.   (Pressure of CS_2 = 10 torr)

DISCUSSION

1. Short wavelength photolysis.

The rapid appearance of the CS spectrum in the flash photolysis of carbon disulfide indicates that the decomposition produces CS and S. This view is further demonstrated by the fact that ethylene episulfide is formed in the flash photolysis of $CS_2 - C_2H_4$ mixtures. Gunning and Strausz[23] showed that S (^3P) atoms add to olefins to produce an episulfide but do not react with paraffins. S (^1D) atoms also add to olefins but the products are an episulfide and a vinylic mercaptan. S (^1D) atoms also insert into paraffinic C - H bonds to produce a mercaptan. Since only ethylene episulfide was formed and no reaction was observed with propane, the sulfur atoms formed in reaction {1} are in the ^3P state.

$$CS_2 \quad + \quad h\nu \quad \rightarrow \quad CS \; (^1\Sigma^+) \quad + \quad S \; (^3P) \qquad \qquad \{1\}$$

This observation is in agreement with the results of Callear[8]. From the short wavelength photolysis of carbon disulfide, he detected S (^3P) atoms by kinetic spectroscopy. S (^1D) atoms were not observed.

For reaction {1} to follow spin conservation rules, the excited CS_2 molecule which dissociates must be in a triplet state. However, the short wavelength absorption region has been shown to correspond to a transition from the $^1\Sigma_g^+$ ground state to the $^1B_2$

excited state. The excited molecule could cross to the nearby $^3B_2$ state[11] and decompose.

At short delays the CS vibrational levels are populated up to the $v''=3$ level indicating that the CS is produced vibrationally excited in reaction {1}. Since $D(SC = S)$ is 110 Kcal/mole[9] and the exciting wavelength has an average energy of about 140 Kcal/mole, the excess energy is capable of populating the $v''=7$ level. However, the mechanism of excitation is uncertain. Vibrationally excited CS is relaxed through collisions with the diluent gas.

$$CS^* + M \rightarrow CS_{v'' = 0} + M^* \qquad \{2\}$$
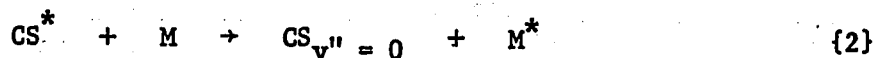
The long lifetime of the ground state CS, 4 minutes in a 2 cm diameter cell and 20 minutes in a 5 cm diameter cell, indicates that the fate of CS is diffusion to the walls and subsequent polymerization. The polymer may return carbon disulfide to the vapor phase.

The appearance of the S_2 ($^1\Delta_g$) and the S_2 ($^3\Sigma_g^-$) spectra indicates that the fate of the sulfur atoms is recombination via

$$2 S (^3P) + M \rightarrow M^* + S_2 (^3\Sigma_g^-) \qquad \{3\}$$

$$\rightarrow M^* + S_2 (^1\Delta_g) \qquad \{4\}$$
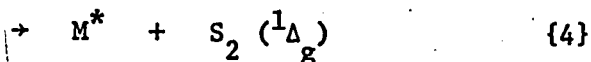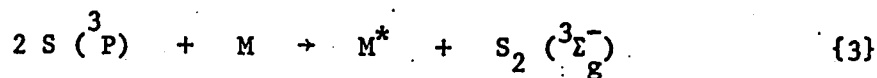
S_2 ($^1\Delta_g$) is relaxed to the ground state by collisions with the diluent gas, (vide infra).

$$S_2 \ (^1\Delta_g) \ + \ M \ \rightarrow \ S_2 \ (^3\Sigma_g^-) \ + \ M^* \tag{5}$$
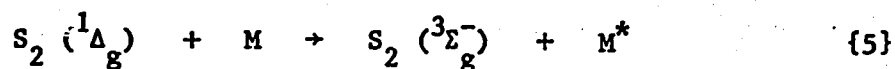
$S_2 \ (^3\Sigma_g^-)$ decays by a pressure dependent, second order process,

$$2 \ S_2 \ (^3\Sigma_g^-) \ + \ M \ \rightarrow \ S_4 \ + \ M^* \tag{6}$$
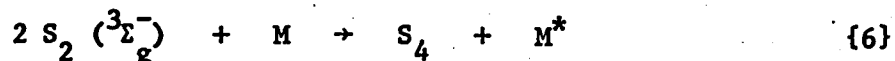
(vide infra).

Basco and Pearson[9] have recently proposed that the recombination of sulfur atoms proceeds by complex formation with carbon disulfide, namely,

$$S \ + \ CS_2 \ \rightleftarrows \ CS_3 \tag{7}$$

$$CS_3 \ + \ S \ \rightarrow \ CS_2 \ + \ S_2 \tag{8}$$
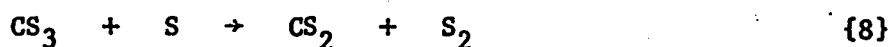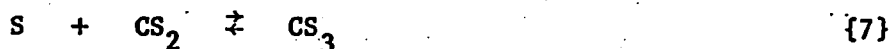
The results of this investigation are consistent with such a mechanism. Figure 1 shows the formation and decay of $S_2 \ (^3\Sigma_g^-)$ as a function of different diluent gases, namely, argon, carbon dioxide, and nitric oxide. Argon is expected to be much less efficient a third body than carbon dioxide or nitric oxide. The fact that the rate of formation of S_2 is very nearly equal for argon and for carbon dioxide suggests that it is not the diluent gas but rather the carbon disulfide that is responsible for the recombination rate. Thus the above mentioned scheme seems reasonable. The presence of a small amount of nitric oxide causes a sharp increase in the recombination rate as shown in Figure 10. This increase is best attributed to a complex formation with nitric oxide,

$$S \ (^3P) \ + \ NO \ \rightleftharpoons \ SNO \qquad \{9\}$$

$$SNO \ + \ S \ (^3P) \ \rightarrow \ NO \ + \ S_2 \qquad \{10\}$$
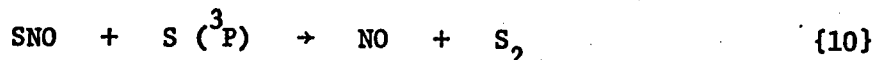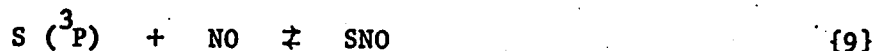
Since S_2 $(^1\Delta_g)$ was detected in the recombination of S (^3P) atoms, the above mechanism must be altered to account for this fact. In the reactions $\{8\}$ and $\{10\}$, S_2 not only represents the $^3\Sigma_g^-$ state as implied by Basco and Pearson, but rather all states that could result from the recombination. By comparison with the O_2 molecule, S_2 has three low lying states, the ground $^3\Sigma_g^-$, and the $^1\Delta_g$ and $^1\Sigma_g^+$ metastable states[45]. All three states correlate with two S (^3P) atoms. Therefore, the recombination of two ground state S atoms should produce these states in the statistical ratios of 3:2:1 respectively. Although the $^1\Sigma_g^+$ state has not been detected, probably due to instrumental limitations, the presence of the $^1\Delta_g$ state does show that ground state atoms can recombine to higher electronic states. From this observation, it follows that reactions $\{8\}$ and $\{10\}$ do not correctly represent the formation of S_2 $(^3\Sigma_g^-)$. The collisional relaxation of the excited states to the ground state must also be considered.

The spectrum observed in the 3500 - 4300 Å region in the presence of nitric oxide was at first attributed to SNO molecule but subsequent work, (vide infra), showed that the spectrum is more plausibly attributed to the species S_3. The formation of S_3 is best described by the mechanism

$$NO \quad + \quad S\ (^3P) \quad \overset{\rightarrow}{\leftarrow} \quad SNO \qquad\qquad \{11\}$$

$$SNO \quad + \quad S_2\ (^3\Sigma_g^-) \quad \rightarrow \quad NO \quad + \quad S_3 \qquad\qquad \{12\}$$
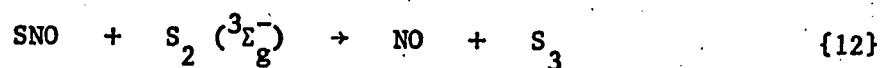
S_3 decays to sulfur polymer. The presence of S_3 causes a further complication in the kinetics of S_2 formation and decay. However, since the amount of S_3 formed could not be determined, its importance could not be established.

Long Wavelength Photolysis

The only products observed when carbon disulfide was photolyzed alone or in the presence of ethylene or propane was a brown polymer. Since there was no product formed with ethylene or propane, the polymerization does not involve S atoms. The flash photolysis of carbon disulfide also produces polymer but again there is no reaction with ethylene or propane. However, CS and S_2 $(^3\Sigma_g^-)$ were observed by kinetic spectroscopy. The transients must have been formed by some means other than S atoms. A reasonable mechanism is

$$CS_2 \quad + \quad h\nu \quad \rightarrow \quad CS_2^* \qquad\qquad \{13\}$$

$$CS_2^* \quad + \quad CS_2 \quad \rightarrow \quad 2\ CS\ (^1\Sigma_g^+) \quad + \quad S_2\ (^3\Sigma_g^-) \qquad \{14\}$$
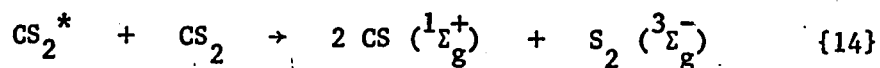
This scheme is consistent with the simultaneous formation of CS and S_2. Further support for this mechanism is given by the observation that the presence of an olefin causes a decrease in the amount of

S_2 formed without the formation of a stable product. Higher pressures of carbon dioxide, a good deactivator, had a similar effect. Thus,

$$CS_2^* + M \rightarrow CS_2 + M^* \qquad \{15\}$$

The absence of the S_2 $(^1\Delta_g)$ state is a further indication that S_2 is not formed by S atom recombination. The absence of the singlet state also gives an insight into the electronic state of the CS_2^* involved in the reaction. It has been suggested that the absorption in the long wavelength region corresponds to a transition from the ground $^1\Sigma_g^+$ state to the B_2 component of the $^3A_2$ state[35,36]. Thus, in reaction $\{14\}$, the formation of S_2 in a singlet state would violate spin conservation rules. This finding also supports the mechanism proposed for S_2 formation.

In the flash photolysis of $CS_2 - O_2$ mixtures, the S_2 spectrum is completely suppressed while the CS spectrum remains essentially unaltered. Sulfur dioxide is the only volatile product and its spectrum only appears at delay times greater than 1 msec suggesting its formation via the superoxide (SOO)[34]. A mechanism consistent with these results is

$$CS_2^* + O_2 \rightarrow CS + SOO \qquad \{16\}$$

$$SOO + M \rightarrow SO_2 + M^* \qquad \{17\}$$
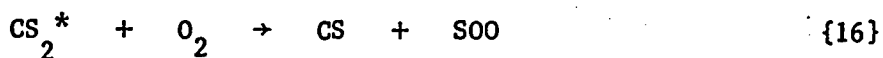
The fact that carbonyl sulfide is formed in static photolysis but not under flash conditions and that the CS spectrum is decreased by a

factor less than two upon the addition of oxygen can be best explained

by the assumption that ground state CS does not react with oxygen

but that electronically excited CS formed by secondary light absorption

does.

$$CS \ (^1\Sigma^+) \ + \ h\nu \ \rightarrow \ CS \ (^1\Pi) \qquad\qquad \{18\}$$

$$CS \ (^1\Pi) \ + \ O_2 \ \rightarrow \ OCS \ + \ O \ (^3P) \qquad\qquad \{19\}$$
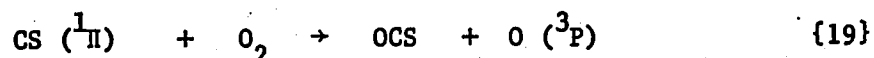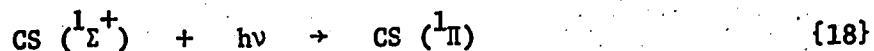
This mechanism is further supported by the fact that carbonyl

sulfide is not formed when the static photolysis is carried out in

a pyrex vessel (transmitted $\lambda > 2900$ Å) (CS does not absorb in the

ultra violet above 2589.6 Å).

Heicklen has observed luminescence from carbon disulfide

vapor illuminated in the long wavelength absorption region[12].

He found that the vibrational energy of the excited state was not

dissipated by collision before emission and the lifetime of the

excited state was estimated to be 3.3×10^{-6} sec. Thus another

relaxation process must be included, namely,

$$CS_2^* \ \rightarrow \ CS_2 \ + \ h\nu \qquad\qquad \{20\}$$

Assuming that only reactions {14} and {16} are quenching processes

in the presence of carbon disulfide and oxygen respectively, the

relative rate constant $k_{14} \ / \ k_{16}$ could be determined by the

measurement of the luminescence intensities. The intensity of

luminescence, I_F, is given by the expression

$$I_F^{-1} = 1 + \frac{k_{14}}{k_{20}} (CS_2)$$

In the presence of oxygen, this expression becomes

$$I_f^{-1} = 1 + \frac{k_{14}(CS_2) + k_{16}(O_2)}{k_{20}}$$

Figures 11 and 12 show reciprocal Stern-Volmer plots for the intensity of luminescence vs. pressure of carbon disulfide and oxygen respectively. The slopes can be equated to k_{14}/k_{20} and k_{16}/k_{20} but since I_F is only proportional to the absolute luminescence intensity, only the ratio of the two slopes has any significance. The ratio of the two slopes and thus k_{14}/k_{16} = 7.6. Therefore, CS_2 is about eight times as effective at relaxing CS_2^* as is oxygen.

In the flash photolysis of CS_2 - O_2 mixtures, it was found that a 4.5 fold excess of oxygen was sufficient to suppress S_2 formation below the limit of detection. However, reaction {16} could only account for about a 50% decrease. Two possible explanations can be offered. First, that S_2 undergoes rapid reaction with oxygen. This can be discounted since Wright[7] found that S_2 did not react with oxygen. The second possibility is that there are more than one kind of CS_2^* involved. The long wavelength absorption region of carbon disulfide has been shown to be made up of transitions to several electronic states[10]. Thus, some of the higher lying states will react via {14} while the lower energy states will react via

$$CS_2^* \; + \; CS_2 \; \rightarrow \; 2 \; CS_2 \qquad\qquad \{21\}$$

Reaction {21} has also been suggested by Heicklen[7] as the luminescence quenching step. Oxygen on the other hand reacts with any of the excited states of CS_2. This high reactivity is consistent with the high combustibility of carbon disulfide.

CHAPTER IV

THE FLASH PHOTOLYSIS OF CARBONYL SULFIDE

RESULTS

DISCUSSION

RESULTS

The transients observed in the flash photolysis of 17 torr COS were S_2 ($^1\Delta_g$) and S_2 ($^3\Sigma_g^-$). The stable products of the reaction were carbon monoxide and sulfur. The series of absorption spectra in Plate 2 show the formation and decay of the transients. S_2 ($^1\Delta_g$) reached maximum concentration within 240 μsec and decayed within 550 μsec. The corresponding times for S_2 ($^3\Sigma_g^-$) were 300 μsec and 3 msec respectively.

The effect of carbonyl sulfide pressure was examined using 7, 17, 31, 65, 192, and 410 torr pressures. Increasing carbonyl sulfide pressure had the following effects:

a) The rate of formation and the rate of decay of S_2 ($^3\Sigma_g^-$) increased as shown in Figure 13.

b) The S_2 ($^1\Delta_g$) spectrum could only be observed at COS pressures of 65 torr or less. At higher COS pressures, the COS continuum caused total absorption in the S_2 ($^1\Delta_g$) region. Table III shows the effect of increasing COS pressure on the rate of formation and the rate of decay of S_2 ($^1\Delta_g$).

c) At 410 torr COS a new transient spectrum appeared in the region of 3500 - 4300 Å. The spectrum consisted of twenty unevenly spaced, diffuse bands degraded to the red. The absorber reached maximum intensity within 100 μsec and decayed within 500 μsec.

$S_2 (B^3\Sigma_u^- \to X^3\Sigma_g^-)$

$S_2 (b^1\Delta_u \to a^1\Delta_g)$
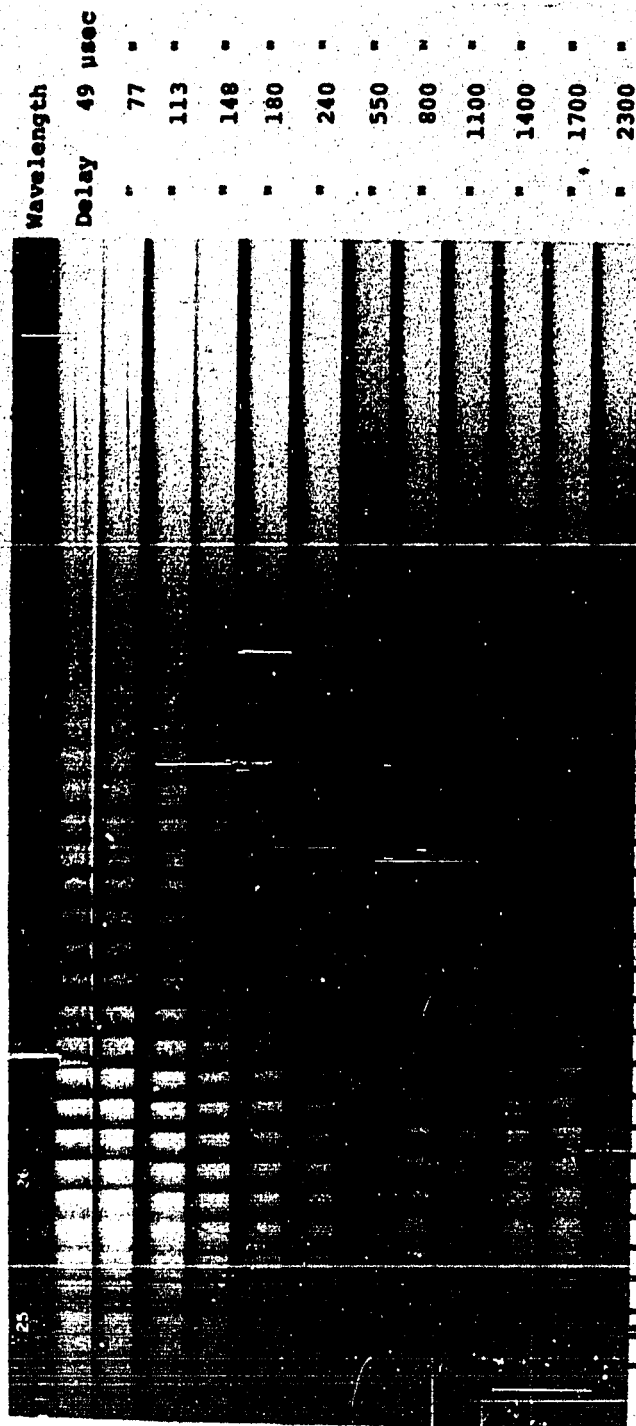
Plate 2. Spectra against time in the flash photolysis of 17 torr COS.

Plate ... Spectra against time in the flash photolysis of 17 torr COS.

S_2 ($B^3\Sigma_u^- \to {}^3\Sigma_g^-$)

S_2 ($b^1\Sigma_u^+ \to {}^1\Delta_g$)
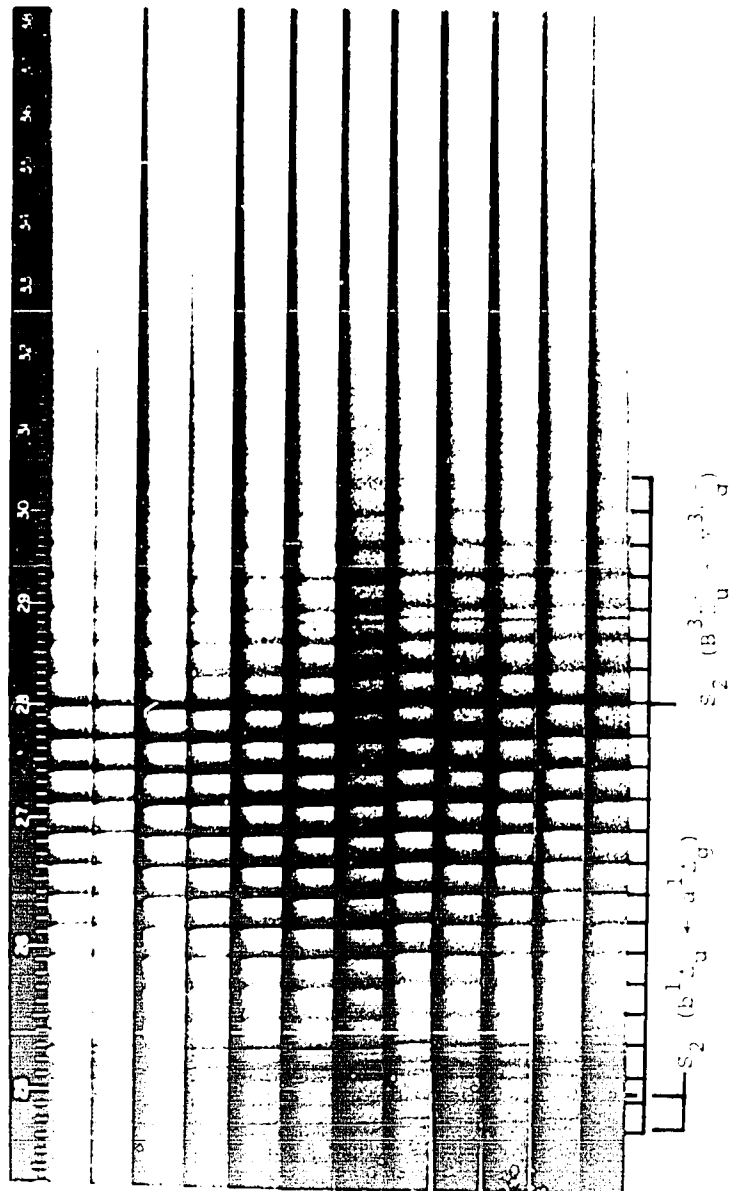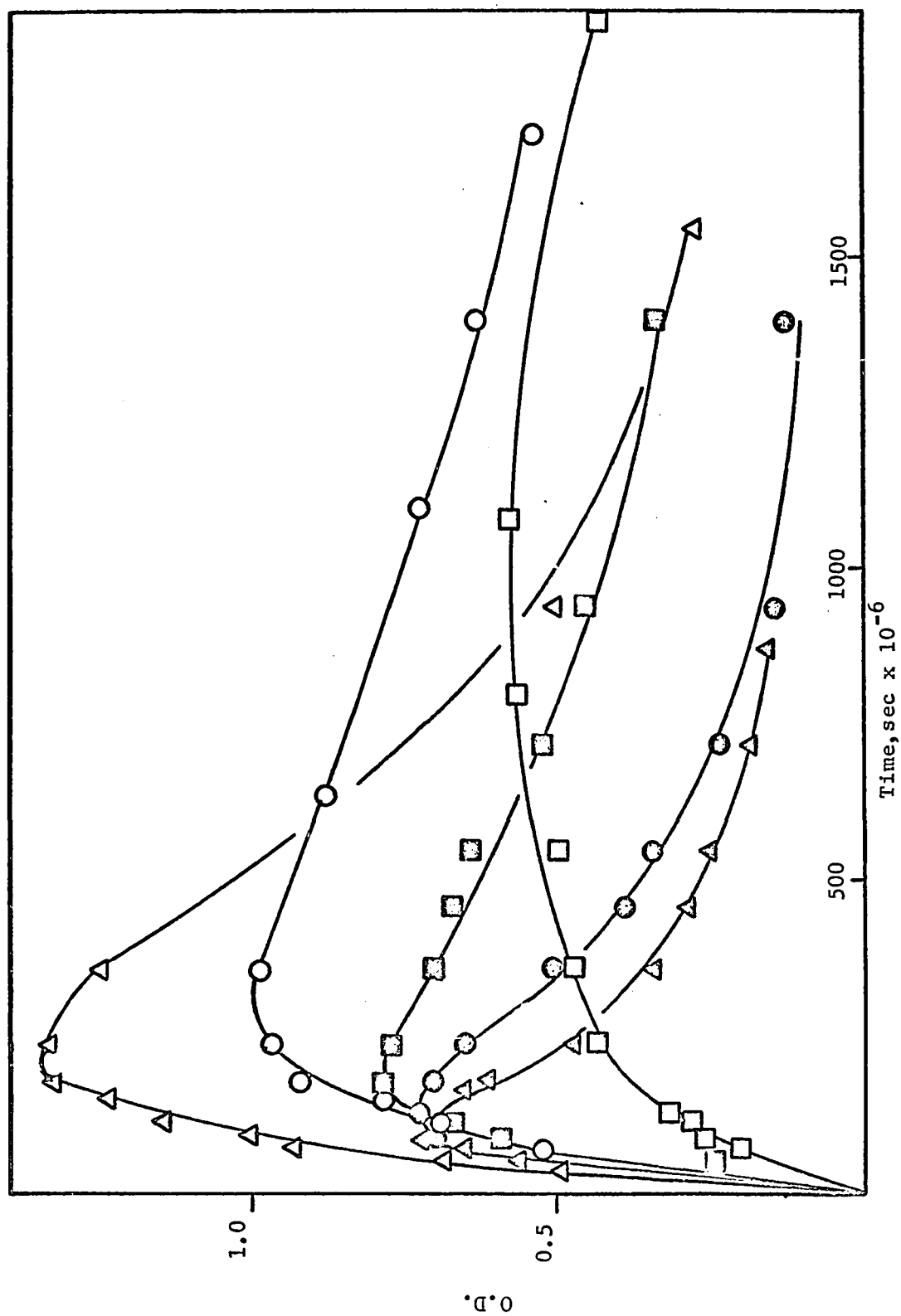
Figure 13. Plot of O.D. against time for S_2 ($^3\Sigma_g^-$) as a function of COS pressure: □ 7 torr

○ 17 torr; △ 31 torr; ▣ 65 torr; ◉ 192 torr; ◭ 410 torr.

TABLE III

THE TIME REQUIRED FOR S_2 $(^1\Delta_g)$ TO REACH MAXIMUM CONCENTRATION AND TO DECAY AS A

FUNCTION OF CARBONYL SULFIDE AND CARBON DIOXIDE PRESSURE

REACTANT	MAXIMUM INTENSITY	DECAY COMPLETE
	time in sec.	time in sec.
17 torr COS	240	500
31 torr COS	113	240
65 torr COS	56	180
17 torr COS + 600 torr CO_2	130	180
31 torr COS + 850 torr CO_2	95	150

The flash photolysis of 7 torr COS in the presence of 400 torr ethylene gave ethylene episulfide, vinyl mercaptan, and carbon monoxide as stable products. No transients were detected. The CO yield was 1.27 μmole/flash. When the photolysis of 7 torr COS was carried out under the same conditions but without the added ethylene, the CO yield was 2.51 μmole/flash. The CO yields from the flash photolysis of 50 torr COS and from 50 torr COS + 500 torr ethylene were 1.01 and 0.53 μmole/flash respectively.

The flash photolysis of carbonyl sulfide was also investigated in the presence of a large excess of carbon dioxide. Two mixtures, 17 torr COS + 600 torr CO_2 and 31 torr COS + 850 torr CO_2 were examined. The transients observed were S_2 $(^1\Delta_g)$, S_2 $(^3\Sigma_g^-)$, and the 3500 - 4300 Å band system. The growth and decay of the triplet S_2 are shown in Figure 14. The S_2 $(^1\Delta_g)$ could not be densitometered due to background absorption by COS but an estimate of the time required to reach maximum intensity and to decay below the limit of detectibility are given in Table III. The yields of CO were 1.61 and 2.25 μmole/flash for the above mixtures respectively. The CO yields for 17 torr and 31 torr COS without the added CO_2 were 3.25 and 4.56 μmole/flash respectively.

The transient spectrum in the λ = 3500 - 4300 Å region was examined under high resolution. The following COS and added
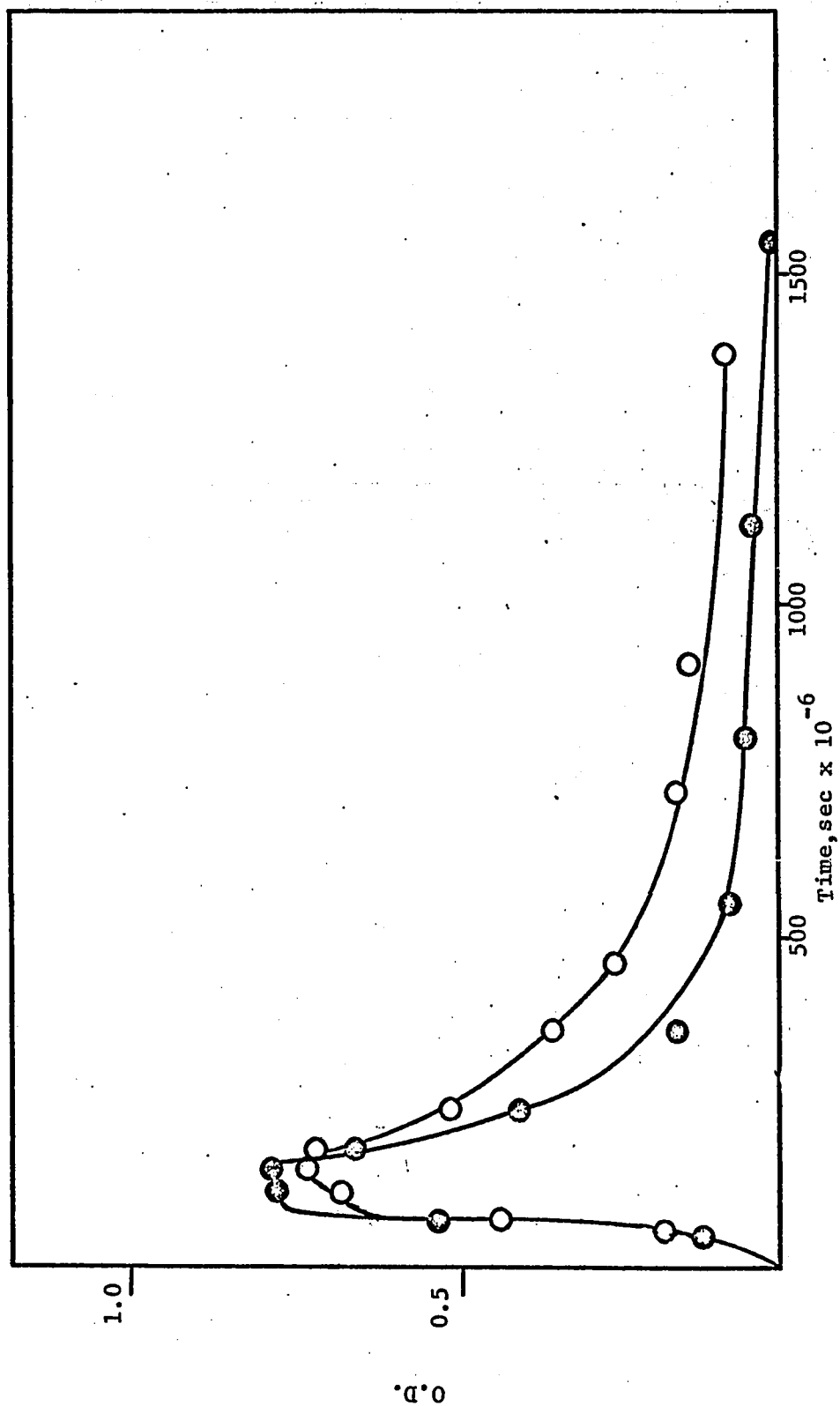
Figure 14. Plot of O.D. against time for S_2 $(^3\Sigma_g^-)$ in the flash photolysis of: ○ 17 torr COS + 600 torr CO_2; ◉ 31 torr COS + 850 torr CO_2.

gas mixtures were used to generate the carrier of the spectrum:
a) 50 torr COS + 70 torr NO; b) 30 torr COS + 390 torr CO_2; c) 400
torr COS. The spectra, taken at 80 μsec delay, are shown in Plate
3. Under high resolution, some of the bands show rotational fine
structure. Some bands which under low resolution appeared as a
single band resolve into two or three separate band heads.

DISCUSSION

The simplest mechanism that will account for the observed
products and for the transients is:

$$COS + h\nu \rightarrow CO + S(^1D) \qquad \{1\}$$

$$COS + S(^1D) \rightarrow CO + S_2(^1\Delta_g) \qquad \{2\}$$

$$S_2(^1\Delta_g) + M \rightarrow S_2(^3\Sigma_g^-) + M^* \qquad \{3\}$$

$$2 S_2(^3\Sigma_g^-) + M \rightarrow S_4 + M^* \qquad \{4\}$$
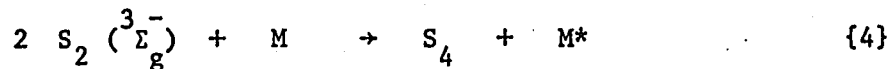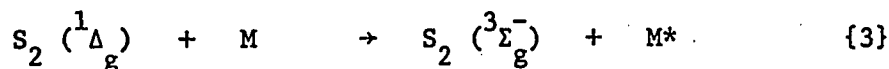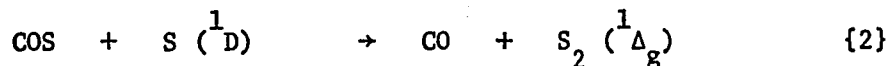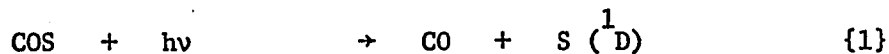
Reaction {1} has been demonstrated by trapping the sulfur atoms
with hydrocarbons[23] and reaction {2} has been proposed to account
for the the quantum yield of CO being 1.8[13]. The importance of
reaction {2} in this study is demonstrated by the fact that the
addition of a large excess of ethylene to carbonyl sulfide reduces
the CO yield exactly to one half owing to the scavenging reactions:
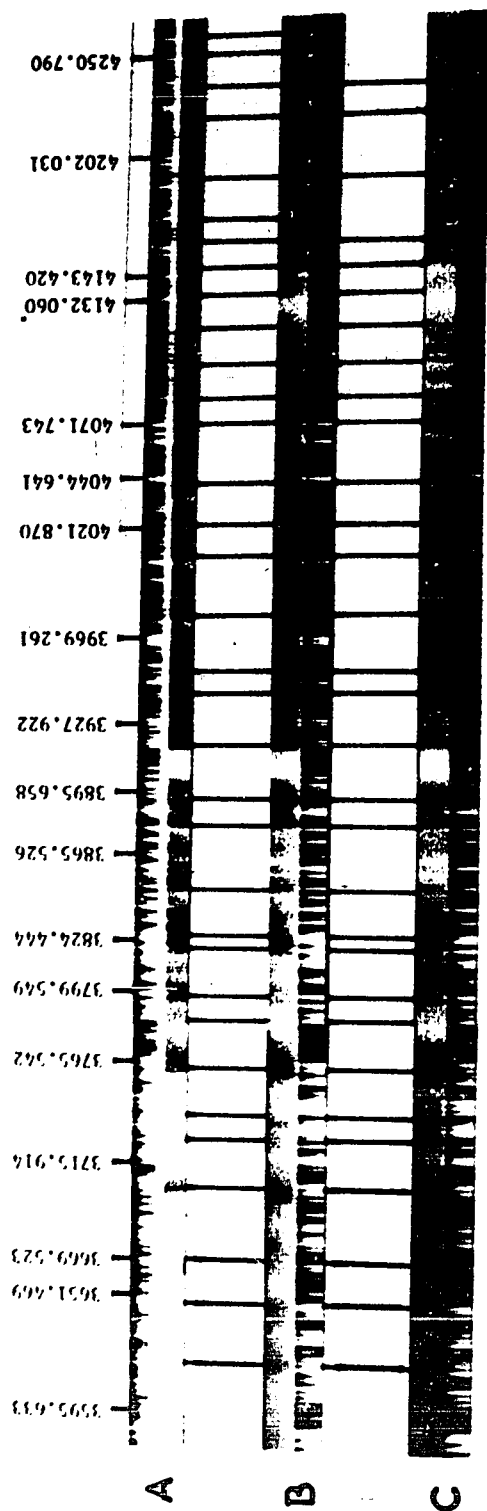
Plate 3. Spectrum of S_3 from the flash photolysis of COS + added gases.

A. 50 torr COS + 70 torr NO; B. 30 torr COS + 400 torr CO_2;

C. 400 torr COS; (Fe arc calibration on each spectrum).

A

B

C

4250.790
4201.031
4143.420
4132.060
4071.743
4040.641
4021.870
3969.261
3927.922
3895.656
3865.526
3825.666
3799.695
3745.
3741.795
3030.
3030.

Plate 3. Spectrum of S_3 from the flash photolysis of COS + added gases.

A. 30 torr COS + 70 torr NO; B. 30 torr COS + 400 torr CO_2;

C. 100 torr COS: (Fe arc calibration on each spectrum).

$$S \; (^1D) \quad + \quad C_2H_4 \quad \rightarrow \quad C_2H_4S \qquad \qquad \{5\}$$

$$\rightarrow \quad CH_2CHSH \qquad \qquad \{6\}$$
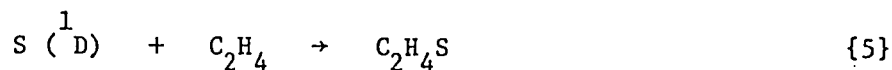
The decrease of the CO yield to exactly one half shows that the fate of the singlet sulfur atoms produced in reaction {1} in the absence of an olefin is abstraction via reaction {2}. This fact precludes the recombination of sulfur atoms.

For spin conservation rules to be obeyed, the S_2 formed in reaction {2} must be in a singlet state. Two low lying singlet states of S_2 are the $^1\Delta_g$ and the $^1\Sigma_g^+$ states, 13 and 24 Kcal/mole above ground state respectively[38]. Since the exothermicity of reaction {2} for the formation of ground state S_2 is 55 Kcal/mole, the formation of both singlet states is energetically possible. $S_2 \; (^1\Delta_g)$ has been observed, Plate 2, but the $^1\Sigma_g^+$ has not been detected. This does not preclude its formation since its absorption spectrum may lie in a region of the spectrum inaccessible with the equipment used.

The abstraction reaction {2} has been stated to be a fast process, proceeding about twice the rate of $S \; (^1D)$ atom insertion into paraffinic C-H bonds which is an indiscriminate process and hence of high efficiency[22]. This point is further demonstrated by the results to be discussed in Chapter VII. In the flash photolysis of $COS - CH_4$ mixtures the transient HS is observed in absorption. Its formation will be shown to be due to the reactions:

$$S \: (^1D) \quad + \quad CH_4 \quad \rightarrow \quad CH_3SH^*$$

$$CH_3SH^* \qquad \rightarrow \quad CH_3 \quad + \quad HS$$
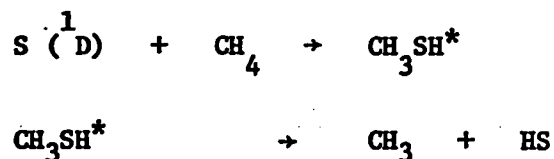
It was observed that the HS appeared at maximum concentration at the shortest delay, further indicating that the insertion reaction is indeed very rapid. Since the insertion reaction is fast, and the rate of reaction {2} proceeds at about twice the rate of insertion, from gas collision frequencies, a rate constant of the order of 10^{11} $M^{-1}sec^{-1}$ would not be unreasonable. However, from Table III, the formation of S_2 $(^1\Delta_g)$ is much slower, corresponding to a rate constant of about 10^7 or 10^8 $M^{-1}sec^{-1}$. Thus there appears to be a slow process between the first interaction of S (^1D) with COS and the formation of S_2 $(^1\Delta_g)$.

This slow process becomes further apparent when the formation and decay of the singlet and the triplet S_2 are examined. The maximum of the triplet curve appears at about 70 to 100 μsec after the singlet S_2 has reached maximum intensity and not after it has decayed, as is the case in other systems (vide infra). This observation indicates that the singlet is formed by a slow process and decays by a fast process. That the S_2 $(^1\Delta_g)$ never attains a high O.D., concentration, is indicative of just such a sequence. This slow step will be discussed later.

The fate of S_2 $(^1\Delta_g)$ is collisional relaxation to the ground $^3\Sigma_g^-$ state by the diluent gas. Radiative relaxation can be

neglected since the transition

$$S_2\ (^1\Delta_g) \rightarrow S_2\ (^3\Sigma_g^-) + h\nu$$
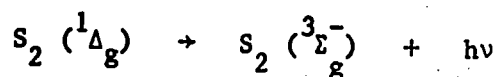
is strongly forbidden. For oxygen, the corresponding transition has a half life of one hour[39]. Diffusion to the walls can be neglected since such a process would be too slow to account for the rapid decay of $S_2\ (^1\Delta_g)$.

Figure 15 shows the plot of O.D.$^{-1}$ against time for $S_2\ (^3\Sigma_g^-)$. Since the data points define straight lines, the decay of S_2 is a second order process with respect to $S_2\ (^3\Sigma_g^-)$. That the slopes increase with increasing pressure indicates that a third body is required for the recombination. The second and third order rate constants for reaction {4} can be calculated from the slopes in Figure 15 using the equation

$$k_4 = S \times \epsilon \times \ell$$

where S is the slope, ϵ is the molar decadic extinction coefficient, and ℓ is the path length in cm. The values of k_4 are listed in Table IV. Since the third order rate constants show good agreement, the decay of $S_2\ (^3\Sigma_g^-)$ is well described by reaction {4}.

The results of the flash photolysis of carbonyl sulfide in the presence of a large excess of carbon dioxide can be best explained by the mechanism:
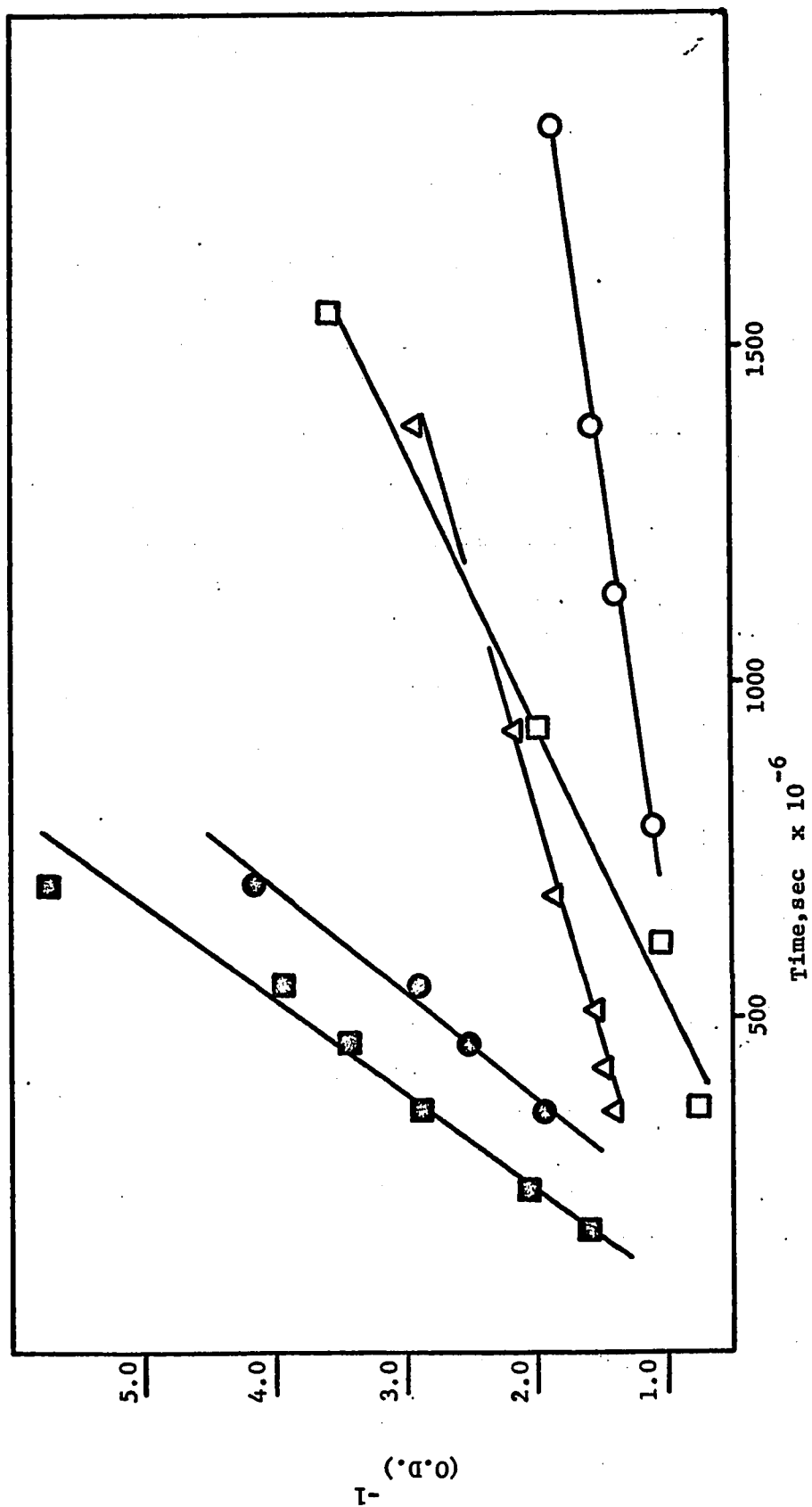
Figure 15. Second order decay plots for S_2 ($^3\Sigma_g^-$) from the flash photolysis of: ◯ 17 torr; △ 31 torr; ☐ 65 torr; ⬤ 192 torr; and ▣ 410 torr COS.

TABLE IV

SECOND AND THIRD ORDER RATE CONSTANTS FOR THE RECOMBINATION OF

$S_2({}^3\Sigma_g^-)$ AT VARIOUS PRESSURES OF COS AND CO_2

P_{COS} torr	P_{CO_2} torr	Slope x 10^{-3} O.D. sec^{-1}	k_4 x 10^{-9} M^{-1} sec^{-1}	k_4 x 10^{-11} M^{-2} sec^{-1}
17	--	0.64 ± 0.11	0.45 ± 0.15	4.92 ± 1.63
31	--	1.51 ± 0.20	1.07 ± 0.32	6.40 ± 1.92
65	--	2.22 ± 0.72	1.56 ± 0.76	4.46 ± 2.19
192	--	5.90 ± 1.44	4.16 ± 1.71	4.04 ± 1.66
410	--	7.10 ± 0.65	5.00 ± 1.30	2.27 ± 0.60
17	600	8.90 ± 1.20	6.27 ± 1.88	1.89 ± 0.57
31	850	26.10 ± 5.60	18.40 ± 6.99	3.88 ± 1.47

$$COS \ + \ h\nu \qquad \rightarrow \quad CO \ + \ S \ (^1D) \qquad \qquad \{1\}$$

$$S \ (^1D) \ + \ CO_2 \qquad \rightarrow \quad S \ (^3P) \ + \ CO_2^* \qquad \qquad \{7\}$$

$$2 \ S \ (^3P) \ + \ M \qquad \rightarrow \quad S_2 \ + \ M^* \qquad \qquad \{8\}$$

$$S_2 \ (^1\Delta_g) \ + \ M \qquad \rightarrow \quad S_2 \ (^3\Sigma_g^-) \ + \ M^* \qquad \qquad \{3\}$$

$$2 \ S_2 \ (^3\Sigma_g^-) \ + \ M \ \rightarrow \ S_4 \ + \ M^* \qquad \qquad \{4\}$$
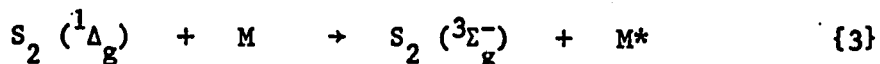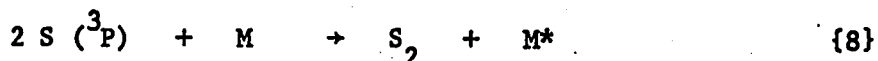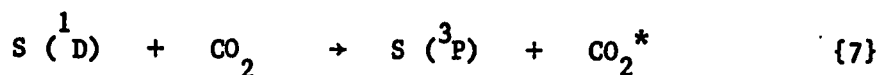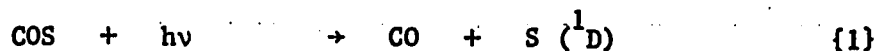
The relaxation of S (^1D) to the ground state by CO_2 has been demonstrated in several studies[21,23]. The fate of the S (^3P) atoms has been shown to be an abstraction reaction when the photolysis was carried out at low light intensities,

$$S \ (^3P) \ + \ COS \ \rightarrow \ CO \ + \ S_2 \qquad \qquad \{9\}$$
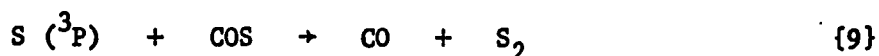
since the quantum yield of CO was found to be 1.8, and the CO yield was reduced to one half upon the addition of a large excess of an olefin. At very high pressures of carbon dioxide, there was a decrease in the CO yield and this was attributed to S atom recombination via reaction {8}. The rate of reaction {9} was shown to be about 30 times slower than reaction [2].

In this study, the addition of a large excess of carbon dioxide reduced the CO yield to one half the yield in the absence of CO_2. This decrease indicates that the sole fate of the S (^3P) atoms under flash conditions is recombination rather than abstraction.

This view seems reasonable since under flash conditions, the momentary concentration of S atoms is at least 10^6 greater than in static systems with the result that radical - radical reactions can compete effectively with radical - substrate reactions.

The fact that under flash conditions S (^{3}P) atoms recombine rather than abstract has an important bearing on the photolysis of carbonyl sulfide. It has been suggested that in the static photolysis of COS up to 26% of the S atoms are formed in the ^{3}P state directly by the spin forbidden step:

$$COS \quad + \quad h\nu \quad \rightarrow \quad CO \quad + \quad S \; (^3P) \qquad \qquad \{10\}$$
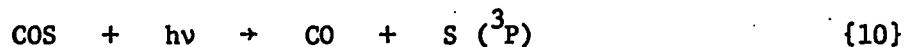
This step was proposed to account for the fact that about 26% of the S atoms produced in the primary step could not be scavenged by paraffins and were thus shown to be in the ^{3}P state. Since in the flash photolysis of pure COS all S atoms underwent abstraction and S (^{3}P) atoms were shown to recombine, the S atoms formed in reaction {1} must be in the ^{1}D state. The accuracy of the CO yield measurements is about ± 5% and thus the gross error in the two CO yields may be as high as 10%. However, the CO yields are the result of 12 flashes and four measurments and the error would not be expected to be as much as 10%. Thus, for the most part, it is not reaction {10} but some other process that is responsible for the production of S (^{3}P) atoms in COS - paraffin systems. This point will be discussed later.

Reaction {8} has been shown in the previous chapter to be the fate of triplet sulfur atoms. The S_2 ($^3\Sigma_g^-$) spectrum reaches a maximum intensity as the S_2 ($^1\Delta_g$) has nearly completely decayed, suggesting the scheme of reactions {3} and {4}. The decay of S_2 ($^3\Sigma_g^-$) is a pressure dependent, second order process, as shown in Figure 16, with second and third order rate constants given in Table IV.

The recombination reaction, {8}, is proposed to proceed via the complex chaperon mechanism similar to that found for the recombination of S (^{3}P) atoms in the presence of carbon disulfide:

$$S\ (^3P)\ +\ COS\ \rightleftharpoons\ COS_2 \qquad\qquad \{11\}$$

$$COS_2\ +\ S\ (^3P)\ \rightarrow\ COS\ +\ S_2 \qquad\qquad \{12\}$$
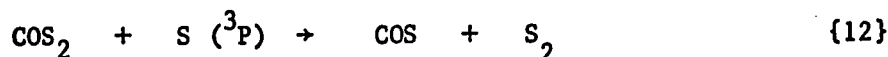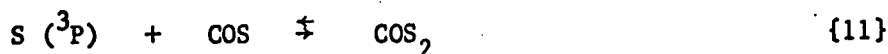
where S_2 again represents the three possible states of S_2, namely, $^3\Sigma_g^-$, $^1\Delta_g$, and $^1\Sigma_g^+$.

The complexity of the transient spectrum in the 3500 – 4300 Å region precludes the fact that the carrier of the spectrum is a diatomic molecule in its ground vibrational state. The carrier of the spectrum is not a vibrationally excited diatomic molecule, since the relative intensities of the bands remain constant as the absorber decays from the system. Basco and Pearson[9] observed this spectrum in the flash photolysis of CS_2 – NO and COS – NO systems but made no assignment as to its origin. They did suggest that the spectrum bore close resemblence to NO_2. The fact that the spectrum is observed even when NO is absent indicates that the carrier can
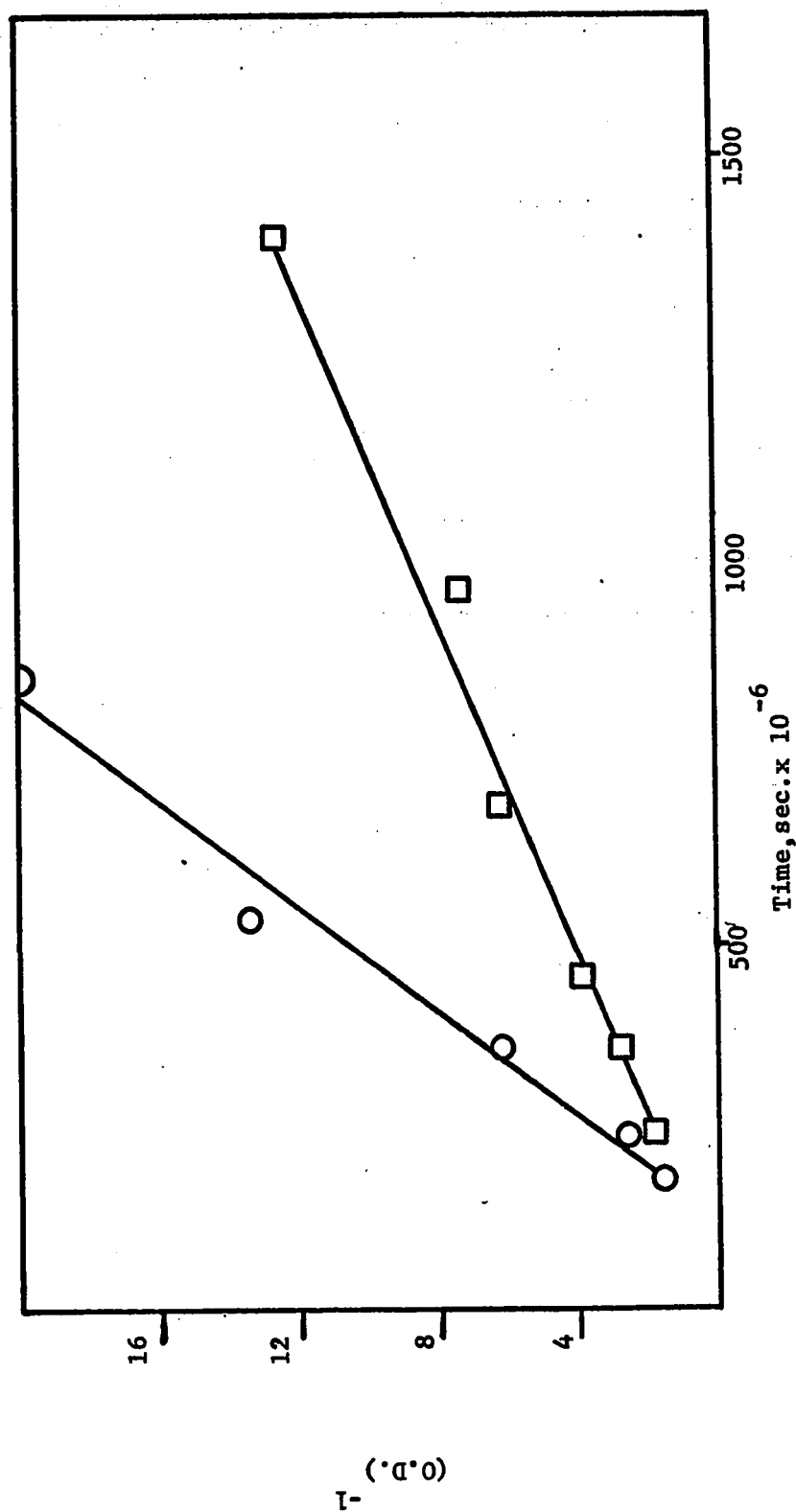
Figure 16. Second order plots for the decay of S_2 $(^3\Sigma_g^-)$ in the flash photolysis of:

□ 17 torr COS + 600 torr CO_2;   ◐ 31 torr COS + 850 torr CO_2.

not be the species SNO. COS_2 is precluded by the fact that the spectrum is observed in the CS_2 - NO system and the bands match the bands observed in the COS system. Therefore the carrier molecule is most likely composed of sulfur atoms only.

S_4 can not be the carrier since in other systems, low pressures of COS, H_2S, H_2S_2, and ethylene episulfide, where S_2 ($^3\Sigma_g^-$) is formed in large amounts and decays by recombination, the spectrum is not observed. The most likely carrier of the spectrum is S_3. This assignment seems reasonable since the spectrum is observed in systems where S (^3P) atoms are not only formed but where the S atoms are capable of forming a complex such as SNO or COS_2. In the presence of NO, S_3 is formed via

$$S\ (^3P)\ +\ NO\ \rightarrow\ SNO \qquad \{13\}$$

$$SNO\ +\ S_2\ (^3\Sigma_g^-)\ \rightarrow\ NO\ +\ S_3 \qquad \{14\}$$
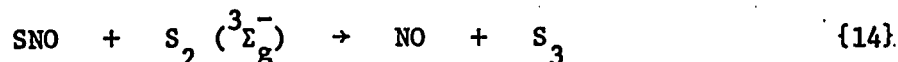
SNO has been suggested by Basco and Pearson[9] . In the presence of COS, the proposed mechanism for the formation of S_3 is

$$S\ (^3P)\ +\ COS\ \rightleftarrows\ COS_2 \qquad \{15\}$$

$$COS_2\ +\ S_2\ (^3\Sigma_g^-)\ \rightarrow\ S_3\ +\ COS \qquad \{16\}$$
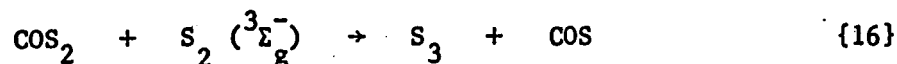
S (^3P) atoms are formed by the relaxation of S (^1D) by CO_2 and NO. That the spectrum of S_3 is also observed at high pressures of COS indicates that COS also relaxes the singlet sulfur atoms. This point is in agreement with previous low intensity results.

Triplet sulfur atoms are also produced in the flash photolysis of H_2S - CO_2 mixtures (vide infra). The fact that the spectrum of S_3 is not observed in that system indicates that CO_2 and S (^3P) do not form a complex such as CO_2S to any significant extent. This is in agreement with the results found in the flash photolysis of CS_2 - CO_2 mixtures where it was found that the S atoms recombine via the CS_3 chaperon and carbon dioxide has little effect on the recombination rate.

It has been shown that although reaction {2} correctly accounts for the stoichiometry of the reaction of S (^1D) with COS, it fails to explain the slow formation of S_2 ($^1\Delta_g$). Basco and Pearson[9] have investigated the flash photolysis of carbonyl sulfide and found that the rate of S_2 formation was proportional to the pressure of COS over a narrow pressure range - 1.0 to 2.0 torr COS - and that the activation energy of S_2 formation was negative. To account for these findings, they proposed that S_2 was formed via

$$COS + S \rightleftarrows COS_2$$

$$COS_2 + S \rightarrow COS + S_2$$
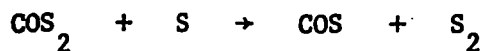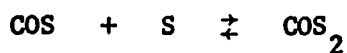
This mechanism does not permit the quantum yield of CO to be greater than 1 nor does it consider the role of S_2 ($^1\Delta_g$) and must therefore be rejected.

A mechanism that will explain the results of this

investigation, the results of Basco and Pearson, as well as earlier low intensity studies, is proposed to be

$$COS + h\nu \rightarrow CO + S\ (^1D) \qquad \{1\}$$

$$COS + S\ (^1D) \rightleftharpoons COS_2 \qquad \{17\}$$

$$COS_2 \rightarrow CO + S_2\ (^1\Delta_g) \qquad \{18\}$$

$$S_2\ (^1\Delta_g) + M \rightarrow S_2\ (^3\Sigma_g^-) + M* \qquad \{3\}$$

$$2\ S_2\ (^3\Sigma_g^-) + M \rightarrow S_4 + M* \qquad \{4\}$$
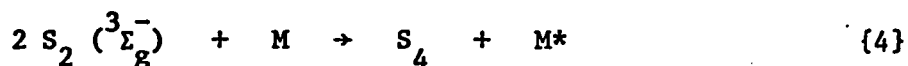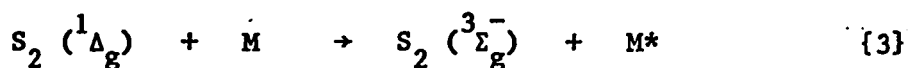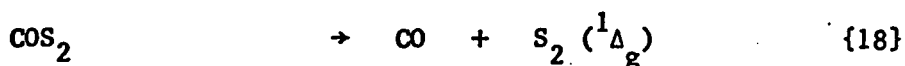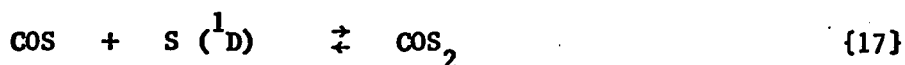
This mechanism does not alter the fact of abstraction but merely proposes a mechanism consistent with the rapid removal of $S\ (^1D)$ atoms by COS and the slow formation of $S_2\ (^1\Delta_g)$.

Thus it is proposed that $S\ (^1D)$ atoms react rapidly with COS to form COS_2 and the equilibrium is rapidly established. Once COS_2 is formed, it will not react with olefins or paraffins and the CO yield will not be reduced to one half, hence the need to use large excesses of hydrocarbons to scavenge the $S\ (^1D)$ atoms. The COS_2 then undergoes unimolecular decomposition to yield S_2 and CO. At low pressures of COS, the rate of $S_2\ (^1\Delta_g)$ formation is slow since the concentration of COS_2 is low. As the pressure of COS is increased, the equilibrium is driven to the right and the concentration of COS_2 increases, resulting in a more rapid formation of $S_2\ (^1\Delta_g)$. At very high pressures of COS, the mechanism predicts that the rate of

S_2 production will be independent of COS pressure and will depend mainly on the amount of S (^{1}D), and hence COS_2, produced in reaction {1}. That this is so can be seen in Table III and Figure 13. In the pressure region of 17 to 65 torr COS, the rate of S_2 production is directly proportional to COS pressure. Above 65 torr, at 192 torr and 410 torr, the rate of triplet S_2 production is independent of COS pressure. At these pressures of COS, the S_2 ($^1\Delta_g$) spectrum cannot be observed due to interference from the COS continuum, but since the relaxation of singlet to the triplet is very rapid, the formation of the triplet closely parallels that of the singlet and so it can be stated that the formation of the singlet is also independent of COS pressure.

The negative activation energy obtained by Basco and Pearson can be explained in terms of the equilibrium reaction {17}. Since the reaction is exothermic, any increase in temperature would shift the equilibrium to the left with the result that the rate of S_2 formation is decreased. The mechanism is also consistent with their finding that the rate of S_2 formation is proportional to the pressure of COS as explained above. They also observed that the addition of an inert gas caused a small increase in the rate of S_2 ($^3\Sigma_g^-$) formation. This may be attributed to the increase in the collisional relaxation of S_2 ($^1\Delta_g$) via reaction {3}.

The quantum yield of CO in the low intensity photolysis of COS - CO_2 mixtures and in the mercury photosensitization of COS is

1.8, while in the flash photolysis of COS - CO_2 mixtures the quantum yield is 0.9. Therefore at low light intensities, S (^3P) atoms abstract from COS while at flash intensities, and hence much higher concentrations, they primarily recombine. This light intensity effect can be best described in terms of the following mechanism

$$S \ (^3P) \ + \ COS \ \rightleftarrows \ ^3COS_2 \qquad \{11\}$$

$$^3COS_2 \ + \ S \ (^3P) \ \rightarrow \ COS \ + \ S_2 \qquad \{12\}$$

$$^3COS_2 \ \rightarrow \ CO \ + \ S_2 \qquad \{19\}$$
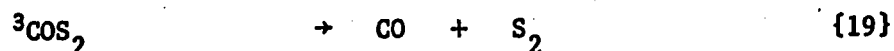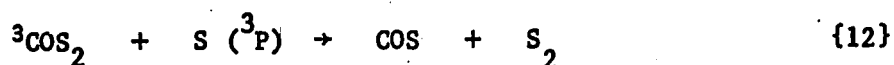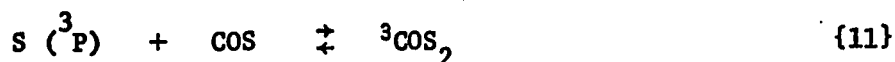
The superscript is used to differentiate the COS_2 formed in $\{11\}$ from that formed in reaction $\{17\}$.

The proposed mechanism is consistent with the results of low and high intensity studies. At low light intensities, the path of the reaction is mainly reactions $\{11\}$ and $\{19\}$ as evidenced by the CO quantum yield of 1.8. This seems reasonable since the concentration of S atoms under static conditions is very low. The abstraction process is slow since the S (^3P) atoms are easily scavenged by added olefins[23].

Under flash conditions, the reaction proceeds mainly via reactions $\{11\}$ and $\{12\}$ as evidenced by the CO quantum yield of 0.9. This seems reasonable since under flash conditions, the S atom concentration is at least 10^6 higher than under static conditions and radical - radical reactions occur more readily.

Therefore under all conditions, reaction {11} is the most likely reaction between S (^{3}P) and COS. If the S atom concentration is sufficiently high, recombination will occur in preference to abstraction. If the S atom concentration is low, the rate of reaction {12} is slow and is replaced by the abstraction reaction {19}.

An estimate of the recombination rate constant can be made from the growth portion of the S_2 ($^3\Sigma_g^-$) curve in Figure 14. This rate constant is about 7×10^{11} $M^{-1}sec^{-1}$ for 17 torr COS + 600 torr CO_2. However, only 50% of the S_2 is formed in the $^3\Sigma_g^-$ state with 33% formed in the $^1\Delta_g$ state and 17% in the $^1\Sigma_g^+$ state. Since these singlet states are relaxed to the triplet at rates that could not be determined in this study, the recombination rate constant is only an estimate. However, the value is of the right order of magnitude since atomic recombinations proceeding by a chaperon mechanism usually have a rate constant about 10^{10} to 10^{12} $M^{-1}sec^{-1}$.

CHAPTER   V

THE FLASH PHOTOLYSIS OF ETHYLENE EPISULFIDE

RESULTS

DISCUSSION

RESULTS

The only important transient in the flash photolysis of ethylene episulfide was S_2 ($^3\Sigma_g^-$). Very weak spectra of CS, HS, and HS$_2$ were also observed. The series of absorption spectra in Plate 4 show the formation and decay of the intermediates. The products of the reaction were ethylene, elemental sulfur, and about 10% each of hydrogen sulfide and acetylene.

The flash photolysis of ethylene episulfide was carried out at three pressures, 10, 13, and 19 torr. The S_2 ($^3\Sigma_g^-$) spectrum was densitometered and the O.D. vs. time plots are shown in Figure 17. The spectra of CS, HS, and HS$_2$ were too weak for densitometry. The yields of ethylene corresponding to 10, 13, and 19 torr ethylene episulfide were 1.18, 1.60, and 1.30 μmole/flash. Plots of O.D.$^{-1}$ vs. time for the decay of S_2 ($^3\Sigma_g^-$) are shown in Figure 18.

Experiments were carried out to determine if the spectrum of S_2 ($^3\Sigma_g^-$) obeyed the Beer - Lambert law. Various lengths of the reaction cell were exposed to the flash and the spectrum of S_2 were recorded. Figure 19 shows the plot of O.D. of S_2 ($^3\Sigma_g^-$) vs. exposed cell length.

Wavelength
Delay 35 µsec

42 "
49 "
56 "
77 "
95 "
113 "
130 "
165 "
180 "
240 "
360 "
460 "

HS_2

HS (0,0)

$S_2 \, (B^3\Sigma_u^- \leftarrow X^3\Sigma_g^-)$
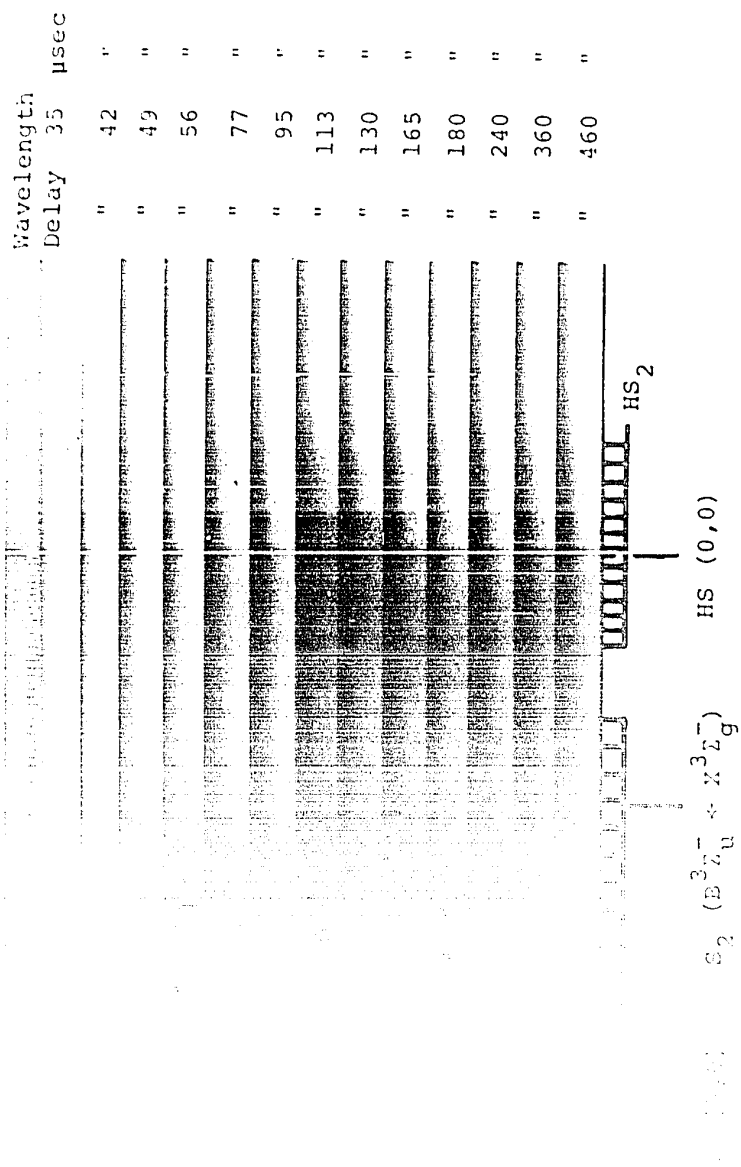
Spectra against time. 19 torr Ethylene Episulfide.
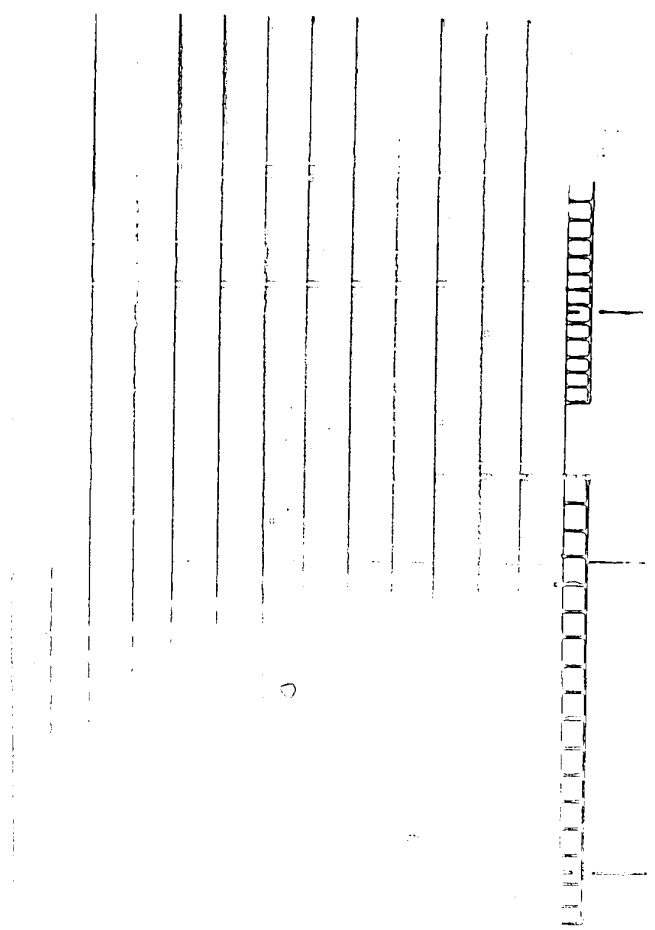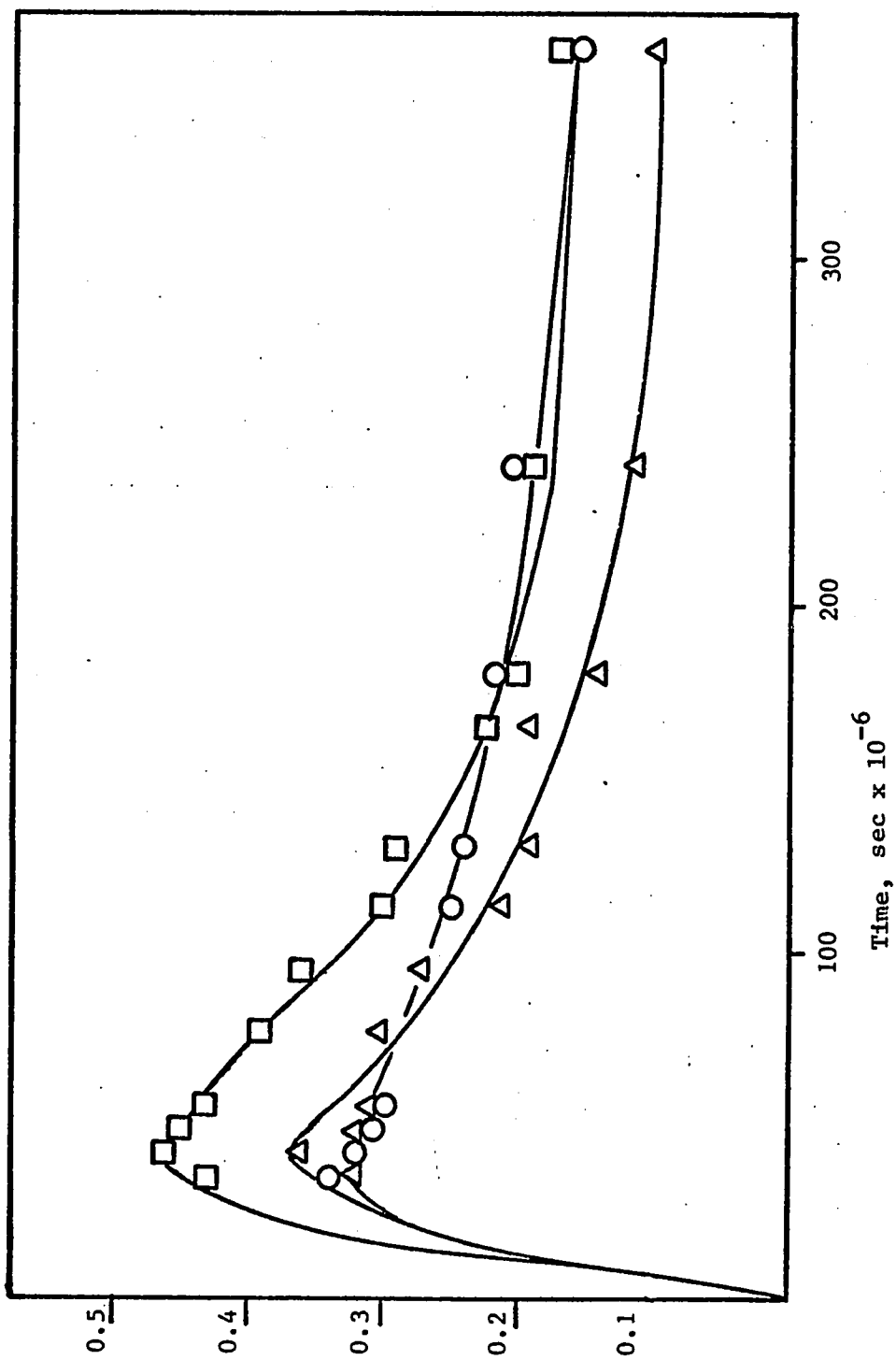
Figure 17. Plots of O.D. vs. time for S_2 ($^3\Sigma_g^-$) at different pressures ethylene

episulfide. ◯ 10 torr; ☐ 13 torr; △ 19 torr.
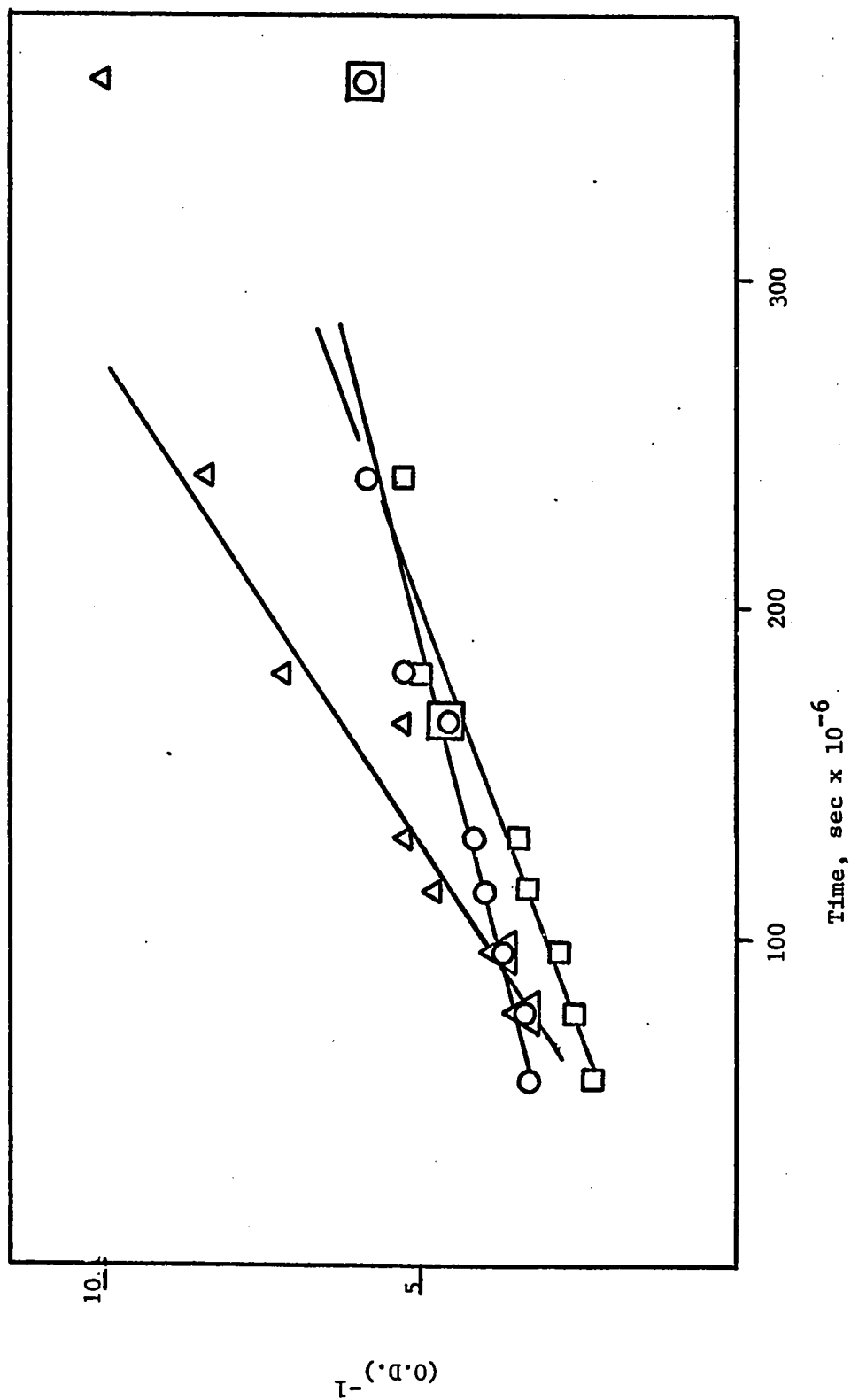
Figure 18. Plots of O.D.$^{-1}$ vs. time for the decay of S_2 ($^3\Sigma_g^-$) as a function of ethylene episulfide pressure. $\bigcirc$ 10 torr; $\square$ 13 torr; $\triangle$ 19 torr.
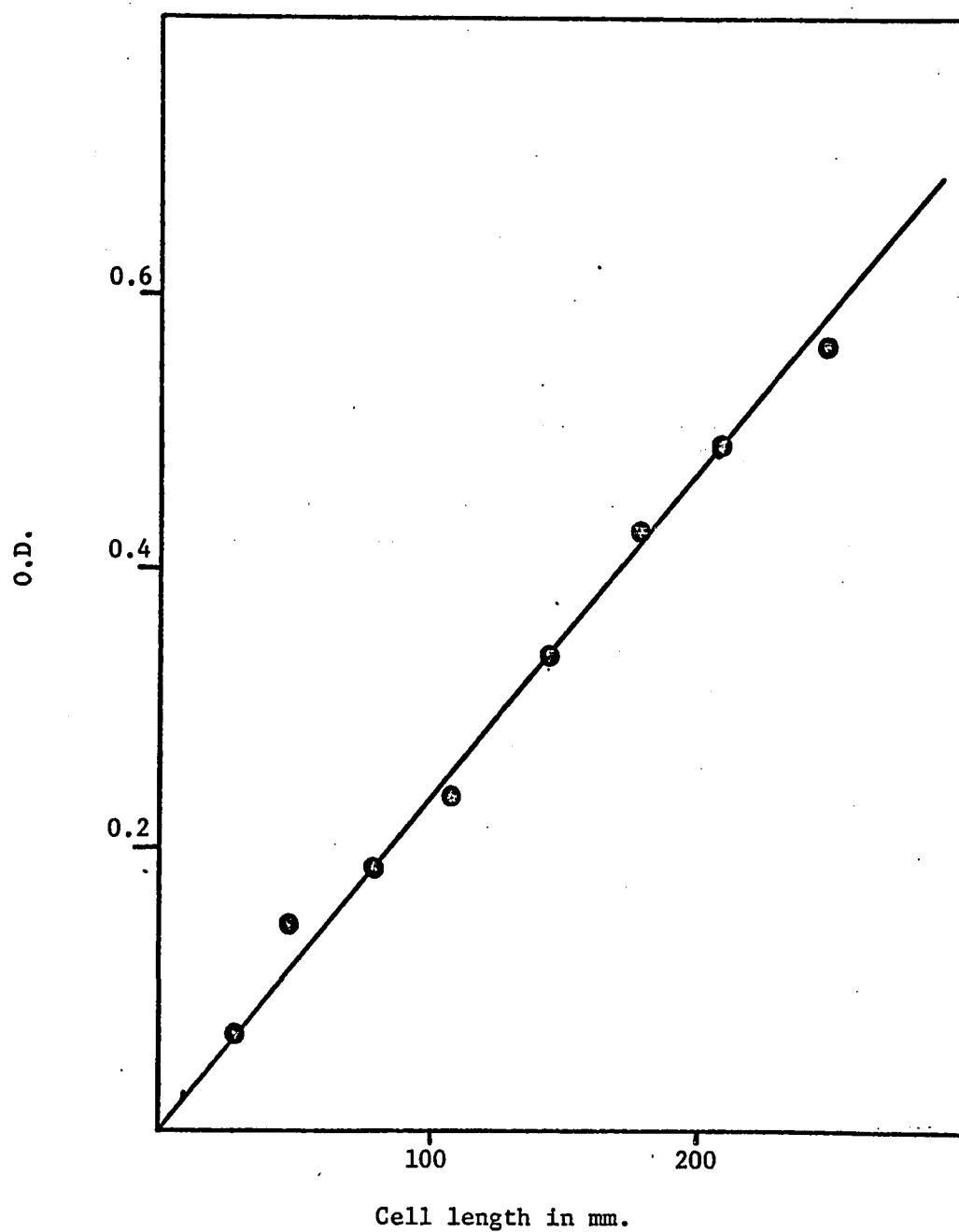
Figure 19.   Plots of O.D. vs. exposed cell length for S_2 $(^3\Sigma_g^-)$
in the flash photolysis of ethylene episulfide.

DISCUSSION

Low intensity studies of the photochemistry of ethylene episulfide[33] have shown that the major product of the reaction is ethylene with a quantum yield of about 1.6. The mechanism proposed for its formation was (E = ethylene episulfide)

$$E \quad + \quad h\nu \quad \rightarrow \quad {}^1E^* \qquad\qquad \{1\}$$

$$^1E^* \quad\qquad \rightarrow \quad {}^3E^* \qquad\qquad \{2\}$$

$$^3E^* \quad\qquad \rightarrow \quad C_2H_4 \quad + \quad S\ ({}^3P) \qquad \{3\}$$

$$^3E^* \quad + \quad E \quad \rightarrow \quad 2\ E \qquad\qquad \{4\}$$

$$^3E^* \quad + \quad S\ ({}^3P) \quad \rightarrow \quad 2\ C_2H_4 \quad + \quad S_2\ ({}^3\Sigma_g^-) \qquad \{5\}$$

$$^3E^* \quad + \quad E \quad \rightarrow \quad 2\ C_2H_4 \quad \pm \quad S_2\ ({}^3\Sigma_g^-) \qquad \{6\}$$
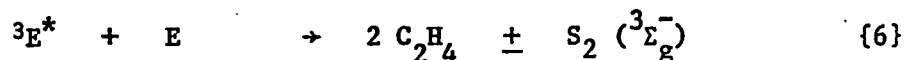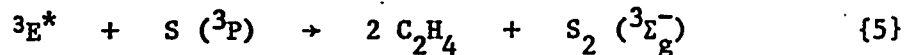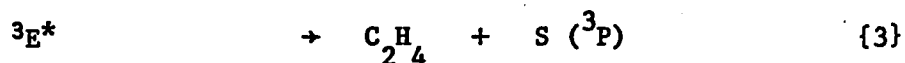
where the superscript denotes the multiplicity of the electronic states. The S atoms are formed in their triplet ground states since mercaptans could not be detected among the products on the addition of paraffinic or olefinic hydrocarbons, although the episulfide of the added olefin was readily detectable[33].

In the flash photolysis of ethylene episulfide, the products volatile at -130°C contained in addition to ethylene about 10% each of hydrogen sulfide and acetylene. These products likely arise from a molecular split of the excited singlet state

$$^1E^* \rightarrow H_2S + C_2H_2 \qquad \{7\}$$

The intermediate CS may also be a cracking product of the excited singlet state but from its low optical density, less than 10^{-2} % of the singlet decomposes to produce this species. The transient HS is most likely the product of the secondary photolysis of the hydrogen sulfide formed in reaction $\{7\}$. HS_2 is formed by the recombination of HS and S. The spectra of these transients are very weak and represent less than 1% of the reaction and can be neglected.

The S_2 formed in reactions $\{5\}$ and $\{6\}$ is in the $^3\Sigma_g^-$ state since spin conservation rules preclude the formation of a singlet state. This view is supported by the absence of the $^1\Delta_g$ state even at the shortest delay. The kinetic expression for the formation of S_2 is simplified by the absence of the $^1\Delta_g$ state and also by the fact that the formation of S_2 is very rapid and can be approximated by the equation for the photo – flash output. This can be seen from the fact that the S_2 curve in Figure 17 reaches a maximum at about 40 µsec, about 85% dissipation of the flash energy. Thus the rate of formation of S_2 is well described by A f(t) where A is the limiting concentration of S_2 produced (i.e., corresponding to t = ∞ and no decay) and is equal to one half the ethylene produced per flash. The function f(t) is the relative intensity of the photo – flash at time t such that $\int_0^\infty f(t)dt = 1$.

The decay of the S_2 is again found to be a second order, pressure dependent process and is best described by

$$2 S_2 \; (^3\Sigma_g^-) \;\; + \;\; M \;\; \rightarrow \;\; S_4 \;\; + \;\; M^* \qquad\qquad \{8\}$$
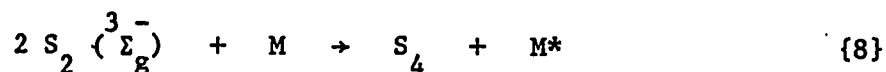
From these facts the kinetic expression for the formation and decay of S_2 becomes:

$$\frac{d(S_2)}{dt} \;\; = \;\; Af(t) \;\; - \;\; k_8 \, (M)(S_2)^2 \qquad\qquad (A)$$

Upon integration, the equation yields

$$(S_2)_t \;\; = \;\; A\!\int_0^t f(t)dt \;\; - \;\; k_8 (M)\!\int_0^t (S_2)^2 dt \qquad\qquad (B)$$

or in terms of optical density

$$(O.D.)_t \;\; = \;\; A\varepsilon\ell\!\int_0^t f(t)dt \;\; - \;\; \frac{k_8}{\varepsilon\ell}\!\int_0^t (O.D.)^2 dt \qquad\qquad (C)$$

The integral $(O.D.)^2 dt$ was evaluated graphically for various value of t from a smoothed out plot of $(O.D.)^2$ against time. The resulting linear differential equation was normalized to $\int_0^\infty f(t) \, dt = 1$. O.D. was plotted against $\int_0^t (O.D.)^2 dt$ as shown in Figure 20 and analyzed by least mean square. The resulting values of $A\varepsilon\ell$ and $k_8/\varepsilon\ell$ together with the measured yields of ethylene are summarized in Table V.

From these data, the molar decadic extinction coefficient, ε, at the peak intensity of the S_2 $(^3\Sigma_g^-)$ (13,0) band can be

TABLE V

RATE CONSTANT AND EXTINCTION COEFFICIENT DATA FROM THE FLASH PHOTOLYSIS

OF ETHYLENE EPISULFIDE

	10	13	19
$P(C_2H_4S)$, torr			
C_2H_4 yield, μmoles	1.18	1.60	1.30
$A\varepsilon\ell$	0.422 ± 0.022	0.615 ± 0.036	0.405 ± 0.015
ε, $M^{-1}cm^{-1} \times 10^{-4}$	1.43 ± 0.07	1.54 ± 0.09	1.25 ± 0.05
$k_8/\varepsilon\ell \times 10^{-4} sec^{-1}$	1.49 ± 0.27	1.83 ± 0.45	3.08 ± 0.93
k_8 $M^{-1}sec^{-1} \times 10^{-10}$	1.05 ± 0.34	1.29 ± 0.51	2.17 ± 0.98
k_8 $M^{-2}sec^{-1} \times 10^{-13}$	1.95 ± 0.63	1.85 ± 0.73	2.12 ± 0.96
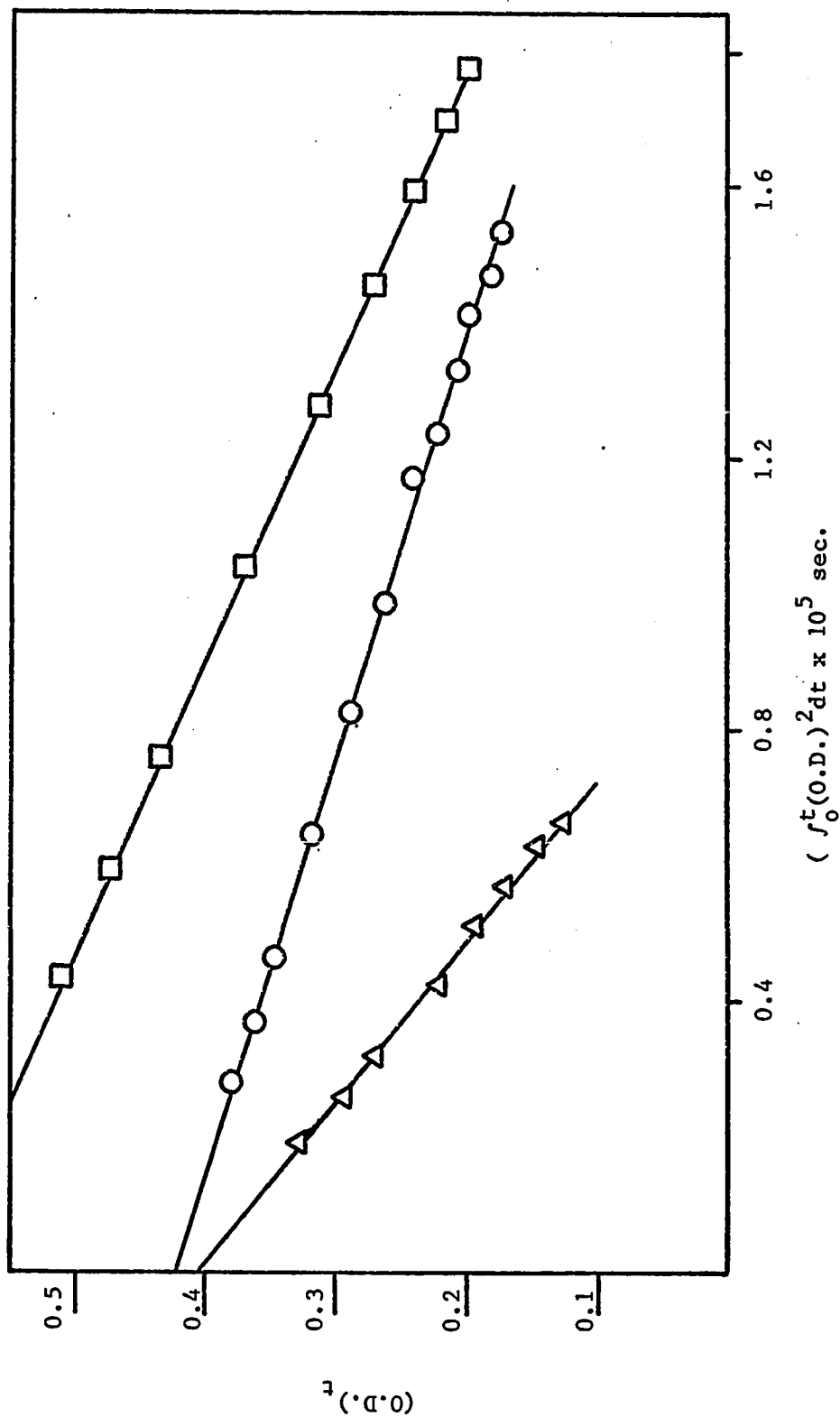
Figure 20. Normalized plots of equation (C). Pressure of ethylene episulfide

○ 10 torr; □ 13 torr; △ 19 torr.

calculated. These values are listed in Table V. The average of the three values is $1.41 \pm 0.21 \times 10^4$ M^{-1} cm^{-1}. This value is in good agreement with the value obtained by Gaydon[40], 3.9×10^3, considering the fact that he obtained his result in shock tube studies at temperatures as high as 3000°K. Also, the extinction coefficient is sensitive to experimental conditions such as the spectral slit width.

Figure 19 shows the plot of O.D. against irradiated cell length for S_2 $(^3\Sigma_g^-)$. The fact that the data points define a straight line indicates that S_2 $(^3\Sigma_g^-)$ (13,0) band obeys the Beer - Lambert law. Similar results were obtained by Callear in the flash photolysis of carbon disulfide. Since the Beer - Lambert law is obeyed, optical density can be used without the need for corrections.

CHAPTER VI

THE FLASH PHOTOLYSIS OF HYDROGEN SULFIDE

RESULTS

DISCUSSION

RESULTS

The flash photolysis of 30 torr H_2S in the presence of 105 torr CO_2 produced the transients S_2 ($^1\Delta_g$), S_2 ($^3\Sigma_g^-$), HS, and HS_2. The stable products of the reaction were hydrogen, hydrogen disulfide, and elemental sulfur. The series of absorption spectra in Plate 5 show the formation and decay of the intermediates. The spectrum of S_2 ($^1\Delta_g$) reached maximum intensity within 42 μsec and decayed within 95 μsec. The spectrum of S_2 ($^3\Sigma_g^-$) reached maximum intensity within 42 μsec and decayed within 550 μsec. HS was at maximum concentration at the shortest delay, 27 μsec, and decayed within 113 μsec. HS_2 reached maximum intensity within 77 μsec and decayed within 240 μsec.

The effect of added inert gas pressure was examined by carrying out the flash photolysis of 30 torr H_2S in the presence of 0, 105, and 335 torr CO_2. The following effects were observed:

a) The hydrogen yield per flash decreased with increasing carbon dioxide pressure. The yields were 3.76, 3.46, and 3.12 μmole/flash respectively.

b) The yield of HS decreased with increasing carbon dioxide pressure. The rate of decay of HS also increased as shown in Figure 21.

c) The rate of decay of S_2 ($^3\Sigma_g^-$) increased with carbon dioxide pressure as shown in Figure 22. The yield of S_2 decreased.
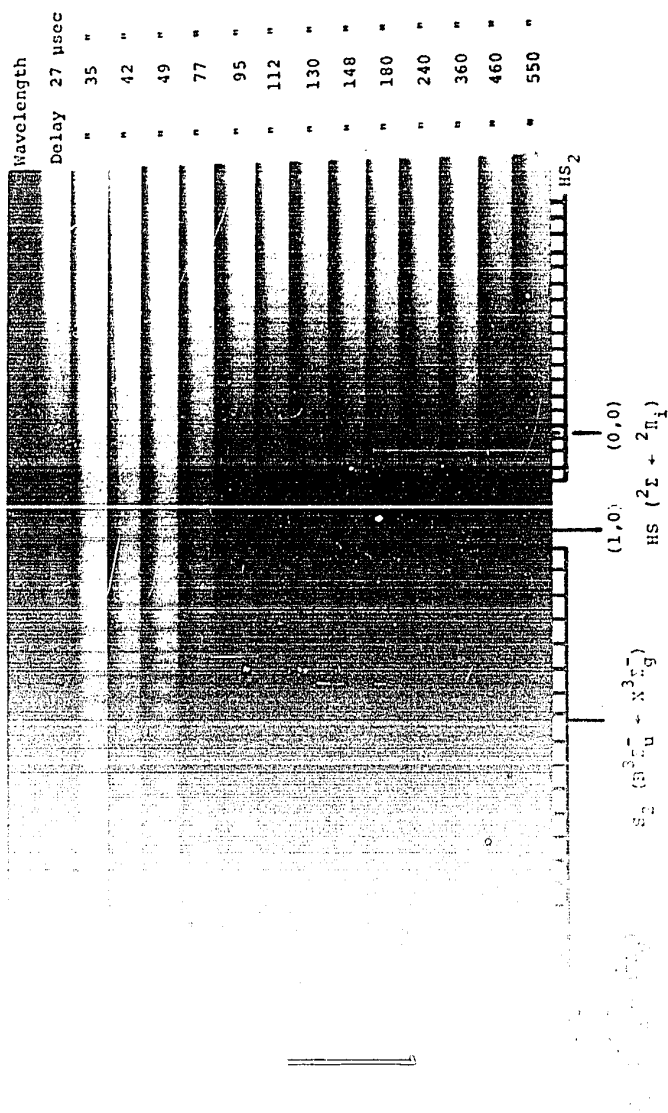
Plate 5. Spectra against time in the flash photolysis of 30 torr H_2S + 105 torr CO_2.
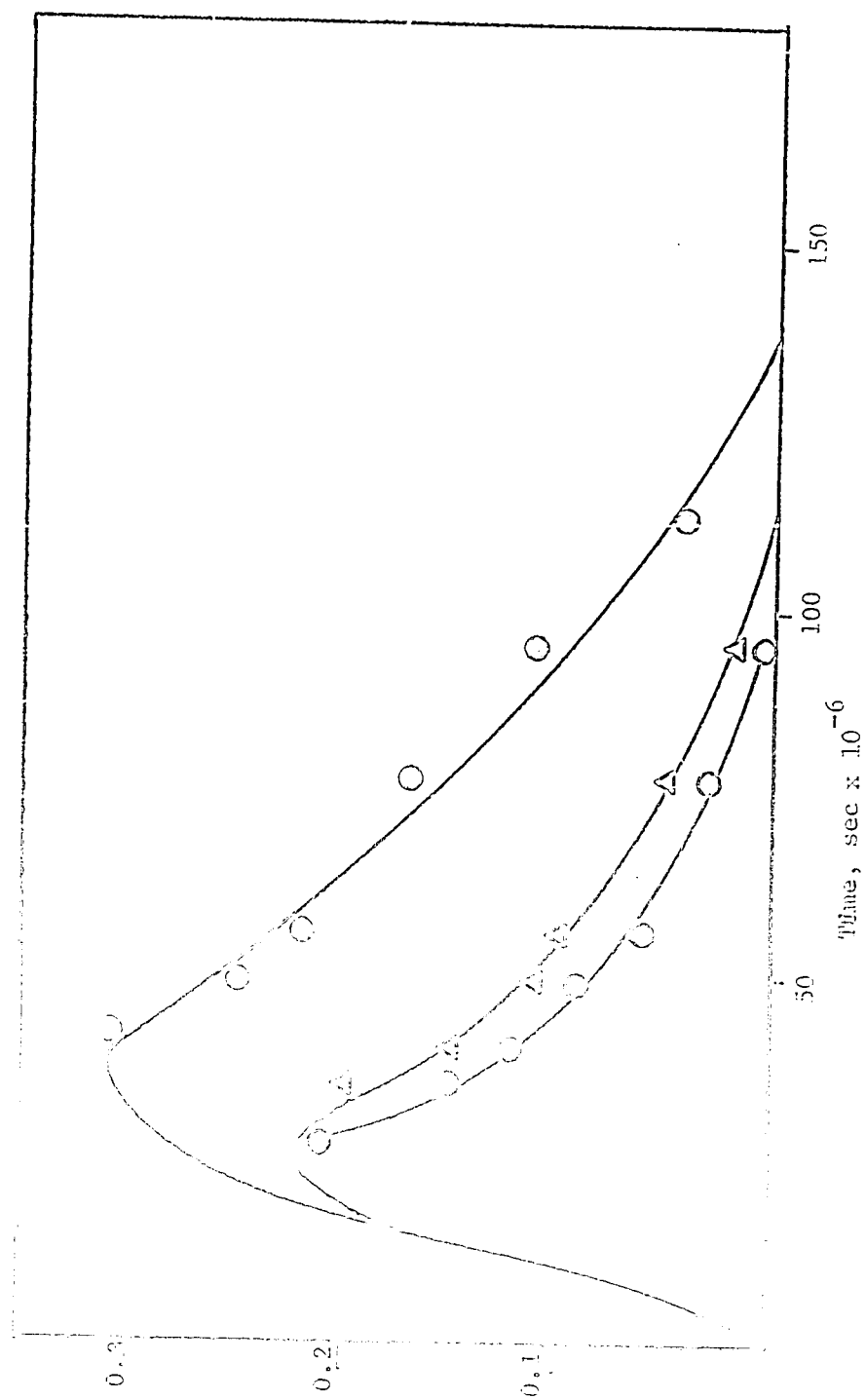
Figure 21.   Plot of O.D. vs. time for HS as a function of added carbon dioxide.

( ) 0 torr;   △ 105 torr;   ○ 335 torr CO$_2$.
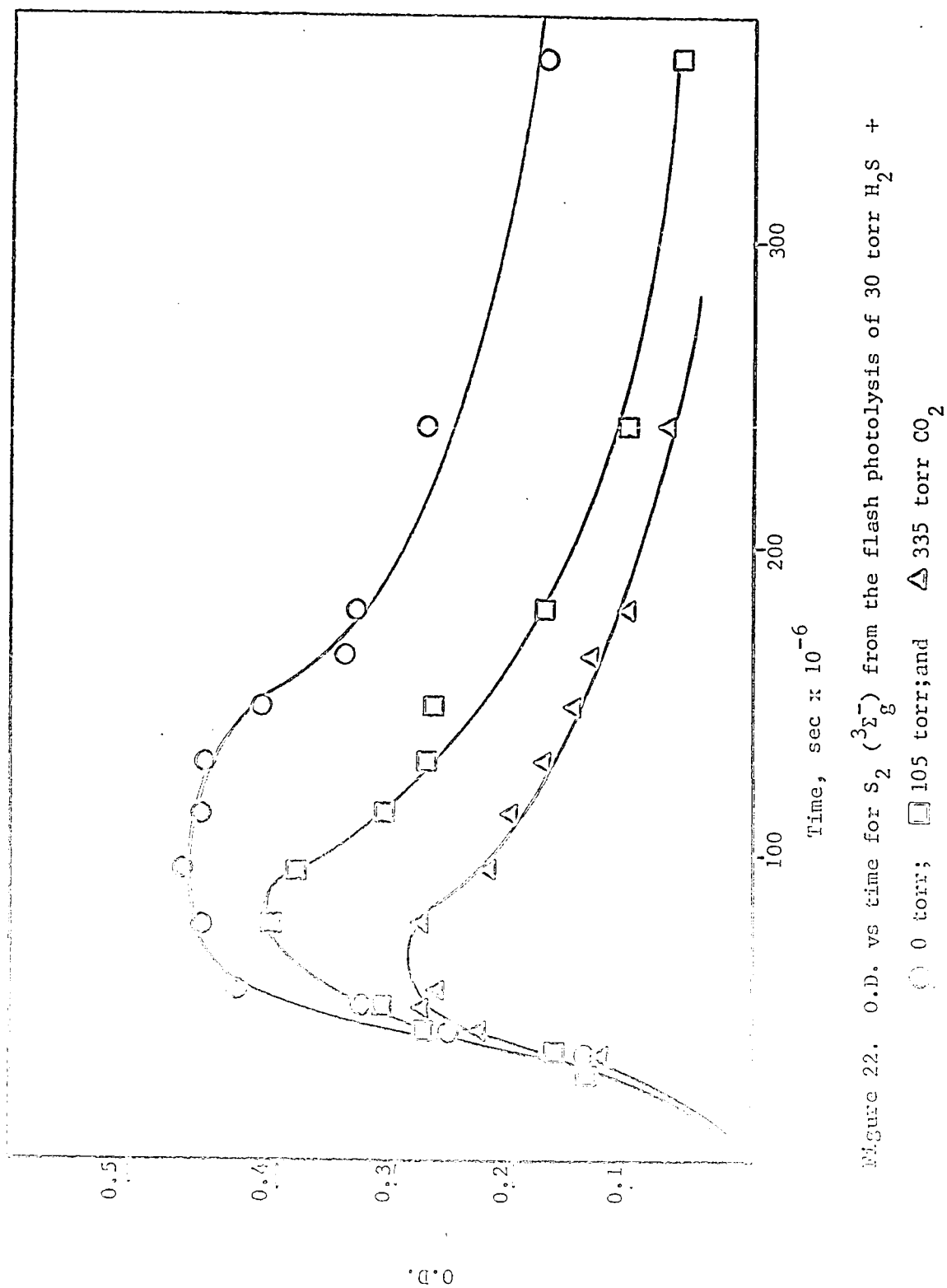
Figure 22. O.D. vs time for S_2 ($^3\Sigma_g^-$) from the flash photolysis of 30 torr H_2S + 335 torr CO_2

○ 0 torr; □ 105 torr;and △ 335 torr CO_2

Time, sec x 10^{-6}

O.D.

d) S_2 $(^1\Delta_g)$ decayed at faster rates at higher carbon dioxide pressures.

e) The HS_2 spectrum was mostly unaffected.

The flash photolysis of 30 torr H_2S in the presence of 100, 325, and 575 torr H_2 gave essentially the same results as the $H_2S - CO_2$ system except for one point. The S_2 $(^1\Delta_g)$ could only be observed at the lowest hydrogen pressure, 100 torr, and only at the shortest time delay, 27 μsec. Its spectrum was very weak. The formation and decay of HS and S_2 $(^3\Sigma_g^-)$ are shown in Figures 23 and 24 respectively.

The flash photolysis of 30 torr H_2S + 210 torr C_2H_4 resulted in the formation of ethyl mercaptan (1.6 μmole/flash) and ethylene episulfide (0.2 μmole/flash) as the only products. The only transient observed was HS but its spectrum was very weak and could only be detected at the shortest delay, 27 μsec. When the same mixture was photolyzed under static conditions, the only product was ethyl mercaptan, 3.5 μmoles.

The flash photolysis of 30 torr H_2S and 30 torr H_2S + 460 torr CO_2 was carried out with varying lengths of the cell exposed to the flash to determine if HS obeyed the Beer - Lambert law. Figure 25 shows the plot of O.D. against path length for the HS (1,0) band. Figure 26 shows the plot of log (O.D.) vs. log (path length) for the HS (0,0) band.

The quantum yield of hydrogen was also measured at 30, 300, 500, and 700 torr H_2S. The light source was a Cadmium resonance
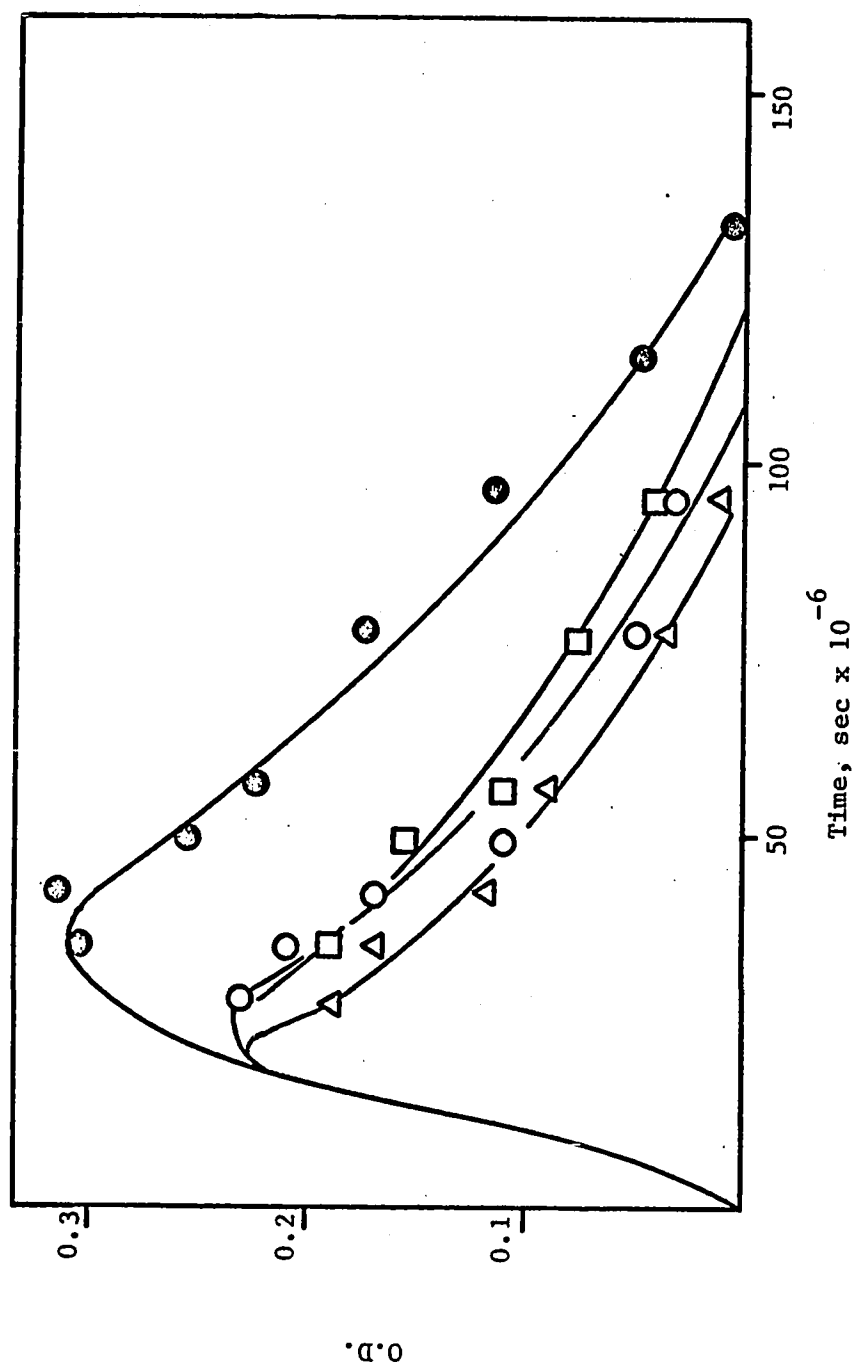
Figure 23. Plot of O.D. vs. time for HS decay at various hydrogen pressures.

⊛ 0 torr; ☐ 100 torr; ○ 325 torr; △ 575 torr H_2.
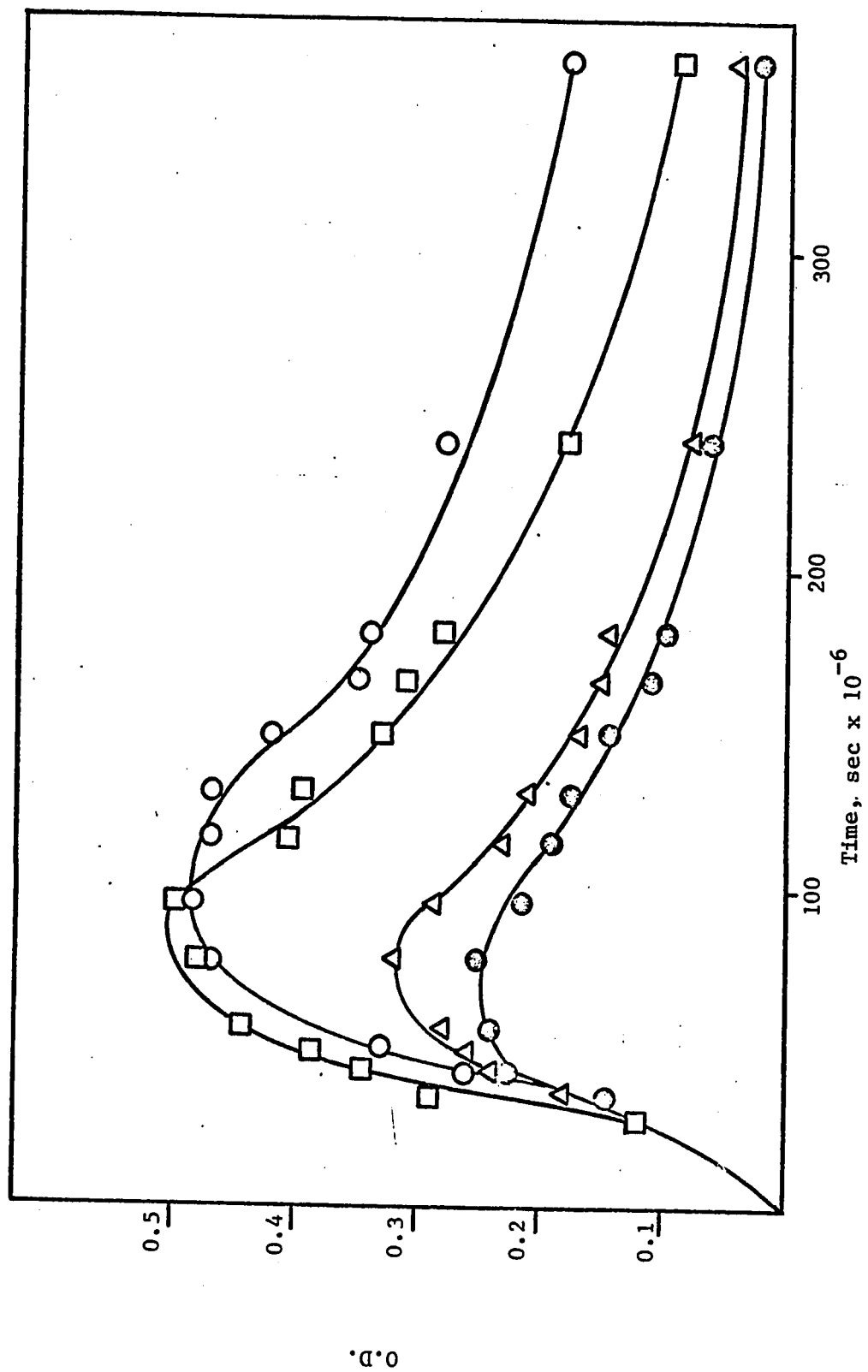
Figure 24. Plot of O.D. vs. time for S_2 ($^3\Sigma_g^-$) decay at various pressures of hydrogen.

○ 0 torr; ☐ 100 torr; △ 325 torr; ◉ 575 torr H_2.

Time, sec x 10^{-6}

O.D.
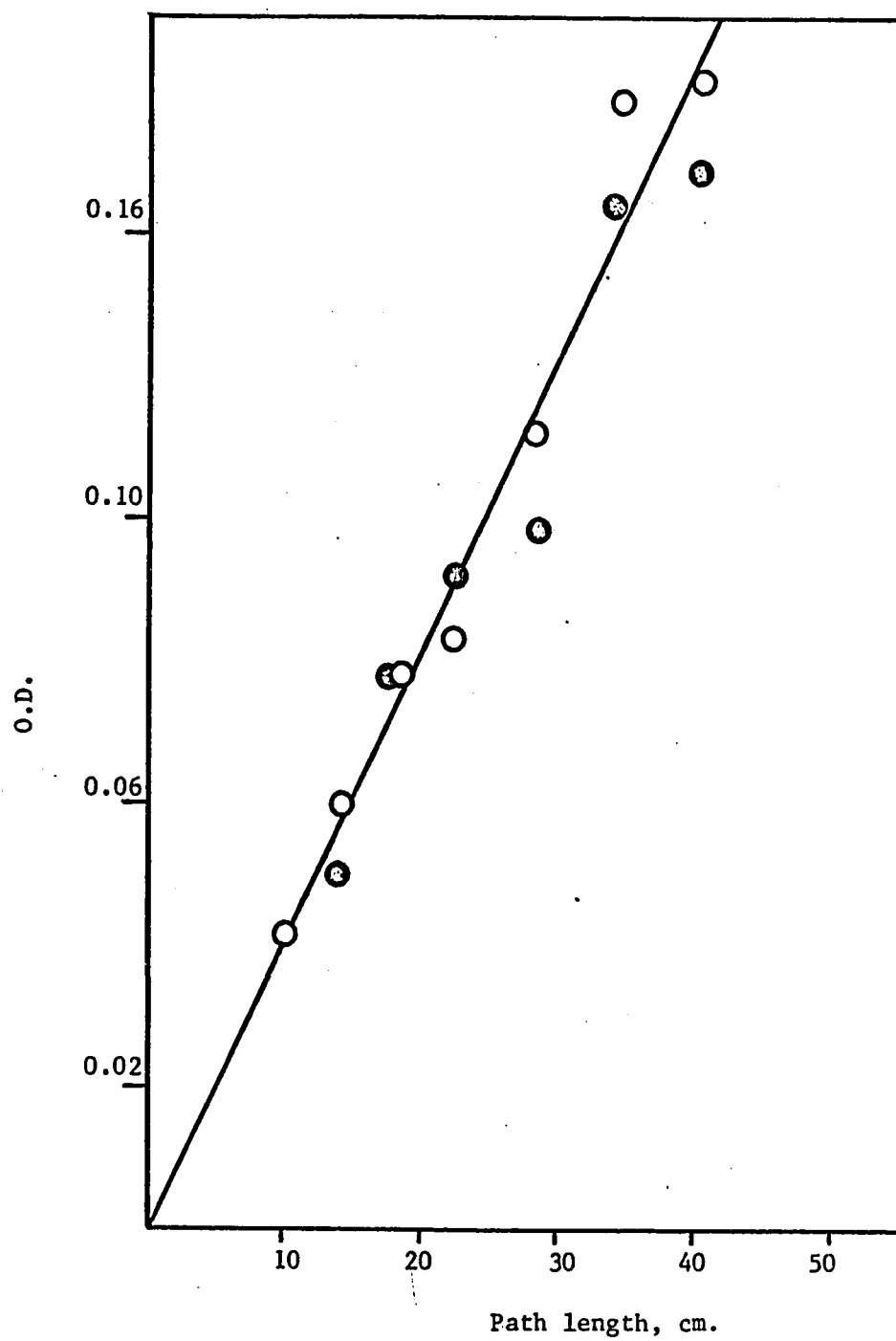
Figure 25. O.D. of HS (1,0) band as a function of the irradiated cell length. ⊙ 30 torr H_2S

○ 30 torr H_2S + 460 torr CO_2.
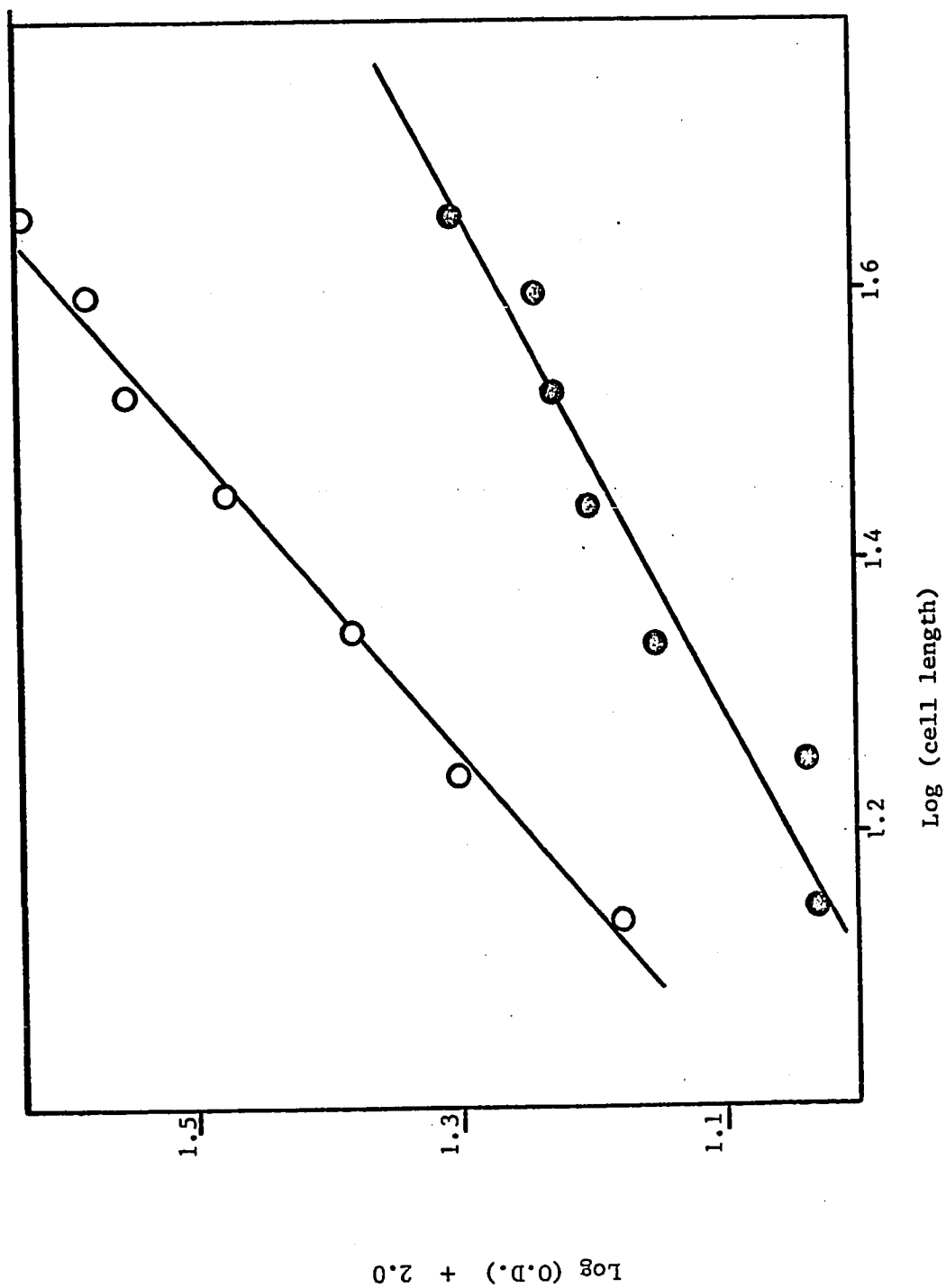
Figure 26. Log – log plot of equation A for the HS (0,0) band.

⊕ 30 torr H_2S; ○ 30 torr H_2S + 460 torr CO_2

Log (cell length)

Log (O.D.) + 2.0

lamp equipped with an interference filter to pass only the 2288 Å resonance line. COS was used as an actinometer. The yields of CO and H_2 are tabulated in Table VI.

DISCUSSION

Porter[41] has shown that the primary photolytic step in the decomposition of hydrogen sulfide is

$$H_2S \ + \ h\nu \ \rightarrow \ H \ + \ HS\cdot \qquad \{1\}$$

This is consistent with the observation that the spectrum of HS in Plate 5 is at maximum intensity at the shortest delay. The fate of the H atoms is

$$H \ + \ H_2S \ \rightarrow \ H_2 \ + \ HS \qquad \{2\}$$

Reaction 2 is known to be fast[29] although its absolute rate is not known with certainty[29]. The H atoms formed in {1} may possess as much as 20 Kcal/mole translational energy and the addition of an inert gas may influence the rate of {2} by removing some of this energy.

The hydrogen quantum yield measurements shown in Table VI indicate that not all the H atoms react via {2} and some must be lost either on the vessel surface or in the reaction

TABLE VI

HYDROGEN QUANTUM YIELD DETERMINATIONS

Reactant	Pressure torr	Irradiation time, min.	H_2 or CO yield moles/min x 10^{-8}	Quantum yield of H_2 or CO
COS	200	75	3.08	1.80
COS	200	37.5	3.09	1.80
H_2S	30	42	1.52	0.89
"	300	42	1.54	0.90
"	500	42	1.54	0.90
"	700	42	1.55	0.91

$$H + HS + M \rightarrow H_2S + M* \qquad \{3\}$$
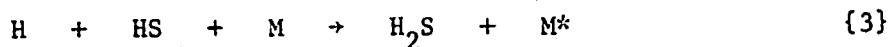
These two processes amount to about 10% of the reaction as shown by the hydrogen yield. Darwent and Roberts[28] have also measured the hydrogen quantum yield and found that at 30 torr H_2S its value is 1.09. From the rates of hydrogen production at different H_2S pressures they inferred that at 200 torr the quantum yield is 1.26. This increase was attributed to reaction $\{5\}$.

There is no obvious explanation for the large difference in the quantum yield values obtained by Darwent and Roberts and the values obtained in this work. One possible explanation could be the fact that they used hydrogen bromide as an actinometer and had to correct for the back reaction. In this study, COS was used as an actinometer since the quantum yield of CO is well established as 1.8[13] and no serious complications are encountered.

Darwent and Roberts proposed that the fate of HS is

$$2 \; HS \rightarrow H_2S + S \qquad \{4\}$$

$$\rightarrow H_2 + S_2 \qquad \{5\}$$

although $\{5\}$ is very much slower than $\{4\}$ at low pressures. Another HS removing step must be considered, namely,

$$2 \; HS + M \rightarrow H_2S_2 + M* \qquad \{6\}$$

since hydrogen disulfide was a product of the reaction. Its

formation was inferred from the presence of a product involatile at

-130°C which underwent surface decomposition to hydrogen sulfide

and elemental sulfur. These same properties were observed for

hydrogen disulfide in later work (vide infra). In an independent

study[41], hydrogen disulfide was shown to be a product of the flash

photolysis of hydrogen sulfide. Using the technique of flash

photolysis kinetic mass spectrometry, they showed that the signal

at m/e = 66 was the parent peak of hydrogen disulfide.

The quantum yield measurements indicate that reaction {5}

is unimportant and that HS is removed primarily by reactions {4}

and {6}. The decrease in the hydrogen yield as the pressure of

carbon dioxide is increased is best attributed to the occurence

of reaction {3} at high pressures of inert gas. Hydrogen atoms

may also diffuse to the walls since considerable photolysis occurs

close to the wall facing the lamp.

The flash photolysis of a mixture of 30 torr H_2S + 210

torr C_2H_4 resulted in the formation of ethyl mercaptan and

ethylene episulfide in the ratio of 8:1. The absence of vinyl

mercaptan shows that S (^1D) atoms are absent and that the S atoms

formed in {4} are in the ground ^3P state. Ethylene episulfide

is formed via

$$S \ (^3P) \ + \ C_2H_4 \ \rightarrow \ C_2H_4S \qquad \{7\}$$
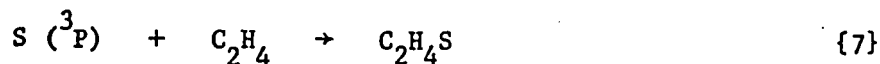
Ethyl mercaptan is formed via

$$HS \; + \; C_2H_4 \; \rightarrow \; CH_2CH_2SH \qquad \{8\}$$

$$CH_2CH_2SH \; + \; H_2S \; \rightarrow \; CH_3CH_2SH \; + \; HS \qquad \{9\}$$

and

$$H \; + \; C_2H_4 \; \rightarrow \; CH_3CH_2 \qquad \{10\}$$

$$CH_3CH_2 \; + \; HS \; \rightarrow \; CH_3CH_2SH \qquad \{11\}$$
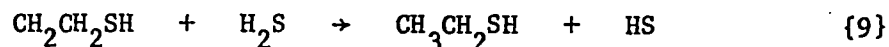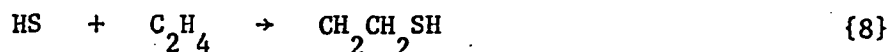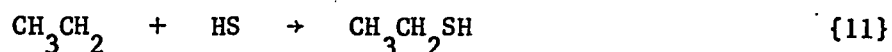
That ethylene episulfide was found indicates that reaction {4} is very rapid since it could compete with the HS scavenging reactions {8} and {11}.

The Beer - Lambert law can be stated as[46]

$$O.D. \; = \; \epsilon(C\ell)^n \qquad\qquad A$$

assuming symmetrical dependence of optical density on concentration and on path length. The law is said to be obeyed if a plot of O.D. vs. path length yields a straight line. Figure 25 shows that the 3060 Å, (1,0) band of HS does obey Beer's law. The 3236 Å, (0,0) band does not obey the Beer - Lambert law since straight lines were not be obtained. The (0,0) band also shows pressure dependence as shown in Figure 26. At 30 torr H_2S, the value of n in equation A is 0.5 while at 490 torr total pressure the value is 0.89. This effect may be due to pressure broadening. For this reason, the (1,0) band must be used in all calculations.

In the absence of a reacting gas, the fate of HS is reaction

via {4} and {6}. Figures 27 and 28 show that the decay of HS follows second order, pressure dependent kinetics. From the slopes the rate constants for HS decay can be calculated using the equation

$$k = slope \times \epsilon \times \ell \qquad \qquad B$$

where k represents the sum of the rate constants $k_4 + k_6(M)$.

The extinction coefficient for the HS (1,0) band can be determined in the following way. The amount of HS formed in the reaction is equal to twice the hydrogen yield. The kinetics of HS decay are described by the equation

$$\frac{d(HS)}{dt} = Af(t) - k(HS)^2 \qquad \qquad C$$

where A is the amount of HS produced per flash, f(t) is the relative intensity of the photo - flash at time t, and k is the sum of the rate constants for HS decay. Equation C upon integration becomes

$$(HS)_t = A\int_0^t f(t)dt - k\int_0^t (HS)^2 dt \qquad \qquad D$$

or in terms of optical density

$$\frac{(O.D.)_t}{\epsilon\ell} = A\int_0^t f(t)dt - \frac{k}{\epsilon\ell}\int_0^t (O.D.)^2 dt \qquad \qquad E$$

When the decay of HS is complete,

$$A = \frac{k}{(\epsilon\ell)^2}\int_0^t (O.D.)^2 dt \qquad \qquad F$$
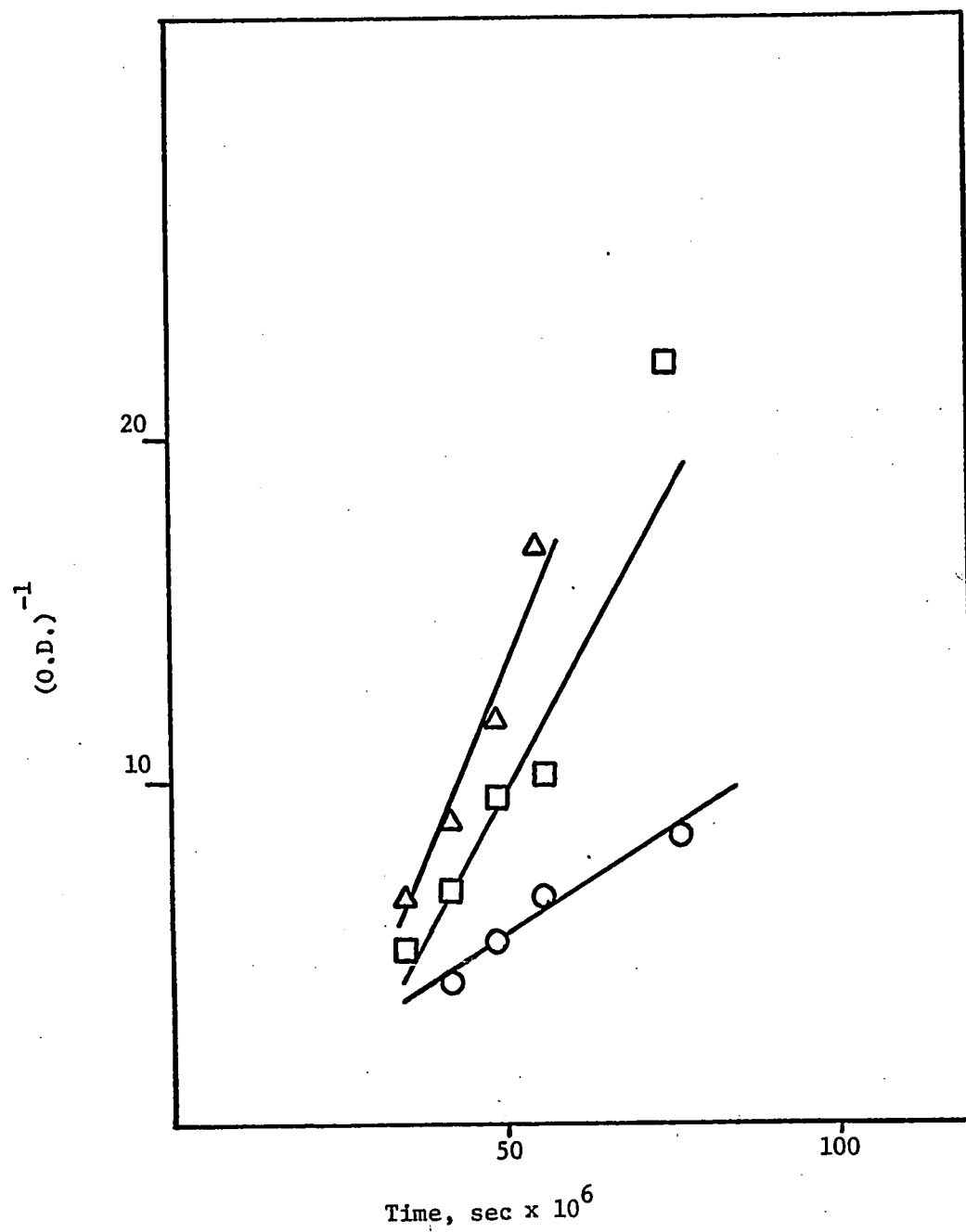
Figure 27. Second order plots for the decay of HS at different pressures of CO_2. $\bigcirc$ 0 torr; $\square$ 105 torr; $\triangle$ 335 torr CO_2.
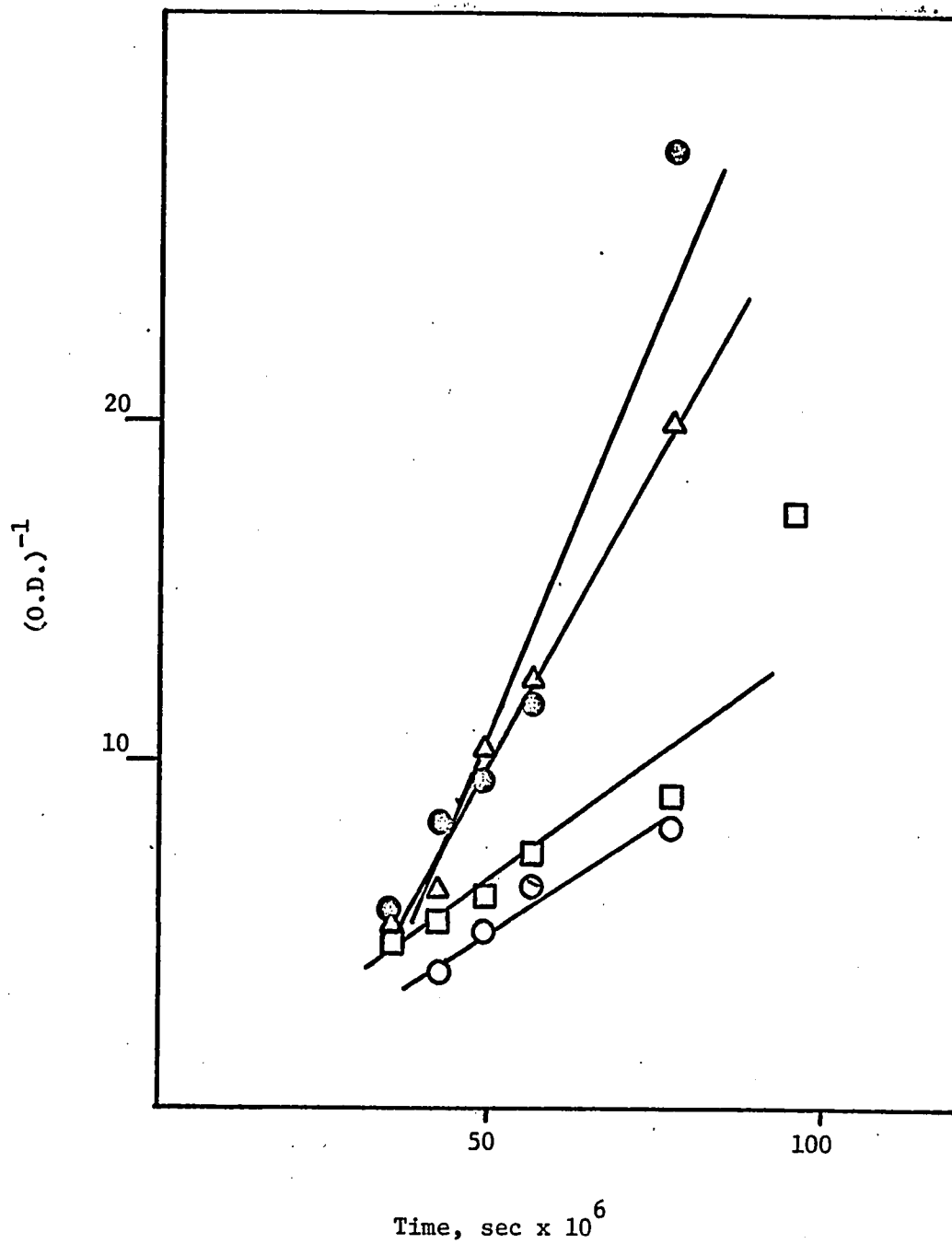
Figure 28.　Second order plots for the decay of HS at different

pressures of H_2.　◯ 0 torr;　□ 100 torr;

△　325 torr;　◐　575 torr H_2.

Combining equations B and F gives

$$A = \frac{slope}{\varepsilon \ell} \int_0^t (O.D.)^2 dt \qquad\qquad G$$

The value of the integral is obtained by graphically evaluating the area under the curve obtained from the plot of $(O.D.)^2$ vs. time, the slope is known from Figure 27, the cell length is ℓ, and A is the yield of HS per flash. The corresponding values for 30 torr H_2S are: $4.36 \times 10^{-6} sec^{-1}$, $1.03 \pm 0.42 \times 10^5$ sec, 50 cm., and 7.64×10^{-6} μmole/flash respectively. Substituting these values into equation G gives $\varepsilon = 1.18 \pm 0.48 \times 10^3$ liter $mole^{1-}$ $cm.^{-1}$

With the value of ε determined, the absolute rate constants for HS decay can be calculated from equation B. These values are listed in Table VII. Inspection of Table VII shows that there is large uncertainty in the values of the rate constants. Some of the more important causes of this are:

a) the decay of HS is rapid and considerable decay will take place during the finite length of the source flash. Since the decay is more rapid at high concentrations, this error will affect the measurements at high optical densities.

b) densitometry of the 3060 Å line of the HS (1,0) band will be greatly affected by the fog level of the spectroscopic plate especially at low O.D. values.

c) a 95% confidence level was used in the least mean square calculations of the extinction coefficient and of the slopes of Figures 27 and 28. This may be described as undue caution, but

TABLE VII

ABSOLUTE RATE CONSTANTS FOR THE DECAY OF HS AS A FUNCTION OF H_2 OR CO_2 PRESSURE

H_2S torr	Added gas	torr	Slope sec $\times 10^{-5}$	k, M^{-1} sec^{-1} $\times 10^{-9}$	k, M^{-2} sec^{-1} $\times 10^{-11}$
30	--	--	1.03 ± 0.42	6.09 ± 5.00	3.78 ± 3.06
30	CO_2	105	2.49 ± 0.47	14.18 ± 8.79	1.93 ± 1.18
30	CO_2	335	3.57 ± 1.16	21.08 ± 15.39	1.08 ± 0.79
30	H_2	100	1.86 ± 0.84	10.97 ± 9.11	1.57 ± 1.30
30	H_2	325	3.43 ± 0.36	20.14 ± 10.52	1.06 ± 0.55
30	H_2	575	4.63 ± 2.32	27.32 ± 24.86	0.84 ± 0.76

owing to large systematic errors, a smaller confidence level was unjustified.

The rate constants in Table VII represent the sum of the two rate constants k_4 and $k_6(M)$. In principle, these two could be determined from the information available but it was felt that the large errors prevented any meaningful calculations. However, the calculated rate constants do have qualitative significance in that there is evidence for the second and third order processes in the pressure dependence observed. They are also in good agreement with the values obtained for the decay of OH[42,43] and HSe[44], viz., 1.55×10^9 and 3.9×10^{10} for OH, and 3.0×10^9 M^{-1} sec^{-1} for HSe.

The fate of the S (^3P) atoms is recombination via

$$2 \text{ S } (^3P) \quad + \quad M \quad \rightarrow \quad S_2 \quad + \quad M \tag{12}$$
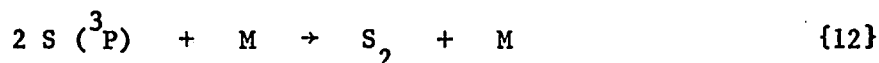
where S_2 is formed in all three possible states, $^3\Sigma_g^-$, $^1\Delta_g$, and $^1\Sigma_g^+$. The appearence of S_2 ($^3\Sigma_g^-$) is rapid indicating that hydrogen sulfide is an efficient third body.

The transient HS_2 is most likely formed in the reaction

$$\text{HS} \quad + \quad \text{S} \quad \rightarrow \quad HS_2 \tag{13}$$

The concentration of HS_2 is low and the amount of HS or S (^3P) removed will not much affect the above calculations. Another possible source of HS_2 is

$$\text{H} \quad + \quad S_2 \ (^3\Sigma_g^-) \quad \rightarrow \quad HS_2 \tag{14}$$

The fate of S_2 ($^1\Delta_g$) is collisional relaxation

$$S_2 \ (^1\Delta_g) \ + \ M \ \rightarrow \ S_2 \ (^3\Sigma_g^-) \ + \ M^* \qquad \{15\}$$
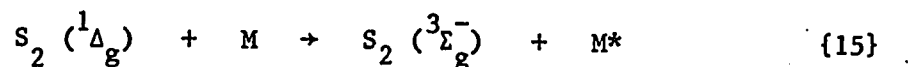
This view is supported by the observation that the S_2 ($^3\Sigma_g^-$) reaches maximum concentration when the S_2 ($^1\Delta_g$) has decayed. In the presence of hydrogen, the spectrum of S_2 ($^1\Delta_g$) is not observed due to the very rapid relaxation to the ground state. This point will be discussed in the following chapter.

Figures 29 and 30 show the plot of O.D.$^{-1}$ vs. time for the decay of S_2 ($^3\Sigma_g^-$). The data points define straight lines and the slopes increase with increasing pressure. Therefore, S_2 ($^3\Sigma_g^-$) removal is accomplished via the process

$$2 \ S_2 \ (^3\Sigma_g^-) \ + \ M \ \rightarrow \ S_4 \ + \ M^* \qquad \{16\}$$
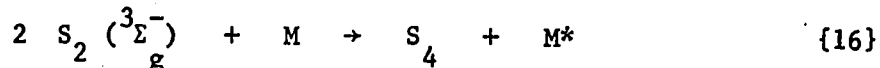
Using equation B and the slopes from Figures 28 and 29, the rate constants for {16} can be calculated. Their values are shown in Table VIII. The third order rate constants can be seen to decrease as the pressure of hydrogen and carbon dioxide are increased. This fact indicates that the assumption that hydrogen and carbon dioxide have the same efficiency in reaction {16} is invalid. The relative efficiencies can be calculated from the data and are seen to be: 3:2:1 for hydrogen sulfide, carbon dioxide and hydrogen, respectively. When the third order rate constants are corrected for this fact, they can be seen to be in good agreement.
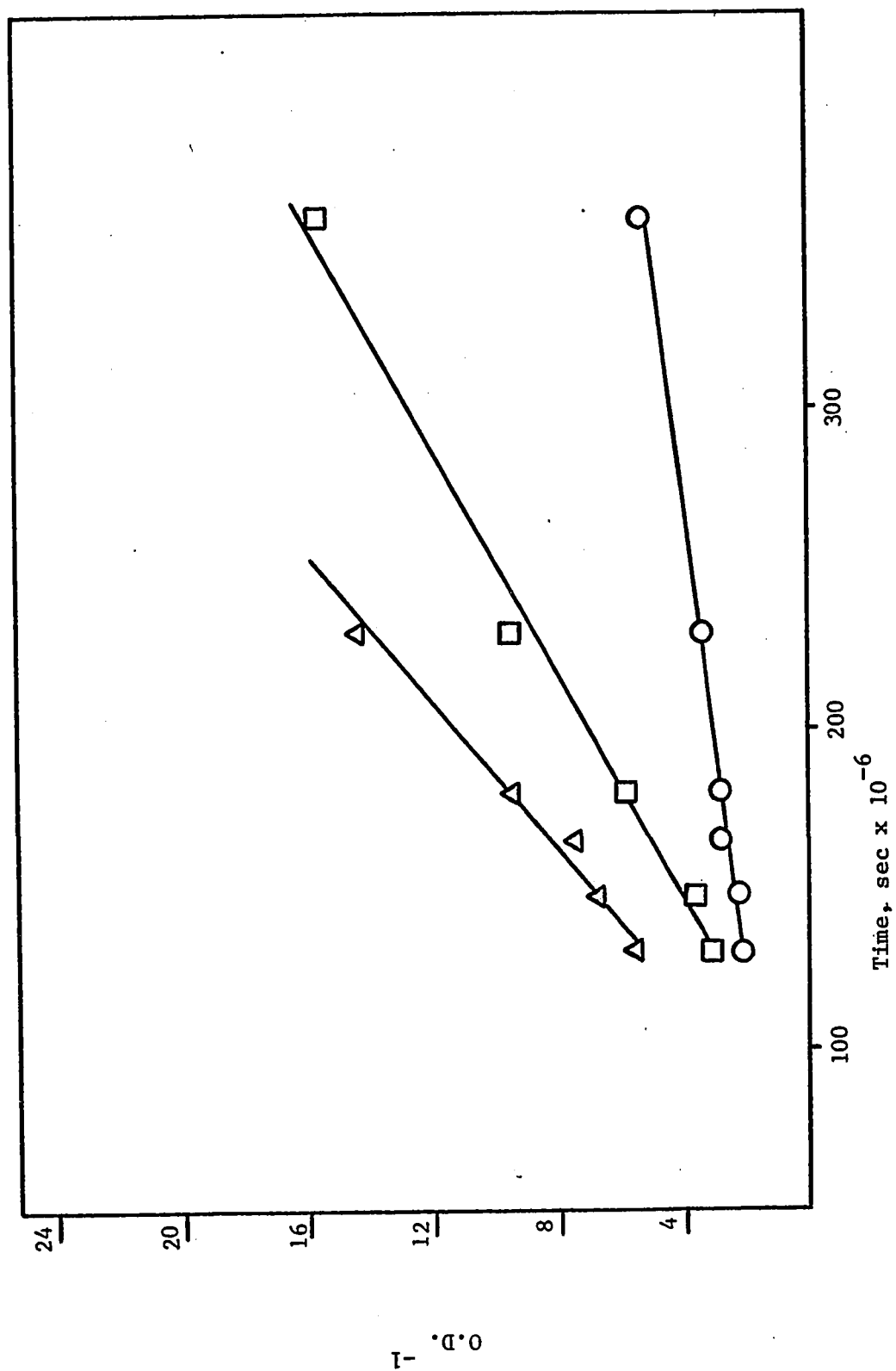
Figure 29. Second order decay plots for S_2 ($^3\Sigma_g^-$) at various CO_2 pressures.

○ 0 torr; □ 105 torr; △ 335 torr CO_2.
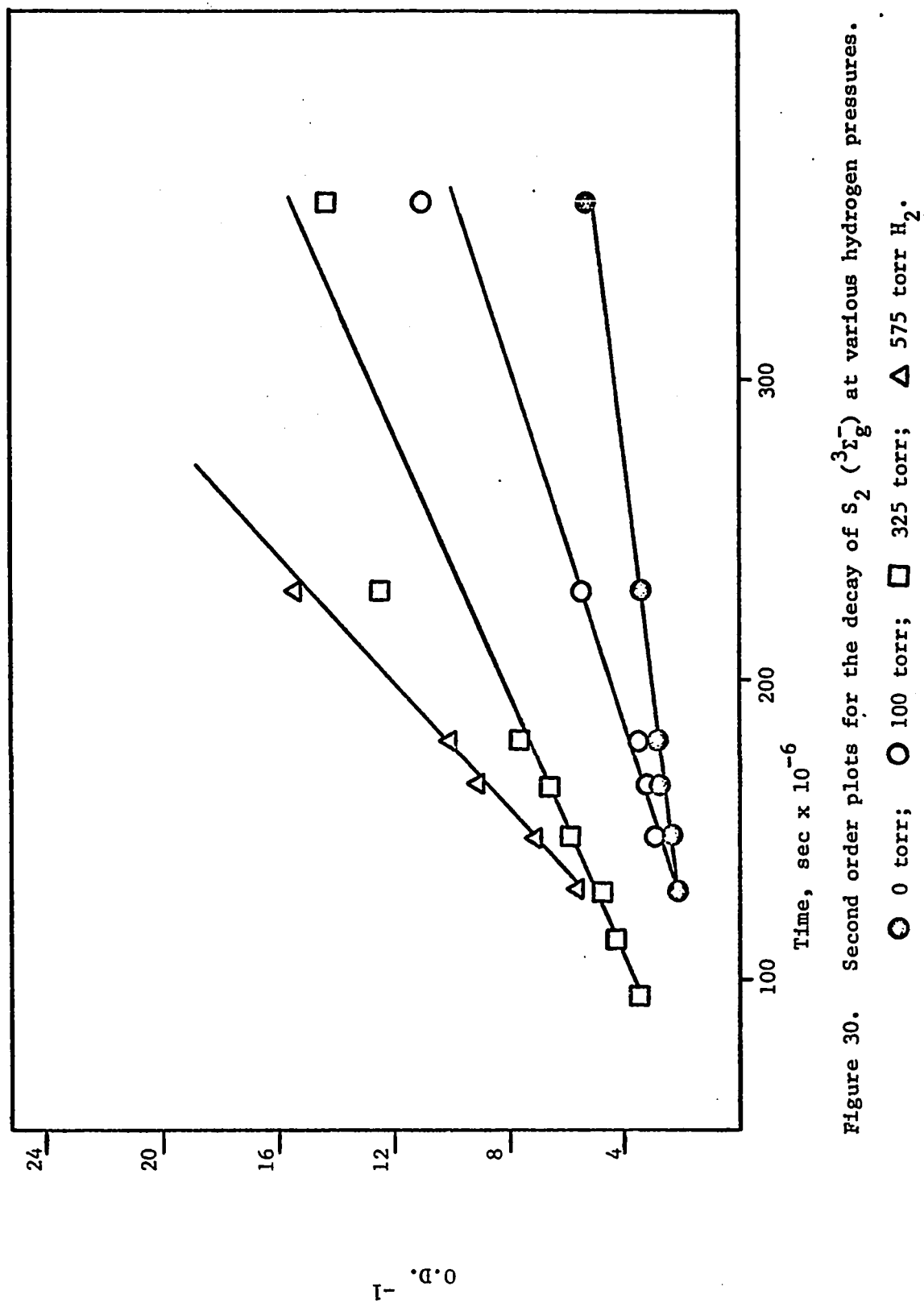
Figure 30. Second order plots for the decay of S_2 ($^3\Sigma_g^-$) at various hydrogen pressures.

⊙ 0 torr; ◯ 100 torr; ☐ 325 torr; △ 575 torr H_2.

TABLE VIII

SECOND AND THRID ORDER RATE CONSTANTS FOR THE DECAY OF S_2 $(^3\Sigma_g^-)$

AS A FUNCTION OF H_2 AND CO_2 PRESSURE

H_2S torr	Added gas	torr	Slope sec $\times 10^{-4}$	k_{16}, M^{-1} sec^{-1} $\times 10^{-10}$	k_{16}, M^{-2} sec^{-1} $\times 10^{-12}$	k_{16}, M^{-2} sec^{-1} $\times 10^{-12}$ *
30	-	-	1.23 ± 0.19	0.87 ± 0.29	5.39 ± 2.32	5.39 ± 2.32
30	CO_2	105	5.04 ± 0.40	3.55 ± 0.92	4.89 ± 1.27	8.00 ± 2.06
30	"	335	8.06 ± 1.86	5.68 ± 2.33	2.89 ± 1.18	5.26 ± 2.16
30	H_2	100	2.49 ± 0.72	1.76 ± 0.83	2.52 ± 1.18	5.45 ± 2.56
30	"	325	4.40 ± 0.99	3.10 ± 1.27	1.62 ± 0.66	4.52 ± 1.85
30	"	575	7.68 ± 1.50	5.41 ± 2.06	1.66 ± 0.63	4.96 ± 1.88

* Corrected for the different efficiencies of H_2S, CO_2, and H_2 as third bodies in reaction

CHAPTER VII

THE REACTION OF S (^{1}D) ATOMS WITH HYDROGEN AND METHANE

RESULTS

    A, Hydrogen

    B, Methane

DISCUSSION

RESULTS

Hydrogen.

In the flash photolysis of 17 torr COS in the presence of 252 torr H_2, the transient spectra detected by kinetic spectroscopy were HS $(^2\Pi_i)$, S_2 $(^3\Sigma_g^-)$, and HS_2. The stable products of the reaction were CO, H_2S, H_2S_2, and sulfur. The series of absorption spectra in Plate 6 show the formation and decay of the transients. All transients were observed in their respective ground vibrational states. The HS spectrum was strongest at the shortest delay used, 27 µsec, and decayed within 200 µsec. The S_2 $(^3\Sigma_g^-)$ spectrum reached maximum intensity in 100 µsec and decayed within 400 µsec. The HS_2 spectrum reached maximum intensity in about 100µsec and decayed within 240 µsec.

The effect of increasing hydrogen pressure was examined by carrying out the flash photolysis of 17 torr COS in the presence of 0, 32.5, 124, 252, 412, and 595 torr H_2. The following effects were observed:

a) In the absence of hydrogen, the spectrum of S_2 $(^1\Delta_g)$ was observed. The addition of 32.5 torr H_2 caused a severe reduction in the intensity of the singlet spectrum and it was only detected at the shortest delay. At hydrogen pressures greater than 32.5 torr, the spectrum could not be detected, Plate 7.

b) Increasing hydrogen pressure had a twofold effect on

Wavelength

Delay 35 usec

42 "
49 "
56 "
77 "
95 "
113 "
130 "
148 "
165 "
180 "
240 "
360 "

HS$_2$

HS (A$^2\Sigma \rightarrow$ X$^2\Pi_i$)

(1,0) (0,0)

S$_2$ (B$^3\Sigma_u^- \rightarrow$ X$^3\Sigma_g^-$)
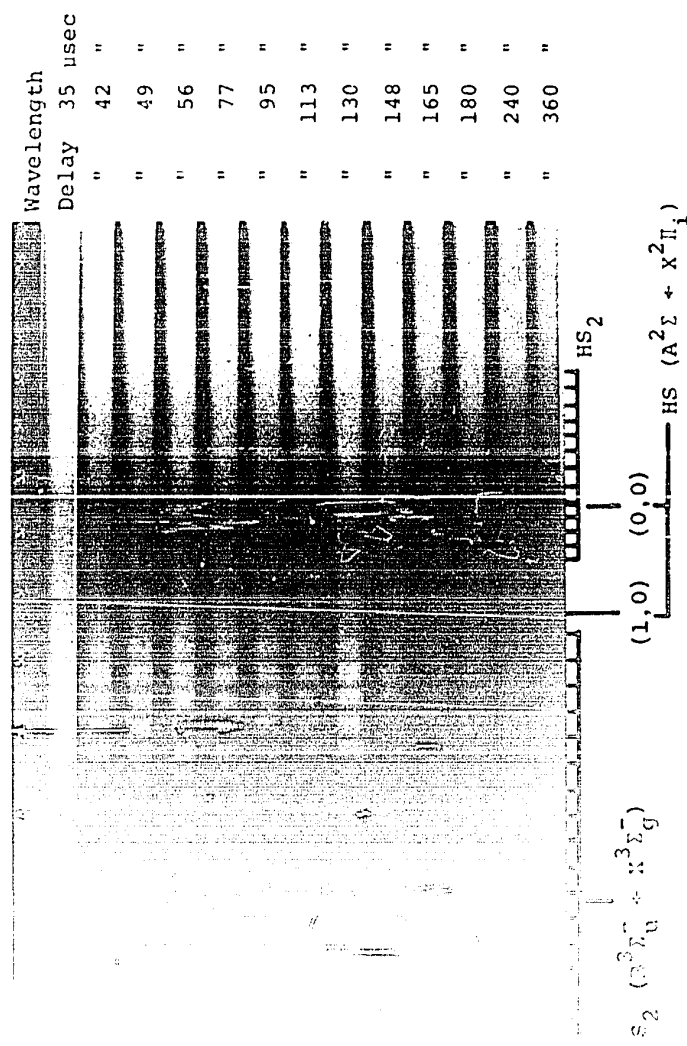
Figure 6. Spectra against time. 17 torr COS

+ 252 torr H$_2$.

C

Wavelength

Delay 35 μsec

" 42
" 49
" 56
" 77
" 95
" 113
" 130
" 148

$S_2 (B^3\Sigma_u^- \rightarrow X^3\Sigma_g^-)$

B

Wavelength

Delay 27 μsec

" 35
" 42
" 49
" 56
" 77
" 95
" 113
" 130
" 148

$S_2 (B^3\Sigma_u^- \rightarrow X^3\Sigma_g^-)$

$S_2 (b^1\Delta_u \rightarrow a^1\Delta_g)$

Wavelength

Delay 40 μsec

" 77
" 95
" 130
" 100
" 240
" 350
" 550

$S_2 (b^1\Delta_u \rightarrow a^1\Delta_g)$
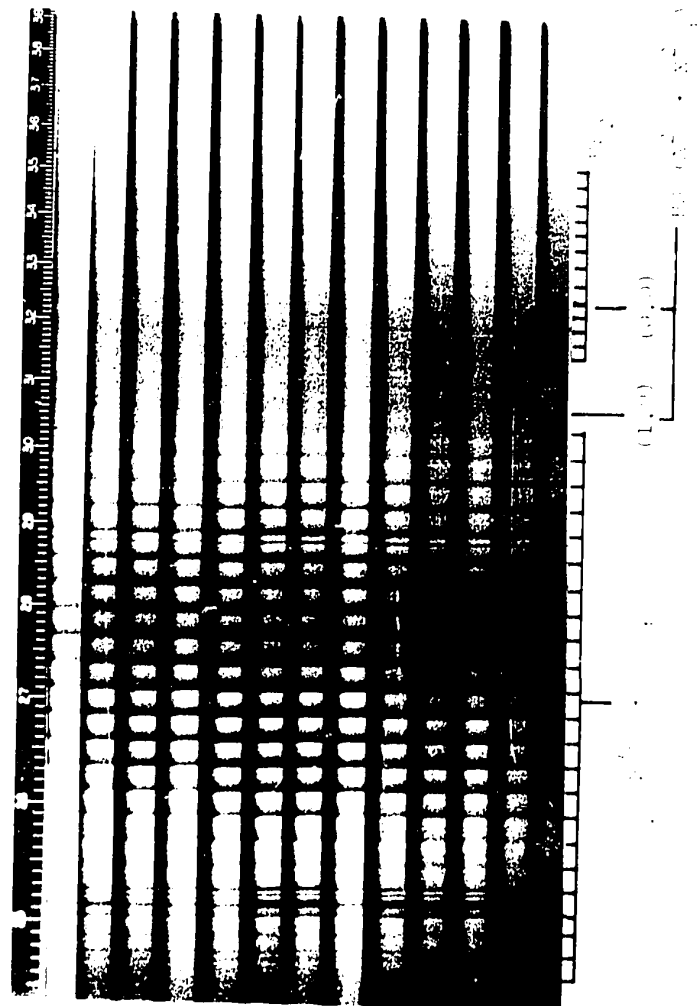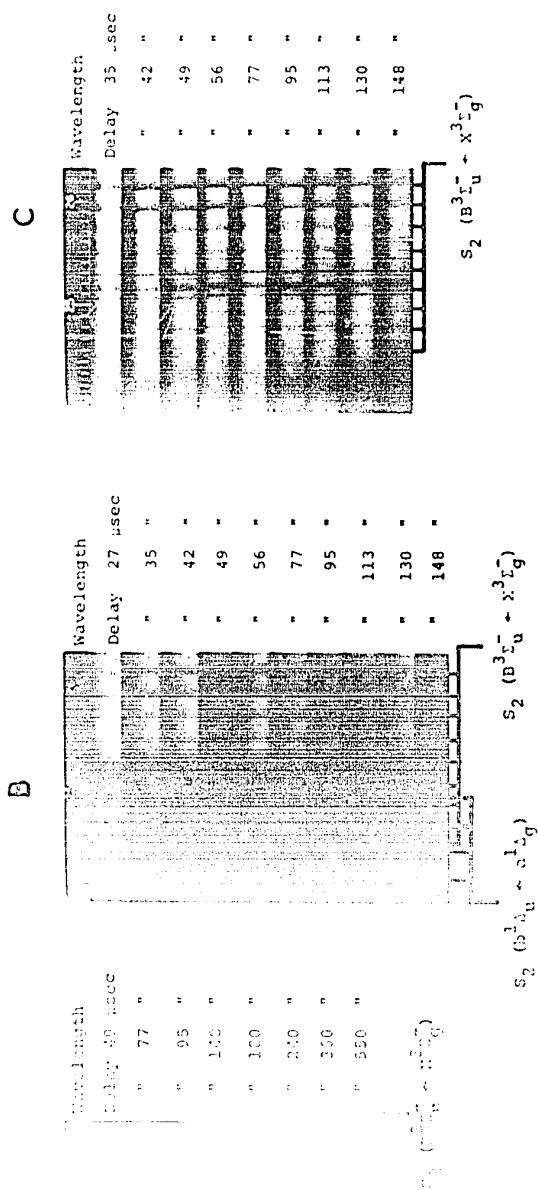
Figure 7. Formation of S_2 $(^1\Delta_g)$ in the flash photolysis of:

A) 17 torr COS; B) 20 torr COS + 300 torr D_2;

C) 17 torr COS + 252 torr H_2.
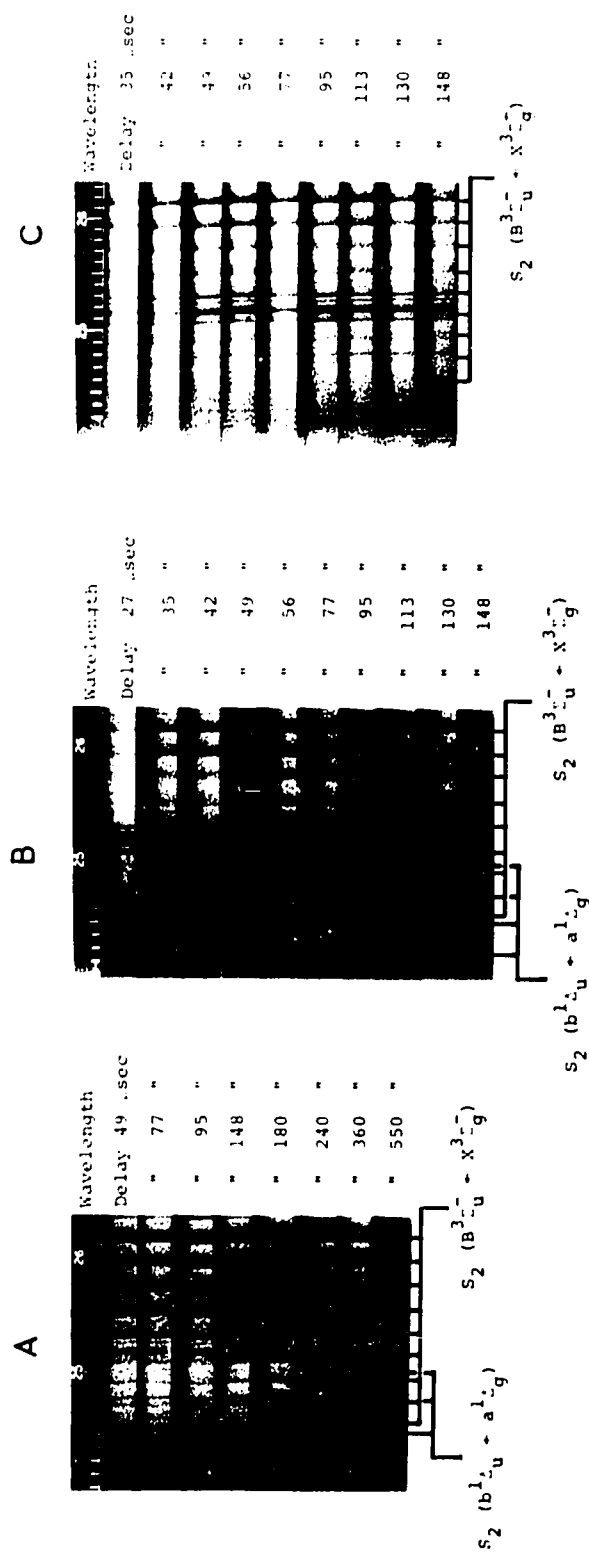
Plate 7. Formation of S_2 ($^1\Delta_g$) in the flash photolysis of:

A) 17 torr COS; B) 20 torr COS + 300 torr D_2;

C) 17 torr COS + 252 torr H_2.

S_2 $(^3\Sigma_g^-)$. First, the rate of formation and the rate of decay increased. In the absence of hydrogen, the maximum of the S_2 curve occurred at 250 usec. In the presence of 32.5, 124, 252, 412, and 595 torr H_2, the corresponding times were 150, 120, 100, 95, and 90 µsec respectively. The rate of decay increased as shown in Figure 32, the second order plots for S_2 removal. Secondly, the amount of S_2 formed decreased as the hydrogen pressure increased.

c) The HS spectrum appeared at the shortest delay times and at maximum intensity at all pressures of hydrogen. The amount of HS formed, as estimated from the O.D. at the shortest delay, was observed to increase at increasing hydrogen pressures, reaching a maximum value at 400 torr H_2. Further increase of hydrogen pressure caused a decrease in the HS yield as shown in Table IX The rate of HS decay also increased with increasing pressure

d) The HS_2 spectrum appeared to increase with increasing hydrogen pressure but even at its greatest intensity, O.D. < 0.02, no meaningful densitometry could be performed. ---

e) The only stable product that could be isolated and quantitatively determined was hydrogen sulfide. Table X shows that the yield of hydrogen sulfide increases as the hydrogen pressure is increased.

The flash photolysis of 20 torr COS + 300 torr D_2 resulted in the formation of the transients DS $(^2\Pi_i)$, DS_2, S_2 $(^3\Sigma_g^-)$, and
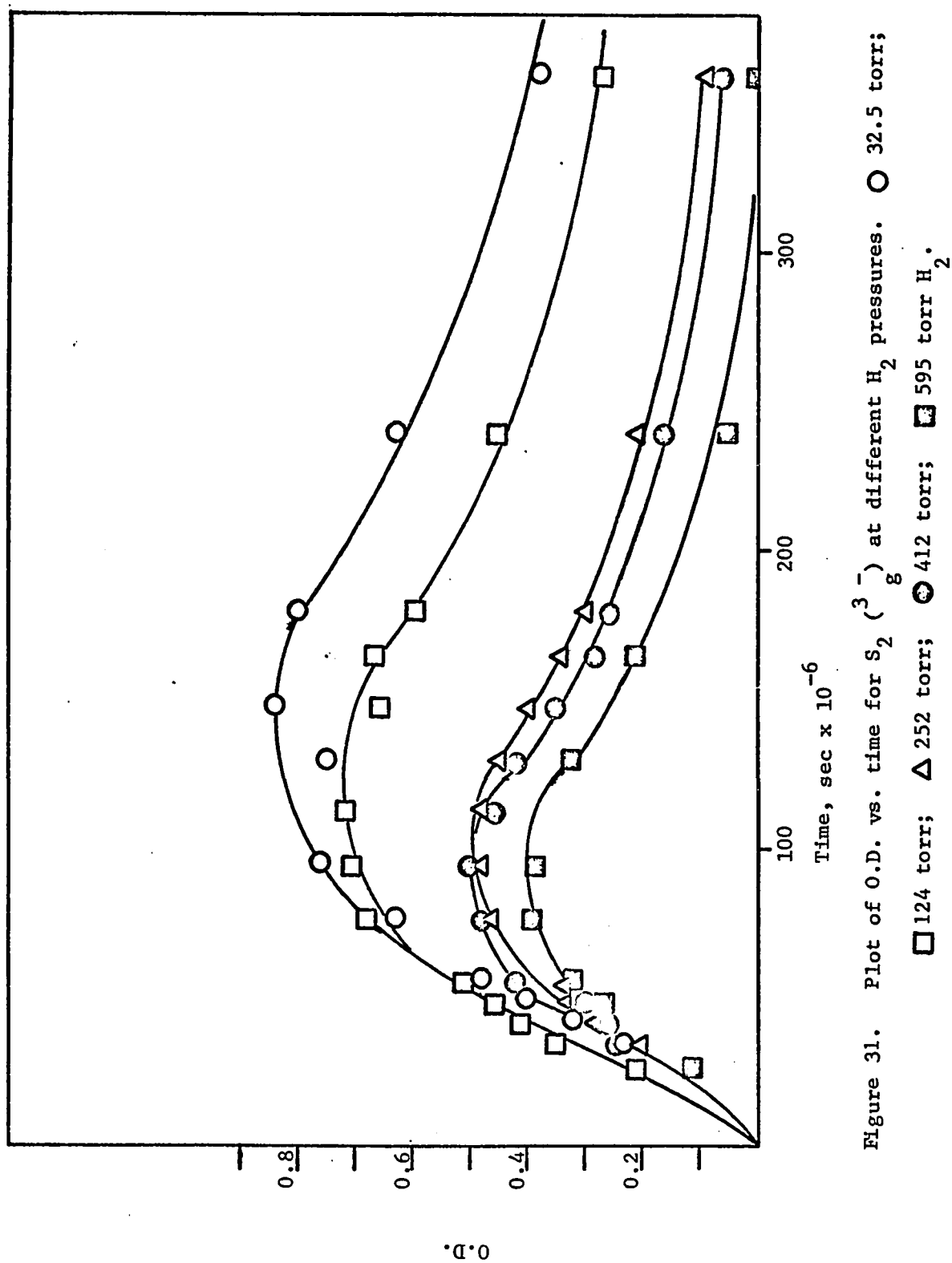
Figure 31. Plot of O.D. vs. time for S_2 ($^3\Sigma_g^-$) at different H_2 pressures. ○ 32.5 torr; □ 124 torr; △ 252 torr; ◉ 412 torr; ▣ 595 torr H_2.
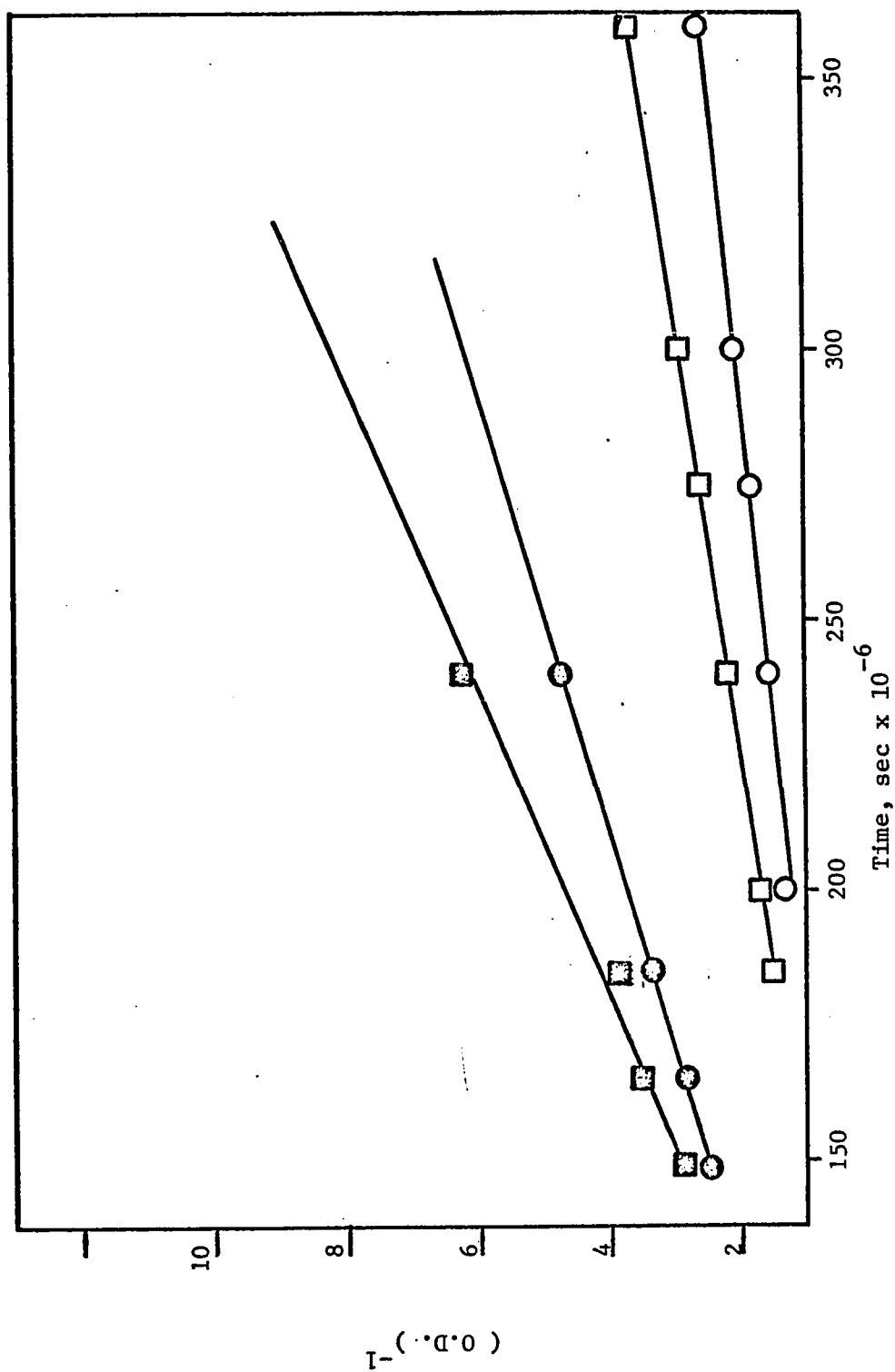
Figure 32. Second order plots for S_2 ($^3\Sigma_g^-$) decay in the flash photolysis of 17 torr
COS + $\bigcirc$ 32.5 torr; $\square$ 124 torr; $\bigcirc$ 252 torr; and $\square$ 412 torr H_2.

TABLE IX

YIELD OF HS AS A FUNCTION OF H_2 PRESSURE

H_2 pressure torr	HS yield O.D.
32.5	0.08
124.0	0.09
252.0	0.14
412.0	0.16
595.0	0.12

TABLE   X

<u>YIELD OF H_2S AS A FUNCTION OF H_2 PRESSURE</u>

H_2 pressure torr	H_2S / CO_o *
88	0.27
180	0.35
370	0.45
550	0.64

*

2 x CO_o is the yield of CO per flash in the absence of hydrogen. CO_o corresponds to the yield of S (^{1}D) atoms per flash

S_2 $(^1\Delta_g)$. The formation and decay of S_2 $(^3\Sigma_g^-)$ and DS are shown in Figure 33. The spectrum of DS_2 is too weak for densitometry but can be seen to reach maximum intensity within 95 μsec and decay within 240 μsec. The spectrum of S_2 $(^1\Delta_g)$ is obscured by the COS continuum but can be seen to reach maximum intensity within about 76 μsec and decay within about 165 μsec.

The flash photolysis of 17 torr COS in the presence of 124 torr H_2 + 600 torr CO_2 was also investigated and the following results were observed. The HS_2 spectrum was suppressed, the HS spectrum intensity was decreased by a factor of three, the S_2 $(^3\Sigma_g^-)$ was unaffected, and a weak absorption due to S_3 appeared. The formation and decay of S_2 $(^3\Sigma_g^-)$ is shown in Figure 34. The HS spectrum is at maximum intensity at 35 μsec and decays by about 100 μsec. The corresponding times for S_3 were 100 and 400 μsec respectively.

Methane.

The flash photolysis of 31 torr COS + 70 torr CH_4 resulted in the formation of the transients: S_2 $(^1\Delta_g)$, S_2 $(^3\Sigma_g^-)$, HS $(^2\Pi_i)$, HS_2, and CS $(^1\Sigma^+)$. The stable products of the reaction were: CO, H_2S, H_2S_2, CH_3SCH_3, $CH_3S_2CH_3$, and sulfur. The series of absorption spectra in Plate 8 show the formation and decay of the transients. The HS spectrum was at maximum intensity at the shortest delay and decayed within 100 μsec. The S_2 $(^3\Sigma_g^-)$ spectrum

Figure 33. O.D. vs. time for S_2 ($^3\Sigma_g^-$) and DS ($^2\Pi_i$). $\bigcirc$ 17 torr COS + 252 torr H_2, S_2 ($^3\Sigma_g^-$).

20 torr COS + 290 torr D_2, $\square$ S_2 ($^3\Sigma_g^-$); $\triangle$ DS ($^2\Pi_i$).
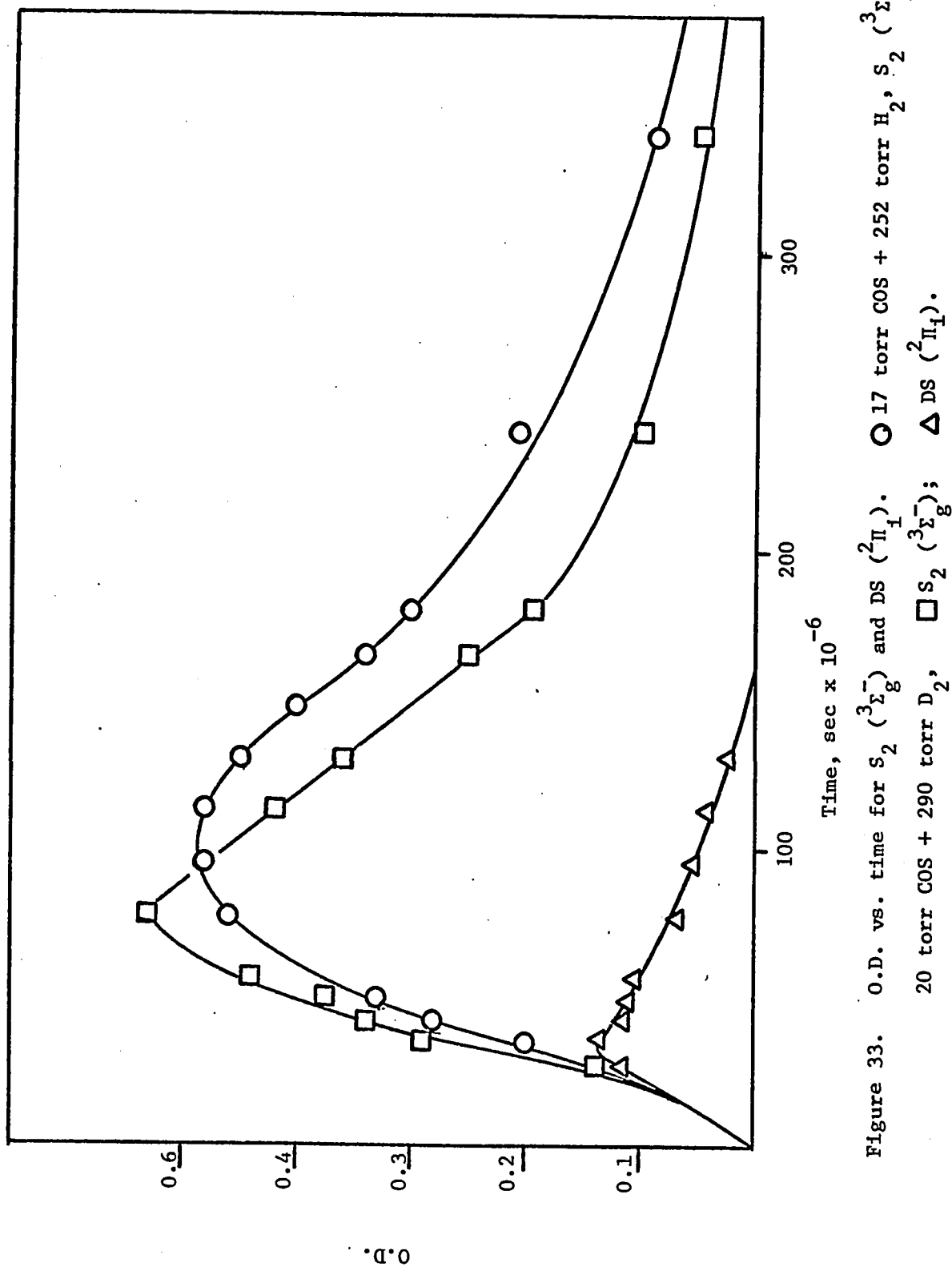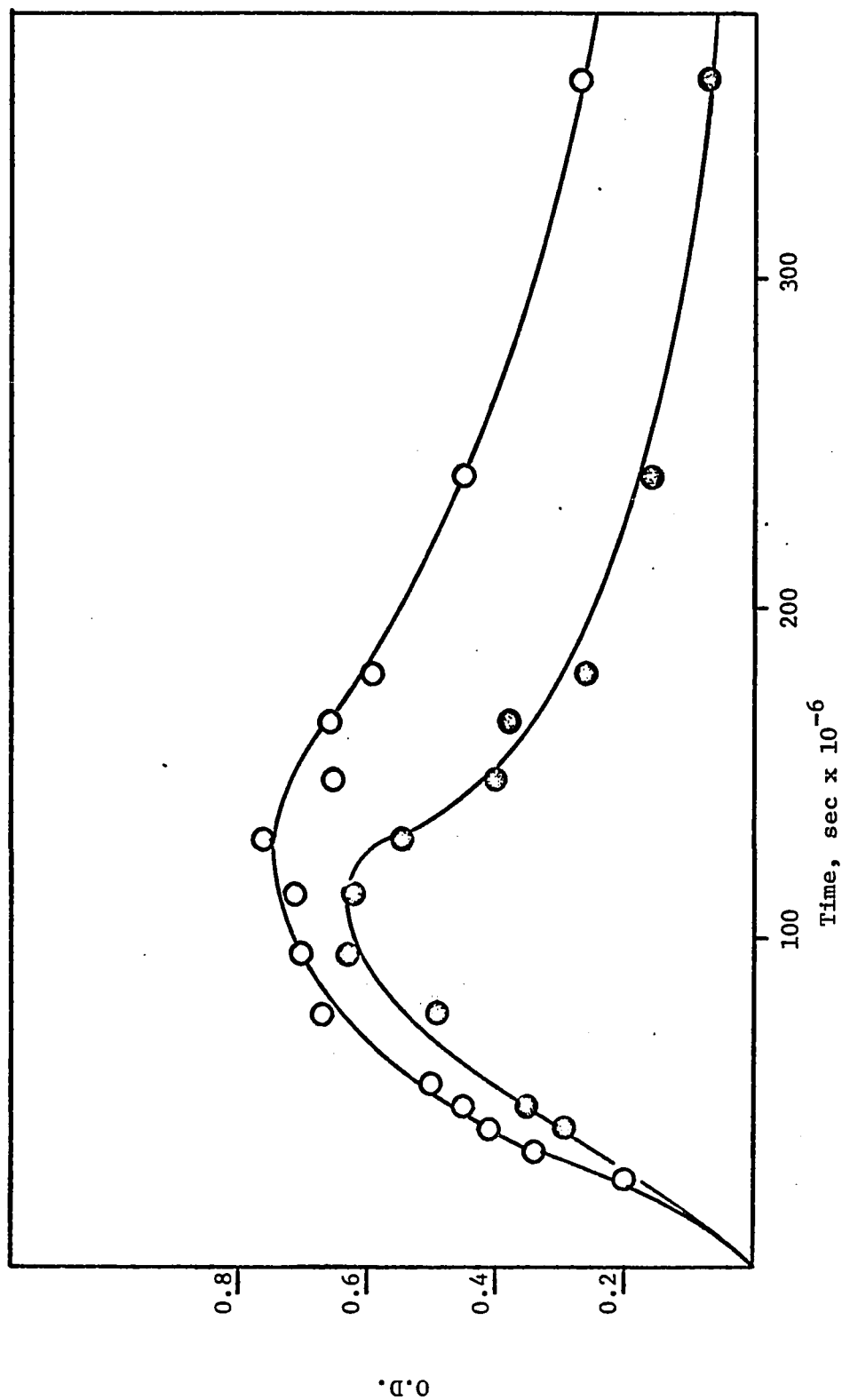
Figure 34. O.D. vs. time for S_2 ($^3\Sigma_g^-$). ⭕ 17 torr COS + 124 torr H_2. ◉ 17 torr COS
+ 124 torr H_2 + 600 torr CO_2.

Plate 8. Spectra against time. 31 torr COS + 70 torr CH$_4$.

Wavelength

Delay	27 μsec
"	35 "
"	42 "
"	49 "
"	56 "
"	77 "
"	95 "
"	113 "
"	130 "
"	148 "
"	165 "
"	180 "
"	240 "
"	360 "

HS$_2$

HS ($A^2\Sigma \rightarrow X^2\Pi_i$)

(0,0)

(1,0)

S$_2$ ($B^3\Sigma_u^- \rightarrow X^3\Sigma_g^-$)

(0,0)(1,1)
CS ($A^1\Pi \rightarrow X^1\Sigma^+$)

S$_2$ ($b^1\Delta_u \rightarrow a^1\Delta_g$)

Wavelength

Delay	27 μsec
"	35 "
"	42 "
"	49 "
"	56 "
"	77 "
"	95 "
"	113 "
"	130 "
"	148 "
"	165 "
"	180 "
"	240 "
"	360 "

(0,0)(1,1)

(0,0)

CS_2

C_2

S_2 (B$^3\Sigma_u^-$ — X$^3\Sigma_g^-$)   (1,0)   (0,0)

HS (A$^2\Sigma^+$ — X$^2\Pi_i$)

Plate 6.   Spectra against time.   31 torr COS
+ 70 torr CH$_4$.

reached maximum intensity within 50 μsec and decayed within 400

μsec. The S_2 ($^1\Delta_g$) spectrum was obscured by the COS continuum but

could be seen to be at maximum intensity at the shortest delay and

decay by 60 μsec. The HS_2 spectrum reached maximum intensity within

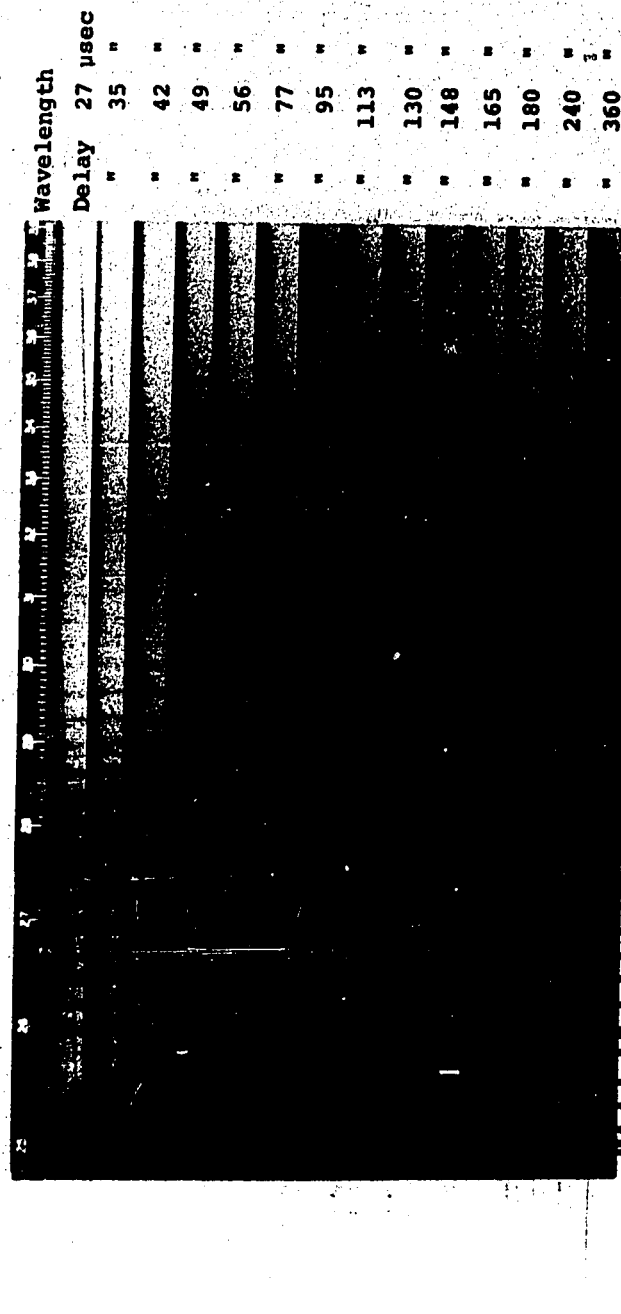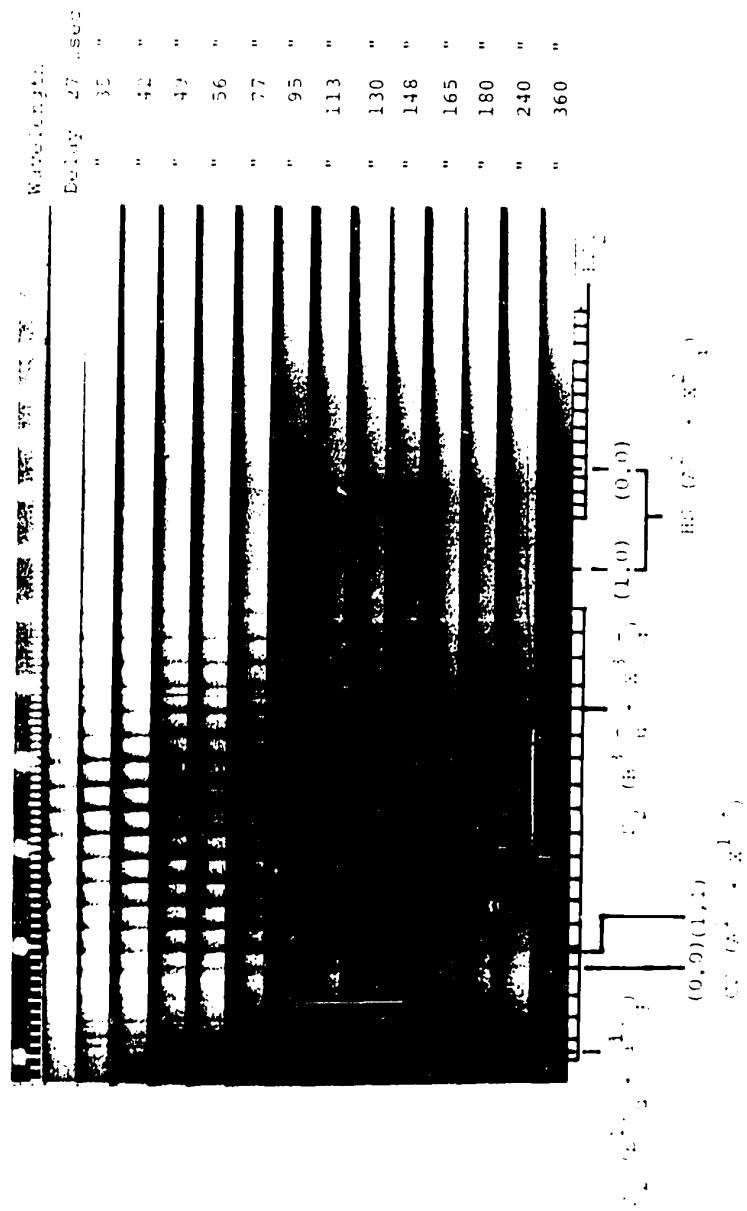70 μsec and decayed within 240 μsec. The CS spectrum was at

maximum intensity at the shortest delay and did not diminish in

intensity over the delay range used. The CS spectrum decayed

below the limit of detectibility within 2 minutes. The vibrationally

excited states CS v"= 1,2, were also detected at short delay times

but they decayed within 50 μsec.

The effect of increasing methane pressure was examined

using 0, 30, 70, 155, 290, and 590 torr CH_4 pressures. The

following results were observed:

a) The intensity of the CS spectrum decreased with

increasing methane pressure. The vibrationally excited states of

CS were relaxed at higher rates. At 590 torr CH_4, only the ground

vibrational state of CS could be observed.

b) The yield of S_2 ($^3\Sigma_g^-$) decreased with increasing

methane pressure as shown in Figure 35. The rate of formation of

S_2 ($^3\Sigma_g^-$) is greatly increased by the addition of the first 30

torr CH_4 but further increase of methane pressure had little effect.

The rate of decay of S_2 is shown in Figure 36 and can be seen to

increase at increased methane pressure.

c) S_2 ($^1\Delta_g$) is decreased by methane pressure. Above
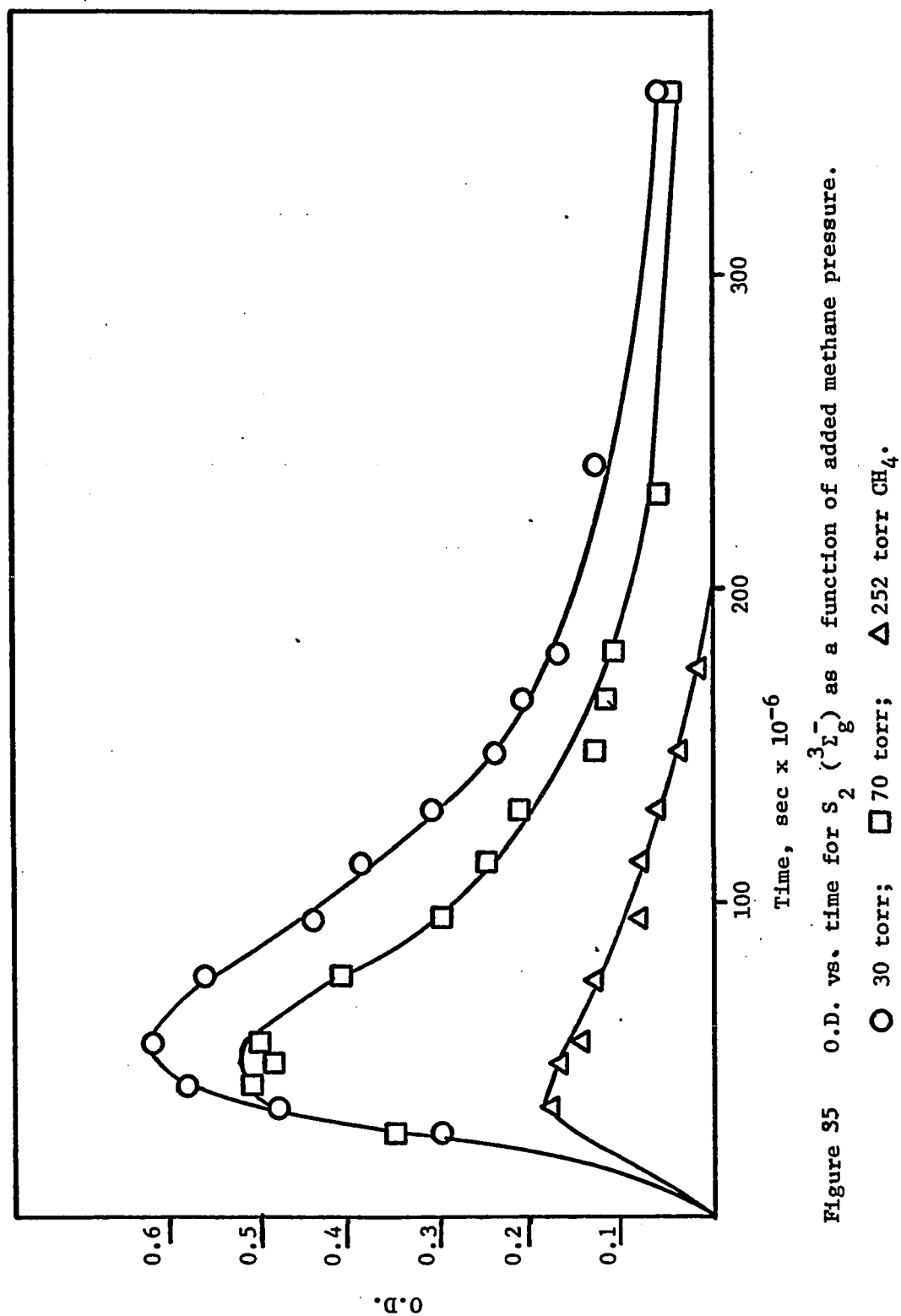
Figure 35   O.D. vs. time for S_2 ($^3\Sigma_g^-$) as a function of added methane pressure.

○ 30 torr;   □ 70 torr;   △ 252 torr CH_4.
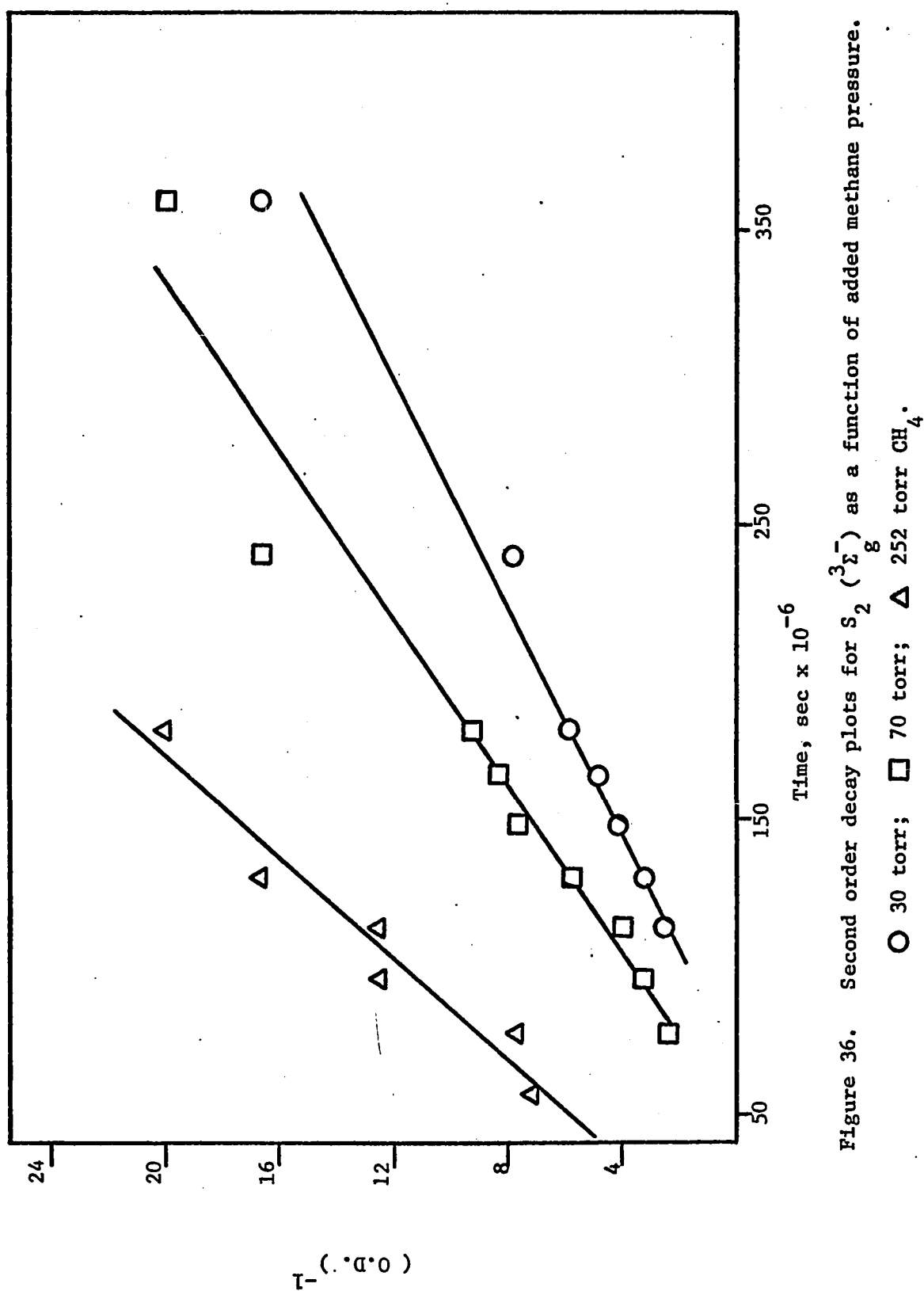
Figure 36. Second order decay plots for S_2 ($^3\Sigma_g^-$) as a function of added methane pressure.

$\bigcirc$ 30 torr; $\square$ 70 torr; $\triangle$ 252 torr CH_4.

300 torr CH_4, the spectrum could not be observed.

     d) The yield of HS decreased and its rate of decay increased with increasing methane pressure. The HS (1,0) band decreased in intensity by a factor of about five as the pressure of methane was increased from 30 torr to 290 torr.

     e) The amount of HS_2 formed decreased with increasing methane pressure but its rate of formation and decay were independent of pressure.

     f) The yield of hydrogen sufide decreased as shown in Table XI.

DISCUSSION

Hydrogen

     The primary reaction between S (^{1}D) atoms and hydrogen can be best envisaged as an insertive attack in close analogy with the insertion into paraffinic C - H bonds, namely

$$S \; (^1D) \; + \; H_2 \; \rightarrow \; H_2S^* \qquad\qquad \{1\}$$
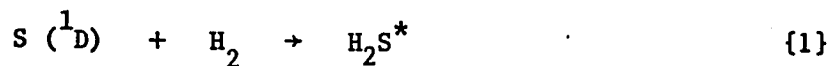
where * represents vibrational excitation. The enthalpy change of the insertion process is -97 Kcal/mole, while the D(HS-H) is only 91 Kcal/mole[47]. Consequently, the hot H_2S molecule may undergo thermal cracking. The presence of HS at short delays indicates that

TABLE XI

YIELD OF H_2S AS A FUNCTION OF ADDED METHANE PRESSURE

CH_4 pressure torr	H_2S / CO_o *
18	0.44
68	0.26
118	0.26
258	0.25
500	0.05

* 2 x CO_o is the yield of CO per flash in the absence of

methane. CO_o corresponds to the yield of S (^{1}D) atoms

produced in reaction 1

the cracking proceeds via

$$H_2S \rightarrow H + HS \qquad\qquad \{2\}$$

In Table IX, the HS yield can be seen to increase, reach a maximum, and start to decrease as the pressure of hydrogen is increased. This behavior of the HS yield demonstrates two points. First, at low pressures of hydrogen, not all the $S(^1D)$ atoms react with hydrogen. Some react with carbonyl sulfide

$$S(^1D) + COS \rightarrow CO + S_2 \qquad\qquad \{3\}$$

As the hydrogen pressure is increased, reaction {1} competes more favorably with reaction {3} as indicated by the increasing HS yield. Secondly, above 400 torr H_2, the HS yield decrease indicates that the hot H_2S molecule is collisonally deactivated via

$$H_2S^* + M \rightarrow H_2S + M^* \qquad\qquad \{4\}$$
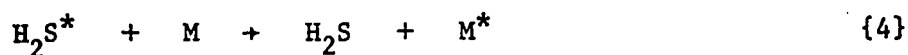
Therefore, the HS yield is detemined by a competition between reactions {1} and {3} and between {2} and {4}.

Hydrogen sulfide is formed in several ways. At high hydrogen pressures, it is formed mainly in reaction {4}. At low pressures it is formed in the reactions of HS, namely,

$$2\ HS \rightarrow H_2S + S(^3P) \qquad\qquad \{5\}$$

$$2\ HS + M \rightarrow H_2S_2 + M^* \qquad\qquad \{6\}$$

$$H_2S_2 + wall \rightarrow H_2S + sulfur \qquad\qquad \{7\}$$
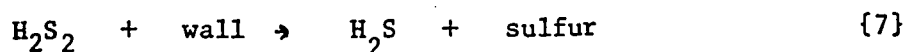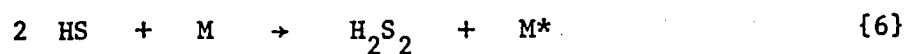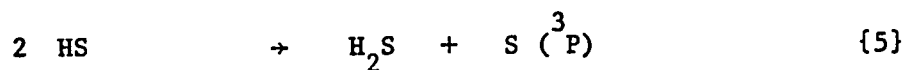
Reaction {7} may occur in the reaction cell or during the analytical process.

The fate of the H atoms produced in reaction {2} is most probably

$$COS + H \rightarrow CO + HS \qquad \{8\}$$

however this could not be demonstrated since HS is produced by other means also. Assuming that all the H atoms react via {8}, then the yield of hydrogen sulfide is independent of the method of its formation. Thus, the ratio of H_2S / CO_o indicates the extent of insertion of S (^1D) into hydrogen. From Table X, at 550 torr H_2, the value of the ratio is 0.65 and only about 65% of the S (^1D) atoms react with hydrogen. This indicates that k_8/k_3 is about 5×10^{-2}. This low reactivity is difficult to justify since the reactivity of methane is about the same as COS (vide infra).

The rapid rate of decomposition of H_2S^* seems reasonable since the reaction is highly exothermic. The hot molecule has 6 Kcal/mole in excess of the energy needed to break the HS - H bond. Also, H_2S has only three vibrational modes into which the excess energy can be partitioned. Unless the molecule will undergo a few collisions within a short time after its formation, it will fragment.

The transient HS_2 is formed via the reaction

$$HS + S (^3P) \rightarrow HS_2 \qquad \{9\}$$

The intensity of this absorber is very low, O.D. < 0.02, and the amount of HS removed from the reaction will not affect the H_2S yield. The fate of the HS_2 radical is disproportionation and recombination.

$$2 \ HS_2 \ \rightarrow \ H_2S_4 \qquad \qquad \{10\}$$

$$\rightarrow \ H_2S_2 \ + \ S_2 \qquad \qquad \{11\}$$
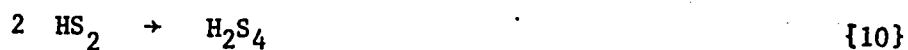
These reactions will be demonstrated in Chapter VIII.

Since considerable cracking of the hot H_2S occurs even at high hydrogen pressures, consideration must be given to the $S\ (^3P)$ atoms formed in reaction {5}.

Triplet sulfur atoms would not be expected to insert and the abstraction reaction

$$S\ (^3P) \ + \ H_2 \ \rightarrow \ HS \ + \ H$$
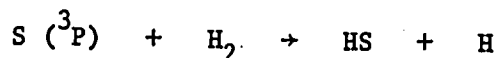
would be endothermic to the extent of 21 Kcal/mole. Consequently, the abstraction is not important at low temperatures. This point was demonstrated by the addition of carbon dioxide to the system. A CO_2/H_2 ratio of about 5 was sufficient to cause a three fold decrease in the HS yield. This decrease is attributed to the relaxation of $S\ (^1D)$ to $S\ (^3P)$ by CO_2 and the fact that triplet sulfur does not react with hydrogen. This decrease could also be consistent with the relaxation of H_2S^*. However, the yield of S_2 in the presence of carbon dioxide is very nearly the same as in its absence, indicating triplet sulfur atoms recombined rather than reacted with hydrogen.

The fate of the S (^{3}P) atoms is recombination via

$$2\ S\ (^3P)\ +\ M\ \rightarrow\ S_2\ +\ M*\qquad\qquad\{12\}$$
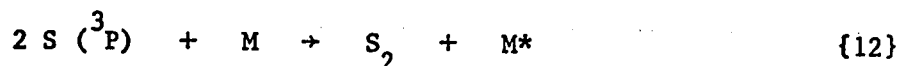
where S_2 represents the three possible states of S_2 namely, $^3\Sigma_g^-$, $^1\Delta_g$, and $^1\Sigma_g^+$. In the recombination, carbonyl sulfide is the more efficient third body since it can act as a chaperon.

S_2 ($^1\Delta_g$) was only detected at the lowest pressure of hydrogen, 32.5 torr, and at the shortest time delay, 27 μsec. Yet, considerable amounts of the singlet should have been formed in the recombination of triplet sulfur atoms. This absence of the $^1\Delta_g$ state can be attributed either to a rapid chemical reaction with hydrogen or to an efficient relaxation of the singlet state by H_2.

In the presence of 300 torr deuterium, the $^1\Delta_g$ spectrum can be seen for about 165 μsec, Plate 7 , while in the presence of 252 torr H_2, the spectrum is absent even at the shortest delay. It is expected that if S_2 ($^1\Delta_g$) underwent reaction with hydrogen, it would also react to the same extent with deuterium, since S (^{1}D) showed the same reactivity to hydrogen as to deuterium. Therefore it can be concluded that the chemical reaction is not the cause of the rapid removal of S_2 ($^1\Delta_g$).

For collisional relaxation to be rapid, there must exist a near resonance condition between the donor and the acceptor. Callear[48] noted that in the relaxation of vibrationally excited NO, only states with closely matched vibrational levels would be

involved in the relaxation process. Thus

$$NO_{v''=n} + NO_{v''=n-2} \rightarrow 2\,NO_{v''=n-1}$$
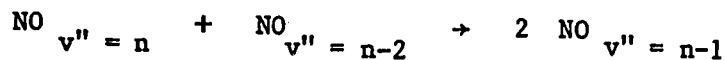
would proceed rapidly while the process

$$NO_{v''=n} + NO_{v''=n-3} \rightarrow \text{relaxation}$$
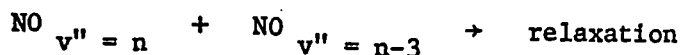
did not occur at a significant rate. This was further substantiated by the observation that the $v'' = 1$ state of NO was long lived since ground state NO was ineffective at relaxing this state.

A similar process is responsible for the rapid relaxation of S_2 ($^1\Delta_g$) state by hydrogen. The energy donated by the excited S_2 is most likely taken up by hydrogen as vibrational energy. $v(1,0)$ for hydrogen is 3927.15 cm^{-1}, or 11.23 Kcal/mole.[45] The $T_{0,0}$ for the $^1\Delta_g \rightarrow {}^3\Sigma_g^-$ transition is still uncertain but Barrow[49] has reported three probable values, 5500, 5400, and > 3800 cm^{-1}, corresponding to 15.72, 15.44, and > 10.86 Kcal/mole respectively. Since even at the shortest delay times, both the singlet and the triplet S_2 are in their respective ground vibrational states, the value 3927 cm^{-1} may be assigned to the $T_{0,0}$ in close agreement with one of Barrow's values. Since deuterium, $v(1,0) = 2993.4$ cm^{-1}, does not meet this resonance condition, the relaxation process is slow and the $^1\Delta_g$ state is long lived. This is observed in the results and supports the above argument.

Thus, S_2 ($^3\Sigma_g^-$) is formed directly in reaction {12} as well

as in the collisional relaxation of the $^1\Delta_g$ state

$$S_2 \ (^1\Delta_g) \ + \ H_2 \ \rightarrow \ S_2 \ (^3\Sigma_g^-) \ + \ H_2^* \qquad \{13\}$$
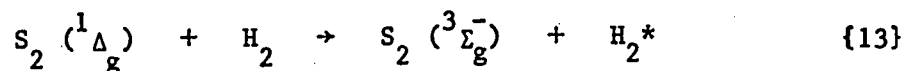
In the absence of hydrogen, the triplet state forms slowly, Figure

4. The addition of 30 torr H_2 greatly increases the rate of formation

of the triplet, further supporting the relaxation process proposed

above. Further increase in added hydrogen pressure has little effect

on the rate of triplet appearence.

Inspection of Figure 31 indicates that the yield of S_2

decreases with increasing hydrogen pressure. This result is

consistent with reaction {3} being important at low hydrogen pressures

while at high pressures, reaction {5} followed by {12} is the more

important S_2 forming step.

$S_2 \ (^3\Sigma_g^-)$ removal is found to obey second order, pressure

dependent kinetics, and is best described by

$$2 \ S_2 \ (^3\Sigma_g^-) \ + \ M \ \rightarrow \ S_4 \ + \ M^*$$

From the slopes of the curves in Figure 32, second and third order

rate constants for {14} are calculated and listed in Table XII.

TABLE XII

RATE CONSTANTS FOR S_2 $(^3\Sigma_g^-)$ DECAY AS A FUNCTION OF ADDED GAS PRESSURE

COS torr	Added gas	torr	Slope $\times 10^{-4}$ sec	k_{13}, M^{-1} sec^{-1} $\times 10^{-10}$	k_{13}, M^{-2} sec^{-1} $\times 10^{-12}$
17	H_2	32.5	0.82 ± 0.05	0.58 ± 0.14	2.18 ± 0.57
17	H_2	124	0.98 ± 0.14	0.69 ± 0.22	0.90 ± 0.29
17	H_2	252	3.23 ± 0.58	2.28 ± 0.83	1.57 ± 0.57
17	H_2	412	3.56 ± 0.67	2.51 ± 0.92	1.09 ± 0.40
20	D_2	300	7.01 ± 0.84	4.94 ± 1.47	2.79 ± 0.83
17	H_2 / CO_2	124/600	4.82 ± 0.48	3.40 ± 0.93	0.85 ± 0.23

Methane

The primary reaction between $S\ (^1D)$ atoms and methane in low intensity studies has been shown to be[22]

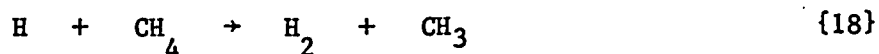$$S\ (^1D)\ +\ CH_4\ \rightarrow\ CH_3SH^* \qquad \{15\}$$

The enthalpy change in reaction $\{15\}$ is -83 Kcal/mole for thermal sulfur atoms and secondary cracking could follow. From the observed product distribution, the secondary decomposition of the hot mercaptan has been shown to be

$$CH_3SH^*\ \rightarrow\ CH_3S\ +\ H \qquad \{16\}$$

Since $D\ (CH_3S - H)$ is 89 Kcal/mole, reaction $\{16\}$ is endothermic to the extent of 6 Kcal/mole, but the $S\ (^1D)$ atoms have up to 12 Kcal/mole translational energy when formed and if this energy can survive the collisions before insertion, then reaction $\{16\}$ will be possible at room temperature. An alternate energetically more favorable decomposition

$$CH_3SH^*\ \rightarrow\ CH_3\ +\ HS \qquad \{17\}$$

had been neglected since the products of the reactions of HS, namely hydrogen sulfide and hydrogen disulfide, were not found. The mechanism proposed for the formation of the stable products was:

$$H\ +\ CH_4\ \rightarrow\ H_2\ +\ CH_3 \qquad \{18\}$$

$$2 \ CH_3S \quad \rightarrow \quad CH_3SSCH_3 \qquad \{19\}$$

$$\rightarrow \quad CH_2S \ + \ CH_3SH \qquad \{20\}$$

$$CH_3S \ + \ CH_3 \quad \rightarrow \quad CH_3SCH_3 \qquad \{21\}$$

$$\rightarrow \quad CH_2S \ + \ CH_4 \qquad \{22\}$$

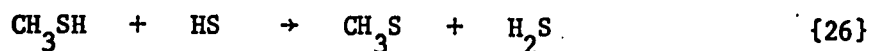$$2 \ CH_3 \quad \rightarrow \quad C_2H_6 \qquad \{23\}$$
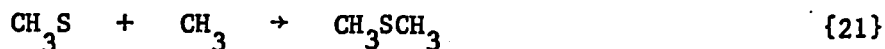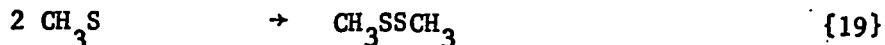
This mechanism was the only reasonable one that would explain the experimental results.

In this study, an important new stable product, hydrogen sulfide, was observed at low methane pressures. Also, the rapid appearence of the transient HS was observed at pressures as high as 600 torr. These two facts which escaped earlier investigations indicate that reaction {17} is important. However, the relative importance of reactions {16} and {17} could not be established. From purely energetic grounds it would appear that reaction {17} should be much more important than {16}.

The enthalpy change of reaction {17} is −7 Kcal/mole. Since the HS yield decreases as the pressure of methane is increased, the hot methyl mercaptan must undergo collisional relaxation via

$$CH_3SH^* \ + \ M \quad \rightarrow \quad CH_3SH \ + \ M^* \qquad \{24\}$$
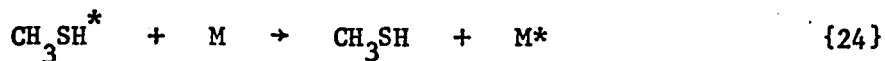
The most likely source of CH_3S is the reaction

$$CH_3SH + CH_3 \rightarrow CH_3S + CH_4 \qquad \{25\}$$

$$CH_3SH + HS \rightarrow CH_3S + H_2S \qquad \{26\}$$
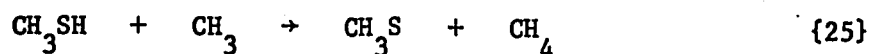
The stable products are explained in terms of reactions [19] to {23} as mentioned before.

An important source of hydrogen sulfide is the sequence of reactions

$$2\ HS \rightarrow H_2S + S\ (^3P) \qquad \{5\}$$

$$2\ HS + M \rightarrow H_2S_2 + M^* \qquad \{6\}$$

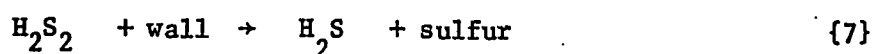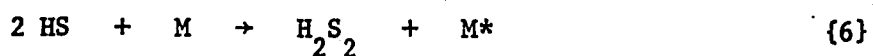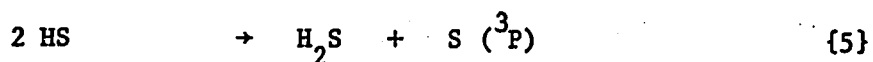$$H_2S_2 + wall \rightarrow H_2S + sulfur \qquad \{7\}$$

Table XI shows that the yield of hydrogen sulfide decreases as the pressure of methane increases. This is consistent with the fact that the fragmentation of the hot mercaptan is prevented at high pressures. At 18 torr CH_4, the H_2S / CO_o is 0.44 indicating that about 44% of the S (^1D) atoms end up as hydrogen sulfide. The mechanism of hydrogen sulfide formation indicates that the quantum yield of H_2S assuming complete scavenging of the S (^1D) atoms is 0.5. Since in this mixture the H_2S / CO_o, and hence the quantum yield of H_2S, is 0.44, about 88% of the sulfur atoms must have reacted with methane and only 12% with COS via reaction {3}. This high reactivity seems unreasonable since hydrogen was shown to be very unreactive and earlier low intensity studies have shown that paraffins have about the same reactivity as carbonyl sulfide.

It is proposed that there is an alternate cracking step, namely,

$$CH_3SH^* \rightarrow CH_2 + H_2S \qquad \{27\}$$

This step will explain the high quantum yield of hydrogen sulfide at low pressures. The enthalpy change of this reaction is +2 Kcal/mole. However, the S atoms may have some translational energy when the insertion takes place making reaction $\{27\}$ energetically feasable at room temperature. The quantum yield of H_2S is seen to decrease rapidly as the methane pressure is increased from 18 to 68 torr probably because the translational energy is more efficiently removed making reaction $\{27\}$ less favorable. Reaction $\{17\}$ is not as easily quenched since the HS spectrum is observed at methane pressures as high as 595 torr. This is due to the high exothermicity of the reaction. Therefore at high pressures reaction $\{27\}$ is unimportant and secondary cracking occurs via $\{17\}$.

HS_2 is formed by the recombination of HS and S. CS may be formed from one of the secondary products or from the secondary photolysis of carbon disulfide, a minor but strongly absorbing product, whose mode of formation is not known. The amounts of these transients formed is very small and will not influence the reaction. The probable fate of CH_2 formed in reaction $\{27\}$ is

$$CH_2 + CH_4 \rightarrow 2\ CH_3 \qquad \{28\}$$

The transient S_2 ($^1\Delta_g$) is produced either in reaction {3} or by the recombination of S (^3P) atoms from the reaction {5}. It suffers collisional relaxation to the ground $^3\Sigma_g^-$ state.

S_2 ($^3\Sigma_g^-$) decays by third body recombination. Second and third order rate constants for the recombination are listed in Table XIII. There is considerable scatter in the rate constants due to experimental error. However, they are of the same order of magnitude as other S_2 recombination rates.

TABLE XIII

RATE CONSTANTS FOR THE DECAY OF S_2 $(^3\Sigma_g^-)$ AS A FUNCTION OF ADDED CH_4

COS torr	CH_4 torr	Slope, sec $\times 10^{-4}$	k_{13}, M^{-1} sec^{-1} $\times 10^{-10}$	k_{13}, M^{-2} sec^{-1} $\times 10^{-10}$
31	30	6.66 ± 1.23	4.69 ± 1.68	14.30 ± 5.15
31	70	4.93 ± 0.90	3.48 ± 1.25	6.41 ± 2.31
31	155	12.70 ± 5.37	8.95 ± 5.37	8.95 ± 5.37
31	290	21.99 ± 7.90	15.50 ± 8.37	8.96 ± 4.83

THE PHOTOCHEMISTRY OF HYDROGEN DISULFIDE

RESULTS

Dark reaction

H_2S_2 with added CO_2

H_2S_2 with added C_2H_4 and C_3H_6

Reaction of CH_3 with H_2S_2

The effect of wavelength

H_2S_2 with added NO

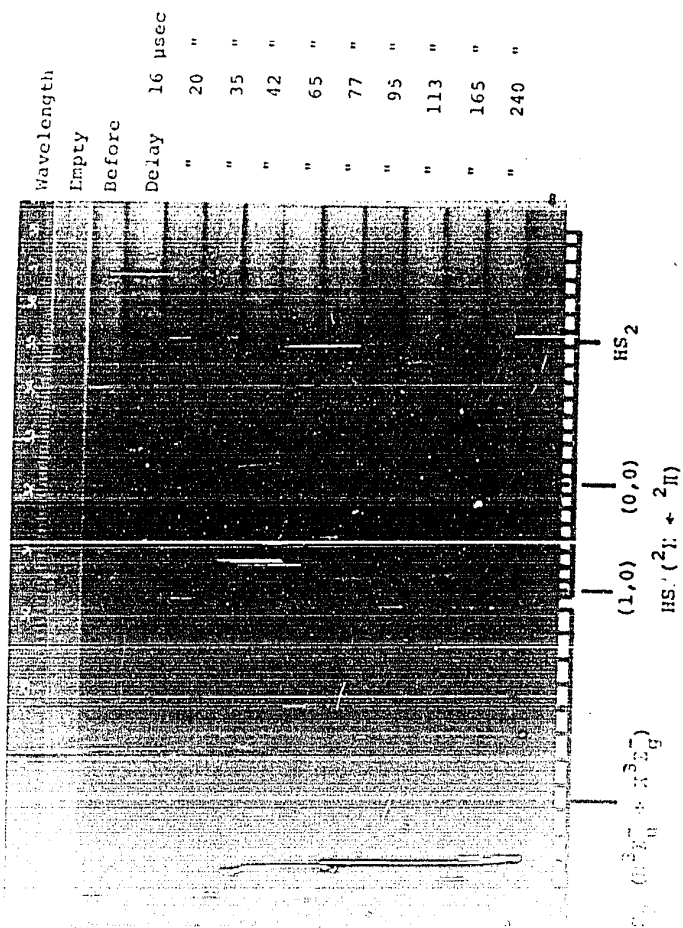Flash photolysis – kinetic mass spectrometry

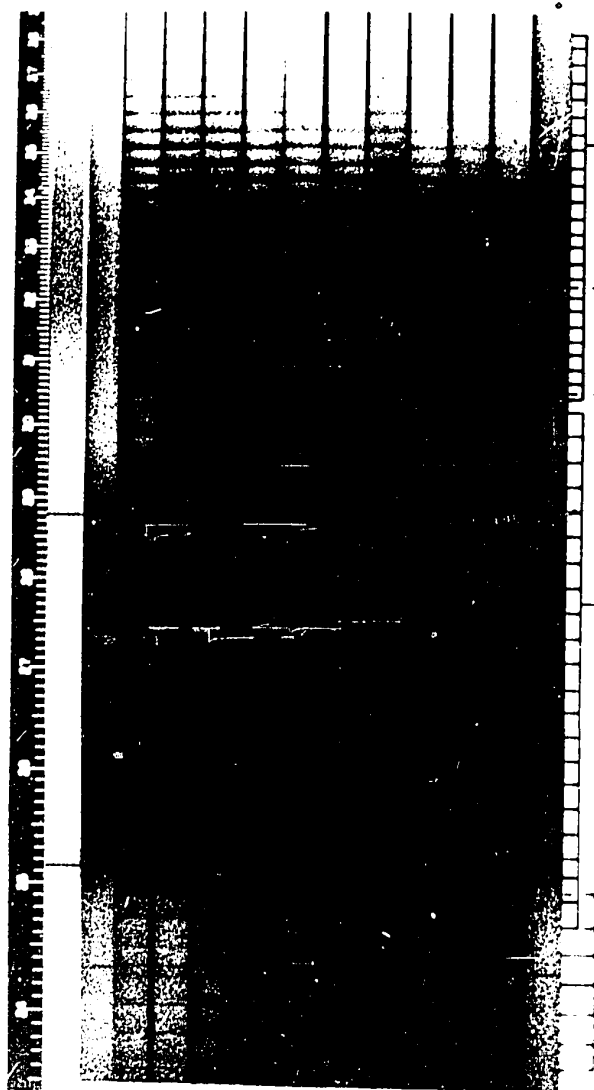## DISCUSSION

RESULTS

Dark reaction

Hydrogen disulfide was found to undergo dark decomposition when the cell was not preconditioned with HCl and when polymeric sulfur was formed as an end product of the photolysis. The products of the dark reaction were hydrogen sulfide and polymeric sulfur. No hydrogen or higher sulfanes could be found. The dark reaction proceeded to completion within minutes after initiation and could be detected by the sulfur polymer formed on the surfaces of the reaction vessel.

Hydrogen disulfide with added carbon dioxide.

The transients detected in the flash photolysis of 1.8 torr H_2S_2 in the presence of 100 torr CO_2 were: S_2 $(^1\Delta_g)$, S_2 $(^3\Sigma_g^-)$, HS $(^2\Pi_i)$, and HS_2. The stable products of the reaction were hydrogen (0.05 µmole/flash), H_2S, H_2S_3, H_2S_4, and sulfur. The series of absorption spectra in Plate 9 show the formation and decay of the intermediates. Both HS and HS_2 are at their maximum concentrations at the shortest delay time, 27 µsec, and decay within 113 and 240 µsec respectively. The S_2 $(^1\Delta_g)$ spectrum reached maximum intensity within 40 µsec and decayed within 95 µsec. The corresponding times for S_2 $(^3\Sigma_g^-)$ were 77 and 360 µsec respectively.

Wavelength

Empty

Before

Delay

16 μsec

20 "

35 "

42 "

65 "

77 "

95 "

113 "

165 "

240 "

HS_2

(0,0)

(1,0) $HS \cdot (^2\Sigma \rightarrow {}^2\Pi)$

point time.   1.8 torr H_2S_2 + 100 torr CO_2.

The effect of increasing diluent gas pressure was examined by carrying out the flash photolysis of 1.8 torr H_2S_2 in the presence of 25, 50, 100, and 200 torr CO_2. The following results were observed:

a) The rate of formation of HS was unaffected but its rate of decay increased as shown in Figure 37.

b) The rates of formation and decay of S_2 ($^3\Sigma_g^-$) were increased as shown in Figure 38.

c) The spectra of S_2 ($^1\Delta_g$) could not be densitometered with any meaningful accuracy due to background absorption by hydrogen disulfide and only qualitative observations could be made. The rate of formation was unaffected but the rate of decay increased. The times required to decay below the limit of detectibility at 25, 50, 100, and 200 torr CO_2 were: 113, 95, 77, and 56 µsec respectively.

d) The formation and the decay of HS_2 were found to be independent of diluent gas pressure as shown in Figure 39.

Hydrogen disulfide with added ethylene and propylene.

The flash photolysis of 1.8 torr H_2S_2 in the presence of ethylene gave two new products in addition to those found with carbon dioxide, namely, ethyl mercaptan and ethylene episulfide. No new transients were observed. Figure 40 shows the formation and the decay of the intermediates. Ethylene had several noticable effects

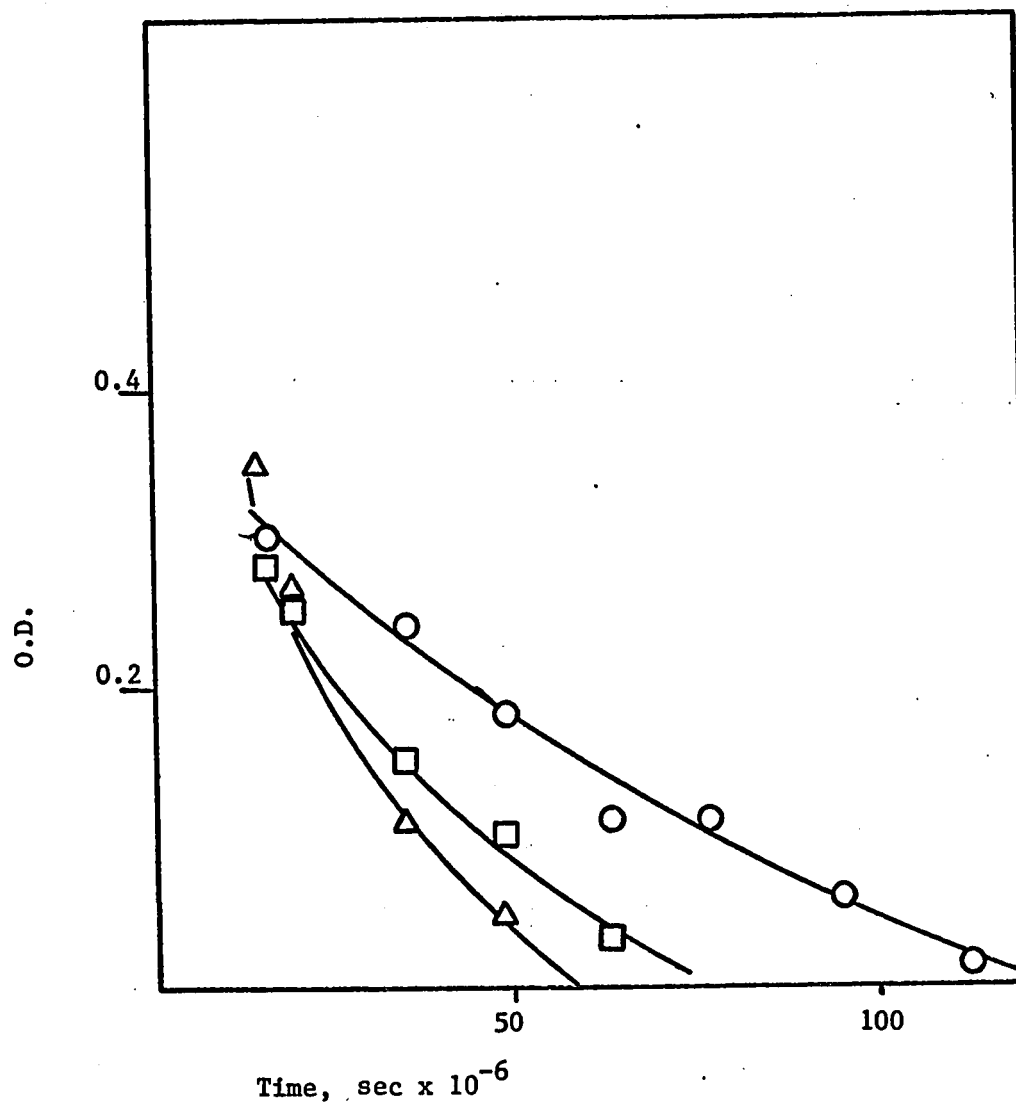Figure 37. Plots of O.D. vs time for HS decay at different pressures of CO_2. ◯ 25 torr; ☐ 100 torr; △ 200 torr.
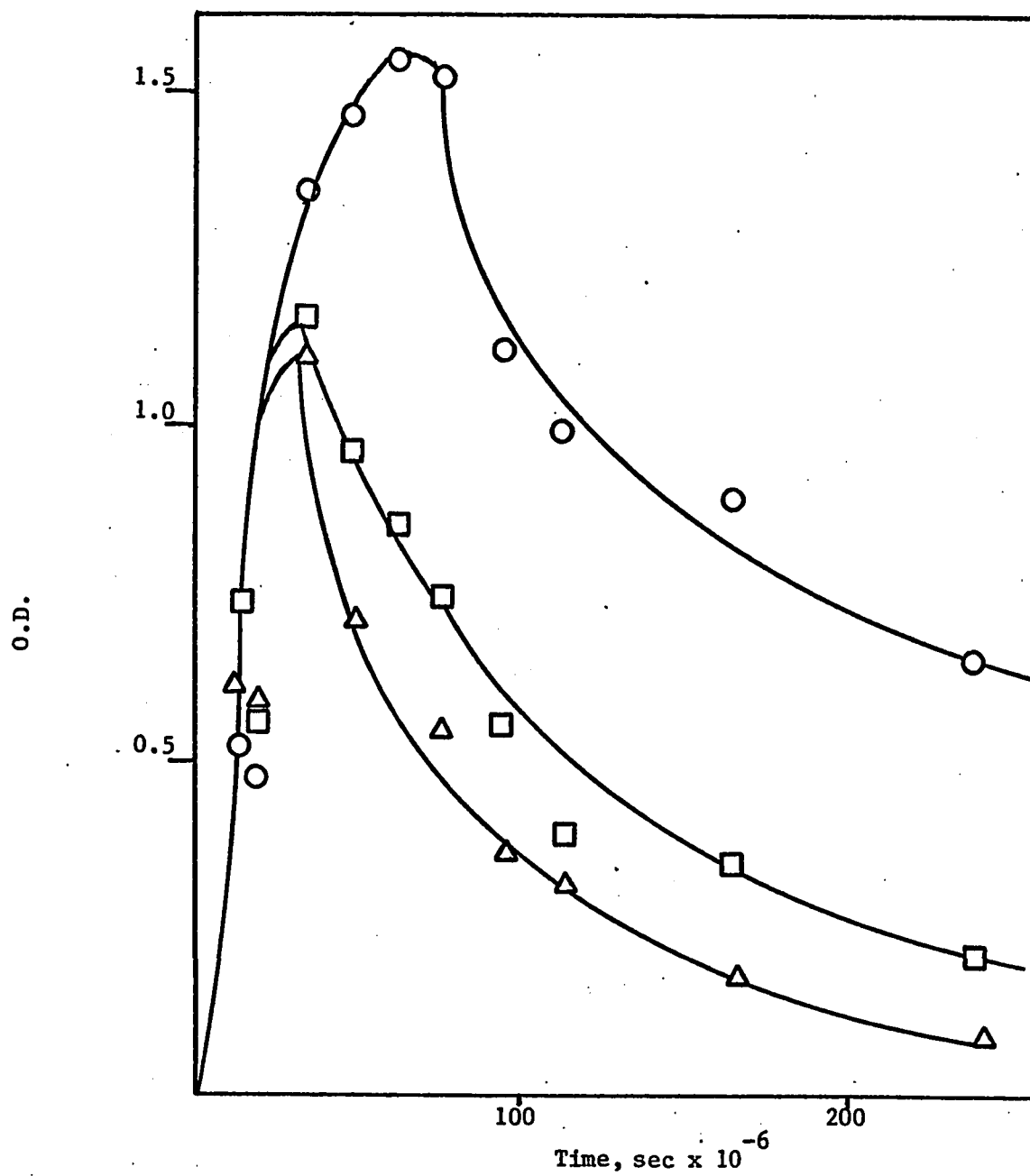
Figure 38. Plots of O.D. vs time for the decay of S_2 ($^3\Sigma_g^-$) at different pressures of CO_2. ○ 25 torr; □ 100 torr; △ 200 torr.
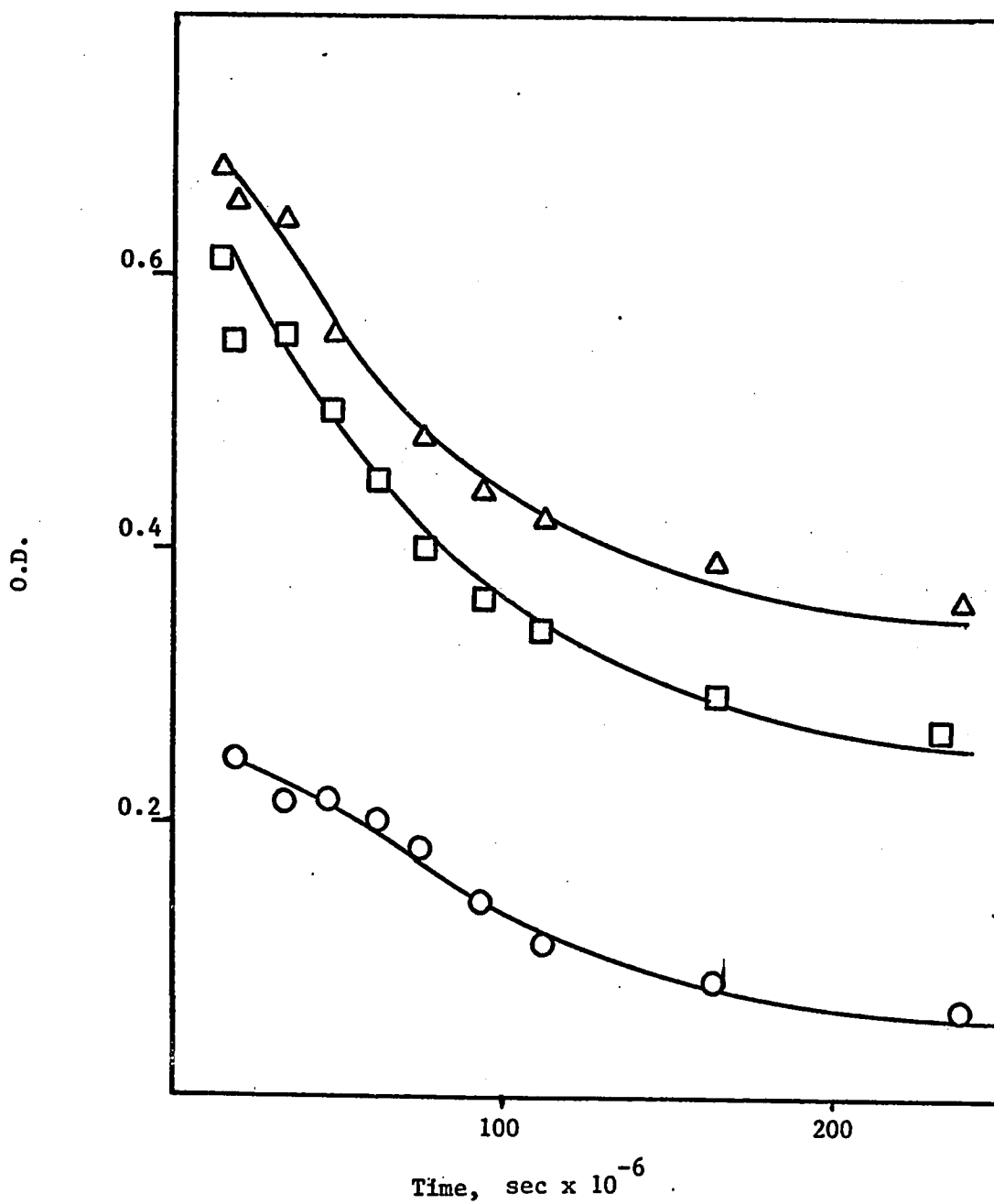
Figure 39.   Plots of O.D. vs. time for the decay of HS_2.

    O 25 torr CO_2, O.D. vs time; □ 100 torr, O.D.
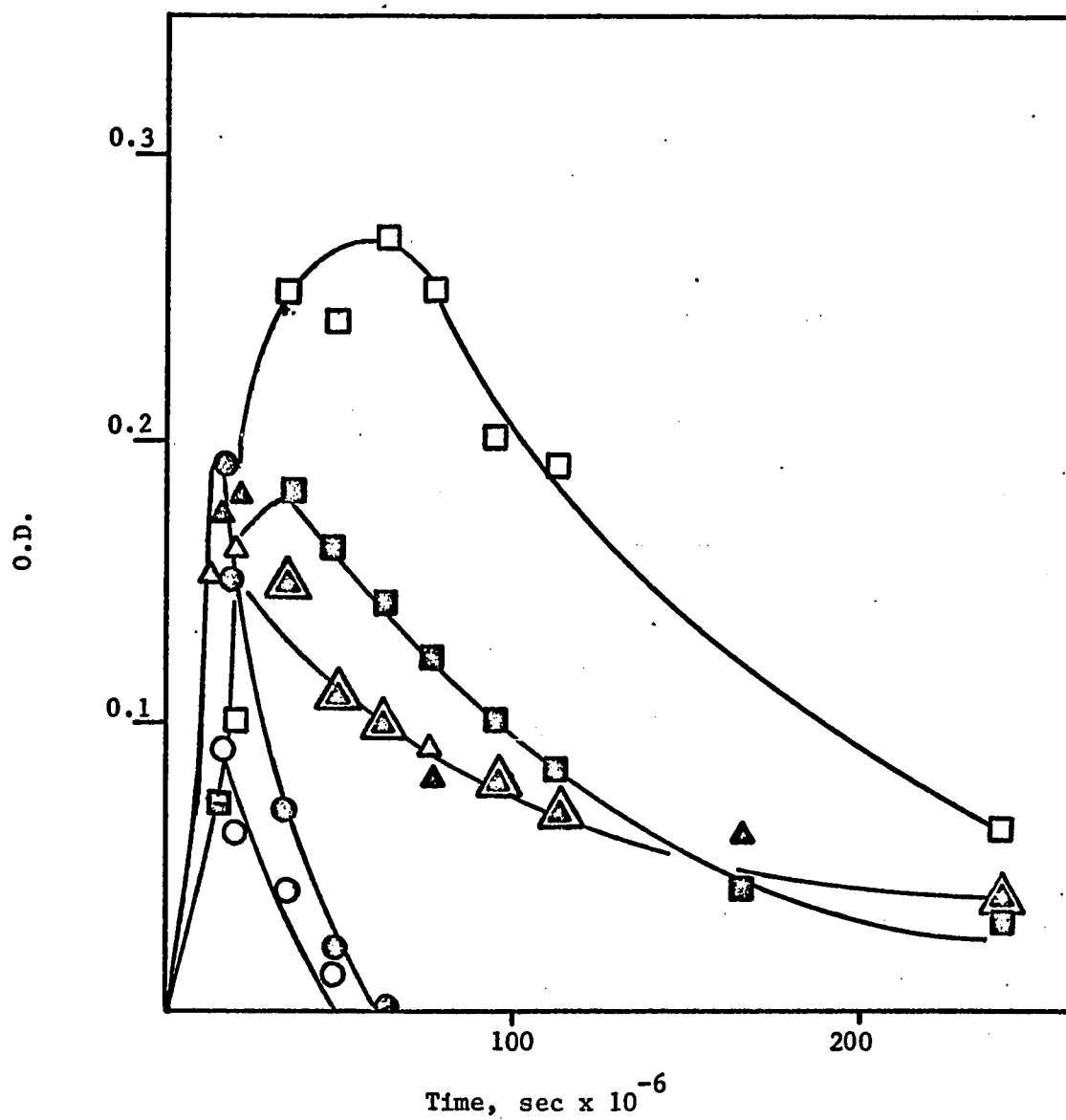
+ 0.2 vs. time;   △ 200 torr, O.D. + 0.3 vs time.

Figure 40. Plots of O.D. vs time for ○ HS, □ S_2 $(^3\Sigma_g^-)$, and

△ HS_2 . Solid figures represent 100 torr C_2H_4,

clear figures, 50 torr added C_2H_4.

on the transients. The rate of decay of HS was markedly increased. Although the rates of formation of S_2 ($^1\Delta_g$) and S_2 ($^3\Sigma_g^-$) were not affected, the amounts of S_2 formed were considerably reduced. The rate of decay of both states of S_2 were increased. The yield of HS_2 was decreased to one half without the formation of an -SSH containing product.

The static photolysis of 1.8 torr H_2S_2 in the presence of 100 torr C_2H_4 gave ethyl mercaptan as one of the products but ethylene episulfide could not be found.

The static photolysis of 1.8 torr H_2S_2 was also carried out in the presence of propylene. Photolysis of a mixture of 1.8 torr H_2S_2 + 100 torr C_2H_4 using a pyrex filter (transmitted $\lambda > 2900$ Å) resulted in the formation of n-propyl mercaptan. No iso-propyl mercaptan could be found. When the photolysis of a similar mixture was performed with a Cadmium resonance lamp using both the 2288 Å and the 2980 Å resonance lines, both n-propyl and iso-propyl mercaptans were formed. The ratio of the two mercaptans was 10:1 for n:iso.

The reaction of CH_3 with hydrogen disulfide.

The flash photolysis of 40 torr acetone in the presence of 1.0 torr H_2S_2 in the pyrex region resulted in the formation of carbon monoxide, ethane, methane, and methyl mercaptan. Other minor products were hydrogen sulfide and sulfur. The transients
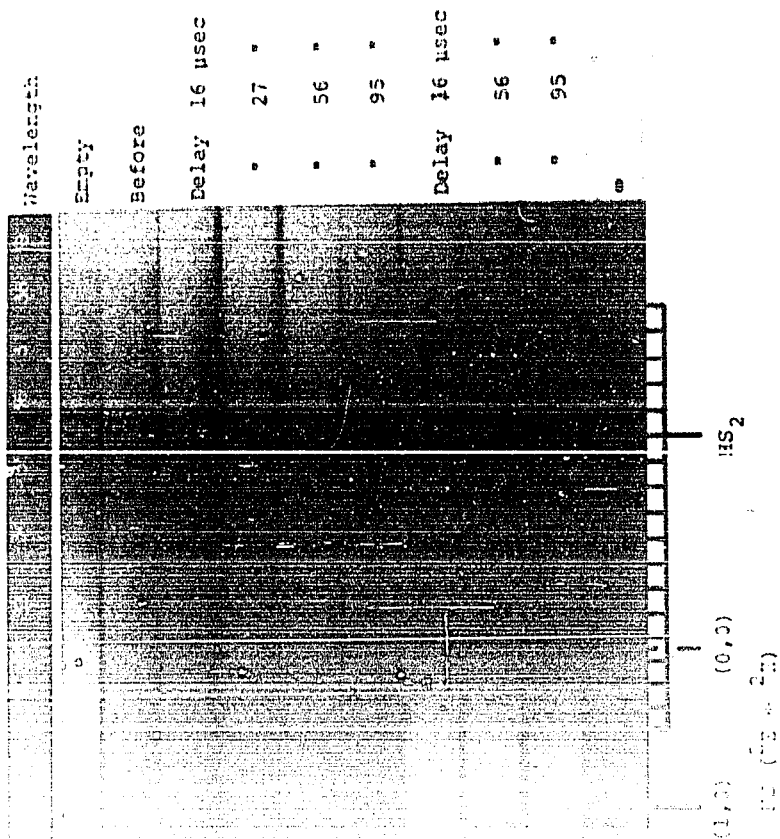
detected by kinetic spectroscopy were HS, HS_2, and S_2 $(^3\Sigma_g^-)$.

S_2 $(^1\Delta_g)$ could not be detected even if formed since the acetone continuum caused complete absorption in that region of the spectrum. The series of absorption spectra in Plate 10 show the formation and the decay of the intermediates. The HS spectrum was at maximum intensity at the shortest delay, 27 μsec, and decayed within 95 μsec. The HS_2 spectrum was weak at short delays but increased at longer delays, reaching maximum intensity at about 95 μsec. The S_2 $(^3\Sigma_g^-)$ spectrum grew in intensity at the same rate as HS_2.

The photolysis of hydrogen disulfide admixed with 90 torr argon was also carried out in the pyrex region. No perceptible decomposition occurred as evidenced by the absence of all transient spectra in Plate 10b.

The flash photolysis of acetone-d_6 was also carried out in the presence of 1.0 torr H_2S_2 under the above conditions. In addition to the products observed with light acetone, CD_3H was also found although in small amounts.

The effect of wavelength.

The effect of wavelength on the photolysis of hydrogen disulfide was examined by carrying but the flash photolysis of 1.8 torr H_2S_2 + 100 torr CO_2 with quartz and Vycor 7905 (transmitted $\lambda > 2300$ Å) filters placed between the lamp and the reaction cell. The only effect observed was a decrease in the intensity of the

Wavelength

empty

Before

Delay 16 µsec

27 "

56 "

95 "

Delay 16 µsec

56 "

95 "

HS$_2$

(0,0)

$HS_2 (^2\Sigma - ^2\pi)$

Spectra against time. 1.0 torr H$_2$S$_2$
... torr C$_3$H$_6$O. (Pyrex cell)
... torr H$_2$S$_2$ + 90 torr Argon. (Pyrex

transient spectra when the Vycor 7905 filter was used. The ratio of HS : HS_2 with quartz and with Vycor 7905 filters were 0.9 and 1.1 respectively.

Hydrogen disulfide with added nitric oxide.

The effect of nitric oxide on the flash photolysis of hydrogen disulfide was examined by flashing 1.8 torr H_2S_2 in the presence of 10 torr NO + 88 torr He. The following effects were observed. All transient spectra were reduced in intensity as shown in Plate 11. The HS and the HS_2 spectra were weak but they appeared at maximum intensity at the shortest delay used, 27 μsec. The spectrum of S_2 $(^3\Sigma_g^-)$ only appeared after a delay of about 100 μsec and its spectrum was very weak. The dark decomposition which normally occurs immediately after the flash did not set in for several minutes. Once initiated, the decomposition went to completion within a few minutes.

Flash photolysis - kinetic mass spectrometry experiments.

The flash photolysis of hydrogen disulfide was also examined by the technique of kinetic mass spectrometry. The products and the transients detected were S_2, S_3, S_4, H_2S, H_2S_3, and H_2S_4. The signal detected at m/e = 98, Figure 41a, represents the formation and the decay of the ion $H_2S_3^+$. A single rapid scan of S_3 from the flash photolysis of carbonyl sulfide is shown in Figure 41b. A

C

96 98 m/e

20 volt/div

B

96 98 m/e

1 volt/div

... m/e = 98 from 0.2 torr H_2S_2 + 25 torr He.

... m/e = 94 – 110 region from 0.5 torr COS + 25 torr He.

... m/e = 94 – 110 region from 0.2 torr H_2S_2 + 25 torr He.

Figure 41. A) Signal at m/e = 98 from 0.2 torr H_2S_2 + 25 torr He.

B) Rapid scan at m/e = 94 – 110 region from 0.5 torr COS + 25 torr He.

C) Rapid scan at m/e = 94 – 110 region from 0.2 torr H_2S_2 + 25 torr He.

similar rapid scan of the m/e = 98 region from the flash photolysis of hydrogen disulfide is shown in Figure 41c.

The signal at m/e = 130 region is shown in Figure 42a and represents the formation and decay of the ion $H_2S_4^+$. Single rapid scans in the m/e = 130 region in the flash photolysis of carbonyl sulfide and hydrogen disulfide are shown in Figures 42b and 42c respectively.

DISCUSSION

Primary reactions.

The ultra violet absorption spectrum of gaseous hydrogen disulfide is shown in Figure 43. There are two distinct maxima, at 2000 Å and at 2550 Å, with possibly a third at 1900 Å. The two maxima in the quartz U. V. region indicate at least two electronic transitions. Thompson et. al.[50] have suggested that the maximum at 2500 Å in dimethyl disulfide contains two transitions, one of which is the promotion of a non bonding electron to a σ^*_{S-S} orbital resulting in S-S bond rupture. Similar observations were made by. Rao et. al.[51]. Disulfides also exhibit a maximum at about 2000 Å. Ramarkrishnan et. al.[52] attributed this absorption in tetra and pentamethylene disulfides to a $\sigma^*_{C-S} \leftarrow n$ transition and demonstrated that C-S bond rupture occured.
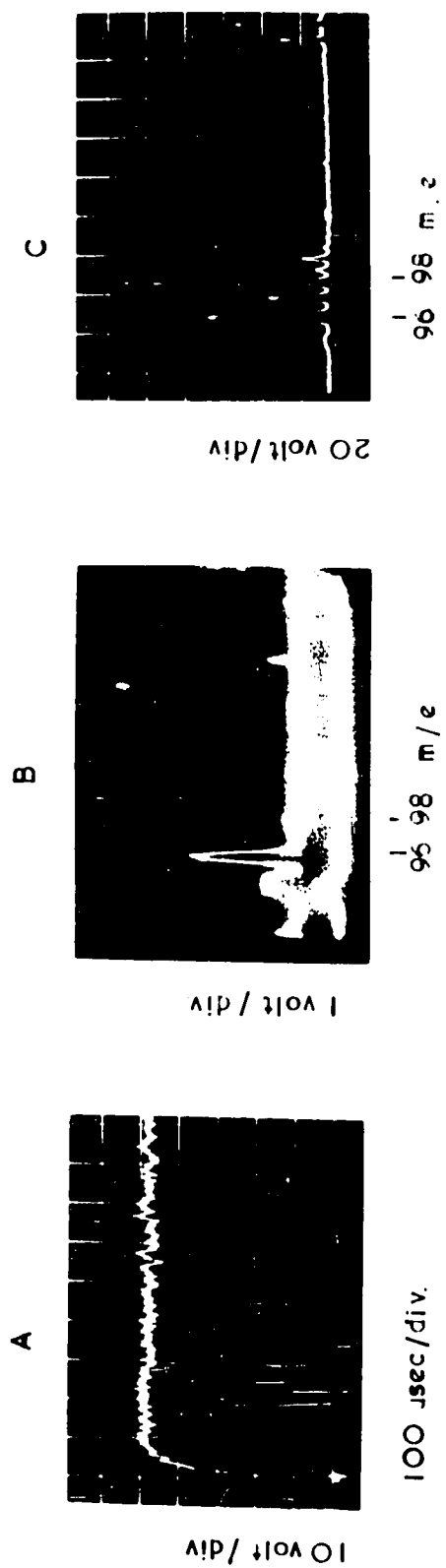
Figure 42. A) Signal at m/e = 130 from 0.2 torr H_2S_2 + 25 torr He.

B) Rapid scan at m/e = 124 - 140 region from 0.5 torr COS + 25 torr He.

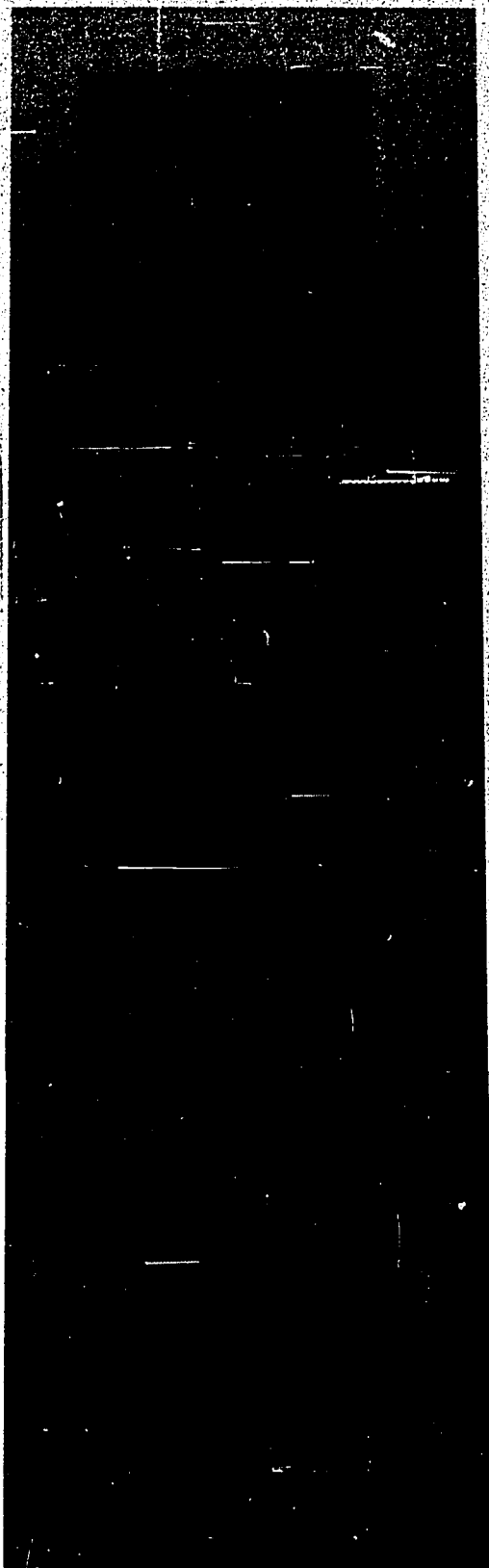C) Rapid scan at m/e = 124 - 140 region from 0.2 torr H_2S_2 + 25 torr He.

Figure 42. A) Signal at m/e = 130 from 0.2 torr H_2S_2 + 25 torr He.

B) Rapid scan at m/e = 124 – 140 region from 0.5 torr COS + 25 torr He.

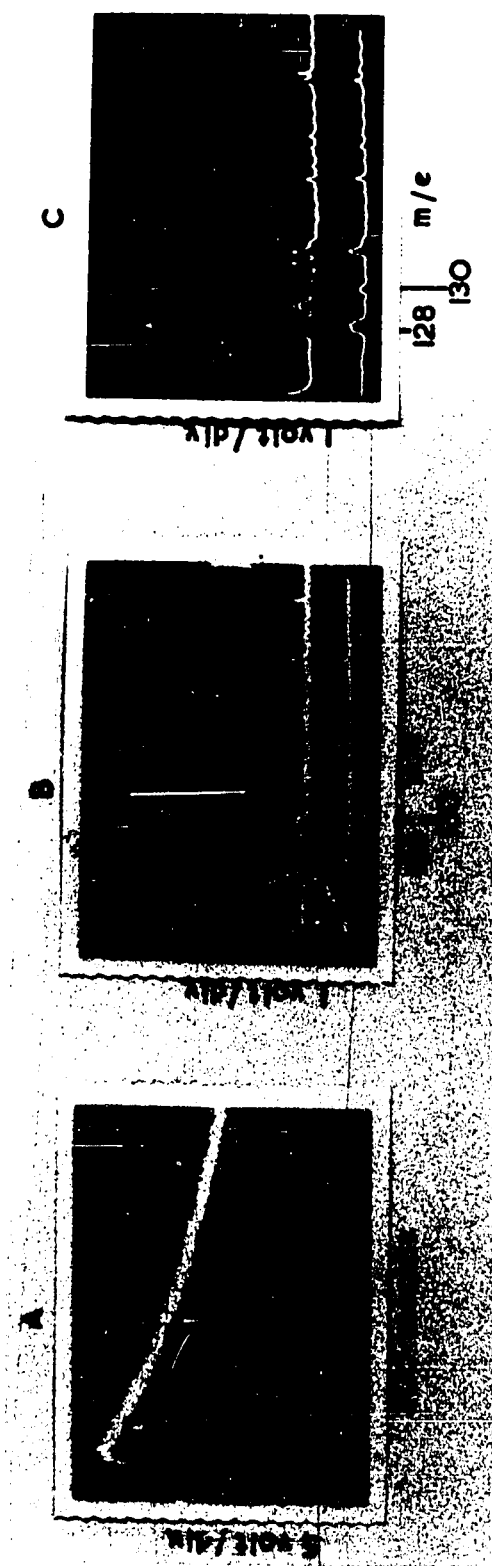C) Rapid scan at m/e = 124 – 140 region from 0.2 torr H_2S_2 + 25 torr He.
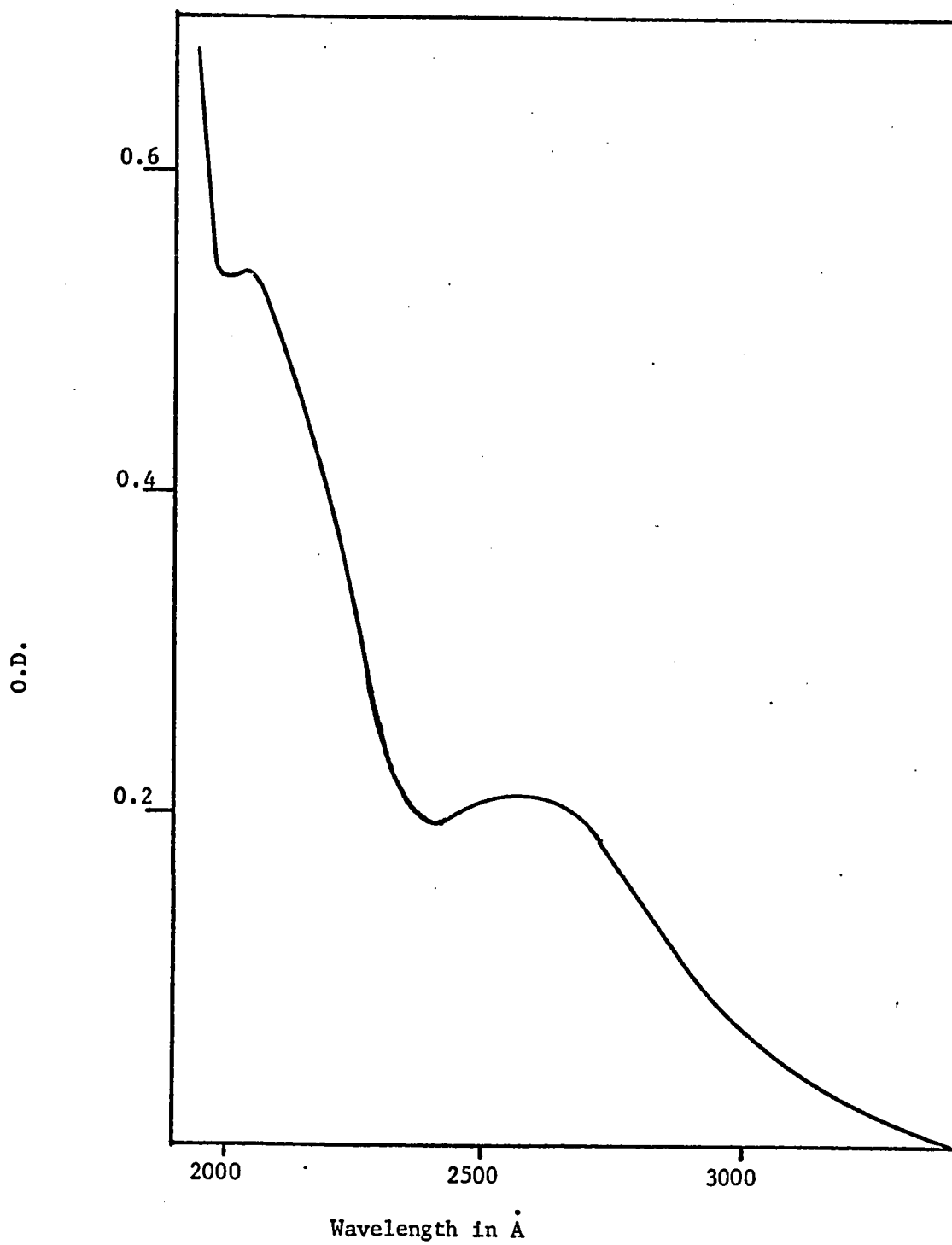
Figure 43. U.V. absorption spectrum of 1.8 torr H_2S_2. (10 cm. path length.)

Since hydrogen disulfide can be expected to show behavior similar to these simple organic disulfides, two probable primary processes that should be considered are:

$$H_2S_2 + h\nu_{2000 \overset{.}{A}} \rightarrow H + HS_2 \qquad \{1\}$$

$$H_2S_2 + h\nu_{2550 \overset{.}{A}} \rightarrow 2 HS \qquad \{2\}$$
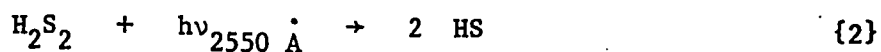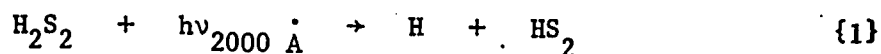
That HS and HS_2 may be formed in the primary process is indicated by the presence of their respective spectra at maximum intensity at the delay time when the output of the flash is at maximum intensity.

The occurrence of reaction $\{2\}$ was demonstrated in the experiments with added propylene. The photolysis of hydrogen disulfide in the presence of propylene in the pyrex region gave only n-propyl mercaptan. No iso-propyl mercaptan could be found. Since pyrex glass only transmits wavelengths greater than 2900 $\overset{.}{A}$, only the tail end of the 2550 $\overset{.}{A}$ region was able to absorb. The formation of n-propyl mercaptan is attributed to the scheme

$$CH_3CH=CH_2 + HS \rightarrow CH_3CHCH_2SH \qquad \{3\}$$

$$CH_3CHCH_2SH + H_2S_2 \rightarrow CH_3CH_2CH_2SH + HS_2 \qquad \{4\}$$
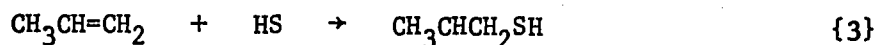
HS is formed in reaction $\{2\}$. If reaction $\{1\}$ had occurred, then iso-propyl mercaptan should also have been formed.

When the photolysis of the same mixture was carried out using both absorption regions, both n-propyl and iso-propyl mercaptans

were formed. The formation of iso-propyl mercaptan is best attributed to

$$CH_3CH=CH_2 \quad + \quad H \quad \rightarrow \quad CH_3CHCH_3 \qquad \{5\}$$

$$CH_3CHCH_3 \quad + \quad HS \quad \rightarrow \quad (CH_3)_2CHSH \qquad \{6\}$$
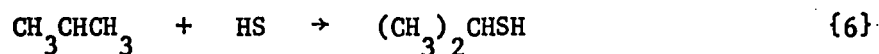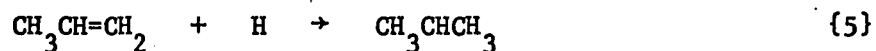
The H atoms are formed in reaction $\{1\}$. n-Propyl mercaptan is again formed by reactions $\{2\}$, $\{3\}$, and $\{4\}$. These observations show that reactions $\{1\}$ and $\{2\}$ are primary processes occuring at 2000 Å and at 2550 Å respectively.

This point was further demonstrated by the observed wavelength dependence of the photolysis of hydrogen disulfide. Identical mixtures were flash photolyzed with either a quartz or a Vycor 7905 filter. The quartz filter was used to correct for any scattering by the Vycor filter placed between the lamp and the cell. The ratio of HS / HS_2 was found to be 0.9 when quartz was used and 1.1 with Vycor 7905. This decrease in the relative yield of HS_2 is best attributed to the fact that Vycor 7905 effectively eliminates all wavelengths below 2300 Å and consequently decreasing the amount of HS_2 formed in reaction $\{1\}$ while having no effect on the 2550 Å absorption region which produces HS.

Other primary processes that should be considered are

$$H_2S_2 \quad + \quad h\nu \quad \rightarrow \quad H_2 \quad + \quad S_2 \qquad \{7\}$$

$$H_2S_2 \quad + \quad h\nu \quad \rightarrow \quad H_2S \quad + \quad S \qquad \{8\}$$
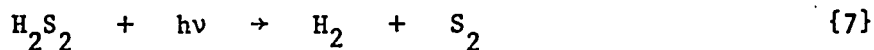
Reaction {7} is not important for two reasons. First, the low hydrogen yield, 0.05 µmoles/flash compared to about 2 µmole/flash total decomposition, shows that even if reaction {7} did occur, its contribution is very small. Secondly, the formation of S_2 is slow when compared to the formation of HS and HS_2, indicating that S_2 is formed in a secondary process.

That S_2 is a product of the reactions of HS and HS_2 was shown in the experiments with added nitric oxide. In the presence of NO, the intensity of the spectra of HS and HS_2 were reduced owing to the reactions

$$HS \;+\; NO \;\rightarrow\; HSNO \qquad\qquad \{9\}$$

$$HS_2 \;+\; NO \;\rightarrow\; HSSNO \qquad\qquad \{10\}$$

Reaction {9} has been demonstrated in the flash photolysis - kinetic mass spectrometry of H_2S - NO mixtures[41]. The spectra of HS and HS_2 were at maximum intensity at the shortest delay. S_2 $(^3\Sigma_g^-)$ on the other hand could not be observed until about 60 µsec delay and even then only very weakly. This clearly indicates that HS and HS_2 are primary products but S_2 is not. These results are shown in Plate 11.

Reaction {8} cannot be a primary process for the following reason. In the static photolysis of H_2S_2 - C_2H_4 mixtures, ethyl mercaptan was isolated but ethylene episulfide was not found. The direct formation of S atoms in the primaty process is precluded by

the absence of the episulfide since sulfur atoms have been shown
to readily add to ethylene.

Secondary reactions.

Since hydrogen atoms are formed in reaction {1}, it was
assumed that they would react with hydrogen disulfide via

$$H + H_2S_2 \rightarrow H_2 + HS_2 \quad\quad \{11\}$$

However, the absence of all but trace quantities of hydrogen
precludes this abstraction reaction. A reasonable reaction that
will account for the reaction of H atoms with hydrogen disulfide
without the formation of hydrogen is

$$H + H_2S_2 \rightarrow H_2S + HS \quad\quad \{12\}$$

i.e., abstraction of an HS group. Reaction {12} could be convincingly
demonstrated by observing the reaction between hydrogen disulfide
and H atoms generated by some means other than the photo-decomposition
of H_2S_2. Several hydrogen atom sources were tried but they either
caused dark decomposition of hydrogen disulfide or absorbed in such
a region of the spectrum that H_2S_2 also underwent photolysis.

Greig and Thynne[53] have observed that CD_3 reacts in two
ways with methyl mercaptan, namely,

$$CD_3 + CH_3SH \rightarrow CD_3H + CH_3S \quad\quad \{13\}$$

$$CD_3 \quad + \quad CH_3SH \quad \rightarrow \quad CD_3SH \quad + \quad CH_3 \qquad \{14\}$$
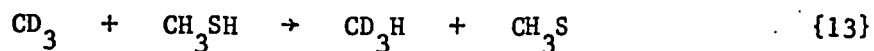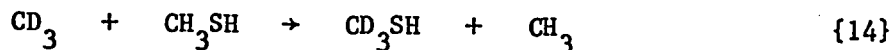
Reaction {14} occurs much slower than {13} and only about 5% of the CD_3 were found to react via {14}. It was felt that if it could shown that methyl redicals do abstract an HS group from hydrogen disulfide, then reaction {12} could also occur.

Acetone, a good source of methyl radicals, was flash photolyzed in the pyrex region of the spectrum to prevent the photo-decomposition of hydrogen disulfide. It can be seen in Plate 10b that flash photolysis of hydrogen disulfide in the pyrex region causes very little decomposition since no transients could be detected. When acetone is added, the spectra of HS, HS_2, and S_2 ($^3\Sigma_g^-$) are detected. It can be seen in Plate 10a that the spectrum observed at the shortest delay is that of HS. The spectra of HS_2 and S_2 only appear after a delay of about 75 μsec. Since the HS spectrum is not the result of direct photolysis, its formation is best attributed to the reaction

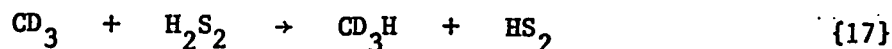$$CH_3 \quad + \quad H_2S_2 \quad \rightarrow \quad CH_3SH \quad + \quad HS \qquad \{15\}$$
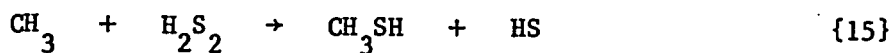
The formation of methyl mercaptan supports this view. The formation of HS_2 is most likely

$$HS \quad + \quad H_2S_2 \quad \rightarrow \quad H_2S \quad + \quad HS_2 \qquad \{16\}$$
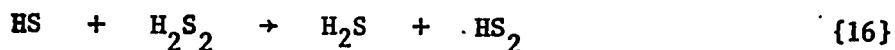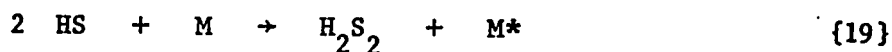
since HS_2 is seen to reach maximum concentration only after the HS

has decayed. Since CD_3H was also formed in the photolysis of C_3D_6O - H_2S_2 mixtures, methyl radicals also undergo

$$CD_3 + H_2S_2 \rightarrow CD_3H + HS_2 \qquad \{17\}$$

but to a lesser extent than reaction $\{15\}$.

The reactions of HS are

$$2\ HS \rightarrow H_2S + S\ (^3P) \qquad \{18\}$$

$$2\ HS + M \rightarrow H_2S_2 + M* \qquad \{19\}$$

$$HS + H_2S_2 \rightarrow H_2S + HS_2 \qquad \{16\}$$
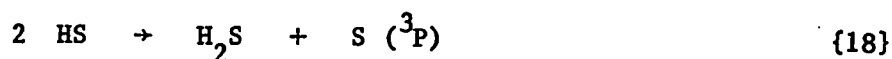
Reaction $\{16\}$, discussed previously, was also proposed[32] to explain the formation of some disulfide products in the liquid phase, thermal decomposition of hydrogen disulfide in the presence of pentenes. Similar reaction between OH and hydrogen peroxide was proposed by Greiner[54] in the flash photolysis of H_2O_2.

Reaction $\{18\}$, proposed in previous chapters, was demonstrated in this study by the detection of ethylene episulfide in the flash photolysis of H_2S_2 - C_2H_4 mixtures. The occurrence of reaction $\{19\}$ is indicated by the pressure dependence of the decay of HS as shown in Figure 37.

The flash photolysis of hydrogen disulfide in the presence of an inert gas produced hydrogen sulfide and sulfur as well as one or more products of low vapor pressure which underwent slow

decomposition to hydrogen sulfide and sulfur before mass spectral or infra red analysis could be performed. To determine the identity of these products, the flash photolysis of hydrogen disulfide was performed in conjunction with the technique of kinetic mass spectrometry. In addition to signals corresponding to H_2S, S_2, and S_4, signals were also detected at $m/e = 98$ and 130 as shown in Figures 41a and 42a respectively. These signals were attributed to the ions $H_2S_3^+$ and $H_2S_4^+$ respectively. However, these signals could also be attributed to the isotopic combinations $S_2^{32}S^{34}$ and $S_3^{32}S^{34}$. To determine the isotopic profile of S_3 and S_4, carbonyl sulfide was flash photolyzed and the signals in the respective regions of S_3 and S_4 were recorded in one rapid scan. These rapid scans are shown in Figures 41b and 42b. It can be seen that the above S^{34} isotopic species only amounts to about 5 to 10% of the total S_3 and S_4 · produced in agreement with the natural abundance of the S^{34} isotope. When the same single rapid scans were carried out in the flash photolysis of hydrogen disulfide, quite different results were obtained. The signals at $m/e = 98$ and 130 are about the same as the signals of S_3 and S_4. From this it can be concluded that the signals at $m/e = 98$ and 130 are due to the species $H_2S_3^+$ and $H_2S_4^+$.
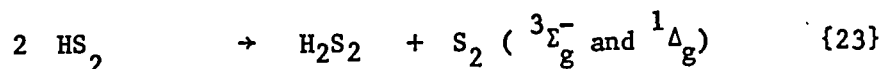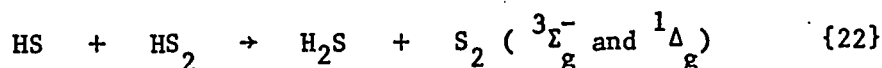
$H_3S_3^+$ may also have been a fragmentation product of the ion $H_2S_4^+$. However, comparison of Figures 41a and 42a shows that the two species have markedly different decay rates and thus they arise from two different molecular species, namely, H_2S_3 and H_2S_4.

The most likely source of H_2S_3 and H_2S_4 is

$$HS + HS_2 \rightarrow H_2S_3 \qquad \{20\}$$

$$2\ HS_2 \rightarrow H_2S_4 \qquad \{21\}$$

Reaction $\{21\}$ is a pressure independent second order process as indicated by Figure 44. The plot of $O.D.^{-1}$ vs. time for HS_2 decay does not yield a straight line until most of the HS has decayed. This is consistent with the complicated kinetics as a result of reactions $\{16\}$ and $\{20\}$. Reaction $\{20\}$ may or may not be pressure dependent. The HS removal does show pressure dependence but this may be due entirely to reaction $\{19\}$.

The cross and self disproportionation reactions of HS_2 must also be considered.

$$HS + HS_2 \rightarrow H_2S + S_2\ (\ ^3\Sigma_g^- \text{ and } ^1\Delta_g) \qquad \{22\}$$

$$2\ HS_2 \rightarrow H_2S_2 + S_2\ (\ ^3\Sigma_g^- \text{ and } ^1\Delta_g) \qquad \{23\}$$

HS can not be the only source of S_2 since in the flash photolysis of hydrogen sulfide, the mount of HS formed was about the same as in this study but the amount of S_2 produced was about one half. This increase in the S_2 yield in the presence of HS_2 is best explained in terms of reactions $\{22\}$ and $\{23\}$.

In the flash photolysis of H_2S_2 - C_2H_4 mixtures, the decay of HS is very rapid owing to the scavenging reaction
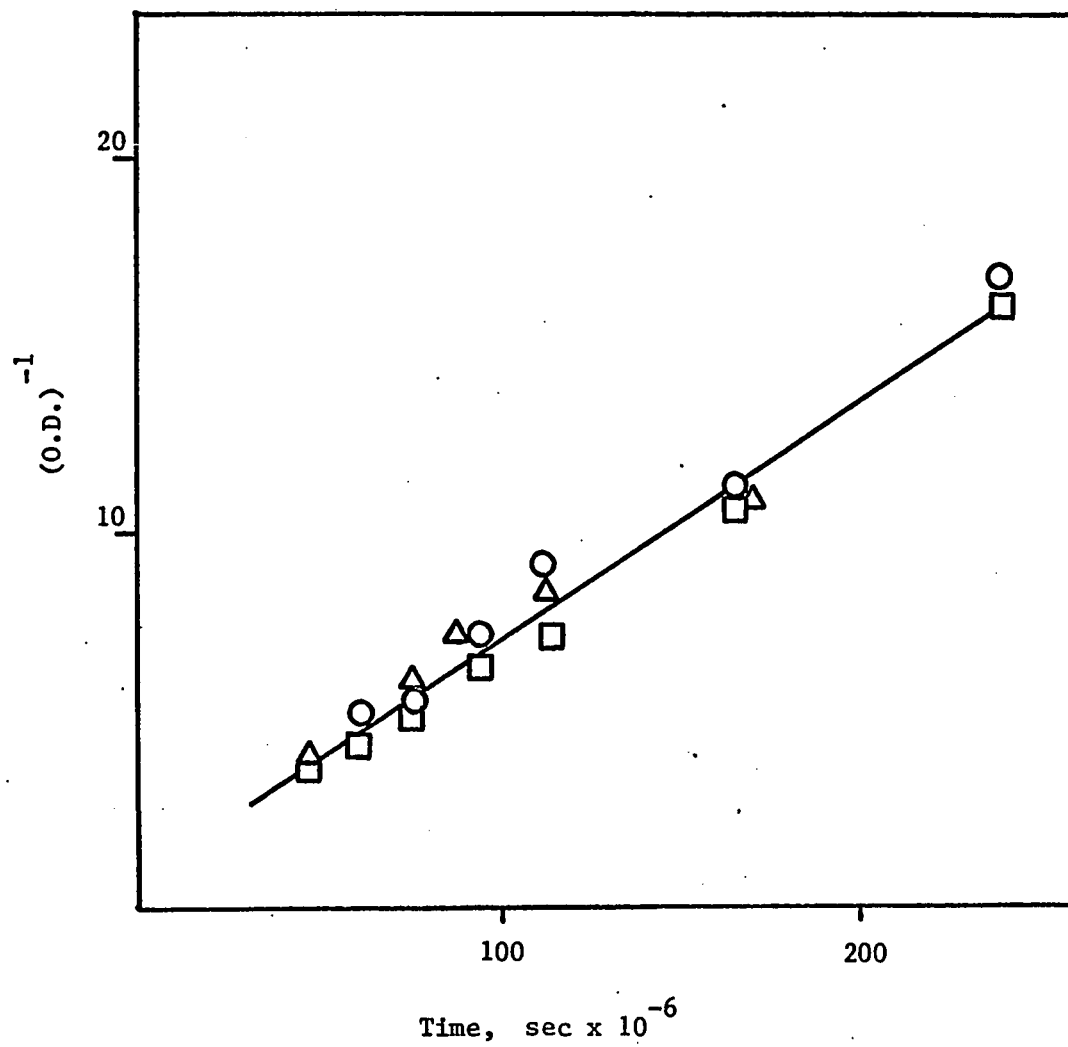
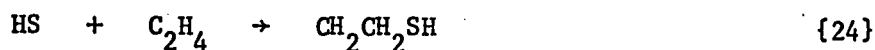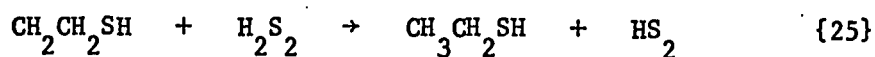Figure 44. Plots of O.D. $^{-1}$ vs time for the decay of HS_2.

○ 25 torr CO_2; □ 100 torr CO_2; △ 200 torr CO_2.

$$HS \quad + \quad C_2H_4 \quad \rightarrow \quad CH_2CH_2SH \qquad \{24\}$$

The formation of ethyl mercaptan can be explained in terms of reactions {24} and {25}.

$$CH_2CH_2SH \quad + \quad H_2S_2 \quad \rightarrow \quad CH_3CH_2SH \quad + \quad HS_2 \qquad \{25\}$$

Hydrogen atoms formed in reaction {1} probably add to ethylene to form ethyl and the ethyl may abstract an H to form ethane. Ethyl may also abstract an HS as was seen for methyl, but this would result in ethyl mercaptan and since it is also formed by reactions {24} and {25}, the two processes can not be distinguished.

The yield of HS_2 decreases by a factor of about two since reaction {16} is eliminated. The S_2 ($^3\Sigma_g^-$) yield also shows about a four fold decrease indicating that reactions {22} and {23} are important S_2 producing steps.

S_2 ($^1\Delta_g$) is formed in reactions {22} and {23} as well as in the recombination of S (^3P) atoms formed in {18}.

$$2 \ S \ (^3P) \quad + \quad M \quad \rightarrow \quad S_2 \ (^3\Sigma_g^- \ \text{and} \ ^1\Delta_g) \quad + \quad M* \qquad \{26\}$$
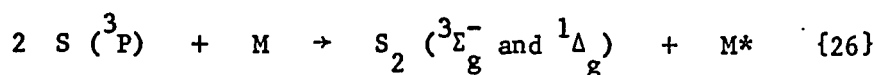
S_2 ($^1\Delta_g$) is relaxed to the ground $^3\Sigma_g^-$ state by collisions with the diluent gas

$$S_2 \ (^1\Delta_g) \quad + \quad M \quad \rightarrow \quad S_2 \ (^3\Sigma_g^-) \quad + \quad M* \qquad \{27\}$$
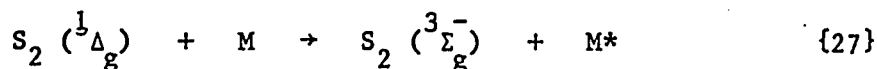
since its rate of removal increases with increasing pressure of diluent gas.

S_2 ($^3\Sigma_g^-$) is formed in reactions {22}, {23}, {26}, and {27}. It decays by a pressure dependent, second order process,

$$2 \ S_2 \ (^3\Sigma_g^-) \ + \ M \ \rightarrow \ S_4 \ + \ M* \qquad \qquad \{28\}$$
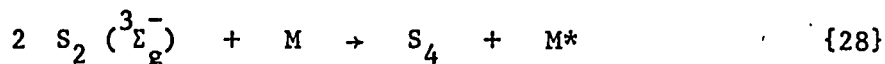
since plots of O.D.$^{-1}$ vs. time result in straight lines as shown in Figure 45. From the slopes, the absolute rate constants for S_2 decay can be calculated and these values are listed in Table XIV. There is good agreement in the third order rate constants indicating that S_2 removal is well described by reaction {28}. It can be seen that ethylene is about seven times as efficient in reaction {28} as is carbon dioxide. This may be compared with ethylene episulfide which is about ten times as efficient as CO_2.

The results of this investigation have an important bearing on the photochemistry of hydrogen peroxide. The only primary process considered was

$$H_2O_2 \ + \ h\nu \ \rightarrow \ 2 \ OH \qquad \qquad \{29\}$$

The absence of hydrogen among the products was taken as evidence that the process

$$H_2O_2 \ + \ h\nu \ \rightarrow \ H \ + \ HO_2 \qquad \qquad \{30\}$$
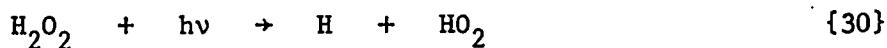
did not occur. However, since it was shown that H atoms abstract an HS group rather than an H atom from hydrogen disulfide, such a process may also occur in the case of hydrogen peroxide with the consequence that hydrogen is not formed.
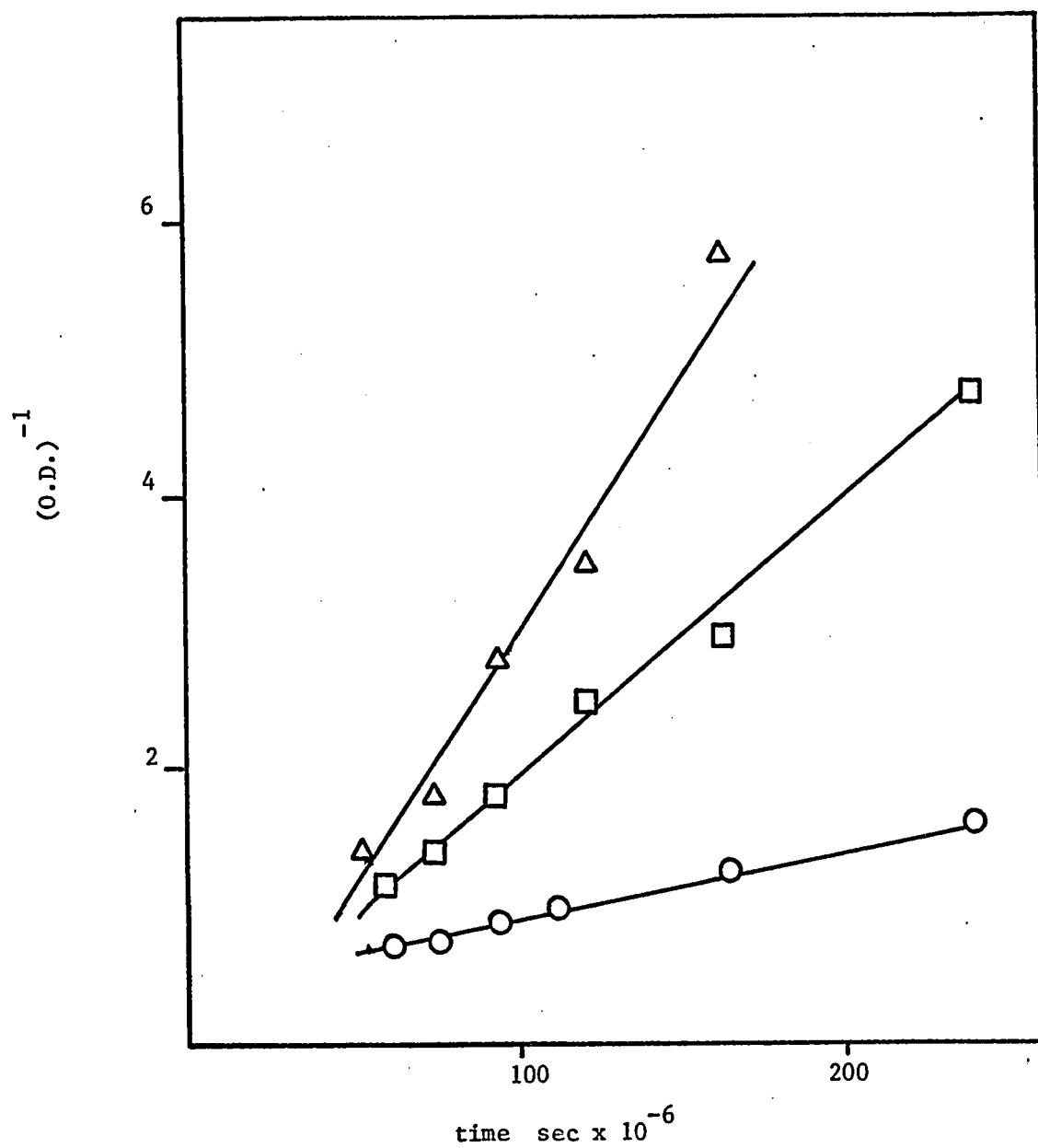
Figure 45. Plots of $(O.\underline{D}.)^{-1}$ vs. time for the decay of S_2 $(^3\Sigma_g^-)$.

at various pressures of CO_2. ◯ 25 torr; ☐ 100 torr;

△ 200 torr.

TABLE XIV

ABSOLUTE RATE CONSTANTS FOR S_2 $(^3\Sigma_g^-)$ RECOMBINATION AT DIFFERENT PRESSURES OF CO_2 AND C_2H_4

Added gas	torr	Slope sec. x 10^{-4}	k_{28}, x 10^{-10} M^{-1} sec^{-1}	k_{28}, x 10^{-12} M^{-2} sec^{-1}
CO_2	25	0.51 ± 0.20	0.40 ± 0.23	2.96 ± 1.60
CO_2	50	1.54 ± 0.22	1.09 ± 0.35	4.04 ± 1.29
CO_2	100	1.96 ± 0.50	1.38 ± 0.61	2.57 ± 1.13
CO_2	200	3.97 ± 1.32	2.80 ± 1.43	2.62 ± 1.34
C_2H_4	50	7.46 ± 1.90	5.25 ± 2.30	19.60 ± 8.50
C_2H_4	100	17.10 ± 3.95	12.10 ± 9.10	22.10 ± 9.80

The process

$$H \quad + \quad H_2O_2 \quad \rightarrow \quad H_2O \quad + \quad OH \qquad \{31\}$$
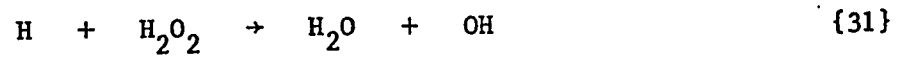
is energetically favorable since the D(HO − OH) is only about 50

Kcal/mole while the D (HO − H) is 119 Kcal/mole.

BIBLIOGRAPHY

(1)   W. A. Noyes Jr., and L. A. Leighton, The Photochemistry of Gases, Reinhold Publishing Corp., New York, 1941.

(2)   J. G. Calvert and J. N. Pitts Jr., Photochemistry, John Wiley and Sons Inc., New York, 1966.

(3)   H. E. Gunning and O. P. Strausz, Advances in Photochemistry, 1, 209 (1963).

(4)   R. G. W. Norrish and G. Porter, Nature, 164, 658 (1949).

(5)   G. Porter, Proc. Roy, Soc., A200, 284 (1950).

(6)   R. G. W. Norrish, G. Porter and B. A. Thrush, Proc. Roy. Soc., A216, 165 (1953).

(7)   F. J. Wright, J. Phys. Chem., 64, 1648 (1960).

(8)   A. B. Callear, Proc. Roy. Soc., A271, 401 (1963).

(9)   N. Basco and A. E. Pearson, Trans. Farad. Soc., 63, 2684 (1967).

(10)   A. D. Walsh, J. Chem. Soc., 2266 (1953).

(11)   R. S. Mulliken, Can. J. Chem., 36, 10 (1958).

(12)   J. Heicklen, J. Am. Chem. Soc., 85, 3562 (1963).

(13)   K. S. Sidhu, I. G. Csizmadia, O. P. Strausz and H. E. Gunning, J. Am. Chem. Soc., 88, 2412 (1966).

(14)   W. Lochte-Holtgreven, C. E. H. Bawn and E. Eastwood, Nature, 129, 869 (1932).

(15)   G. S. Forbes and J. E. Cline, J. Am. Chem. Soc., 61, 151 (1939).

(16)   O. P. Strausz and H. E. Gunning, J. Am. Chem. Soc., 84, 4080 (1962).

(17) T. F. Palmer and F. P. Lossing, J. Am. Chem. Soc., 84, 4661 (1962); J. Berkowitz and J. R. Marquart, J. Chem. Phys., 39, 275, (1963).

(18) Selected Values of Chemical Thermodynamic Properties, Circular of the National Bureau of Standards, No. 500, 1952.

(19) Circular of the National Bureau of Standards, No. 467, 1949.

(20) H. A. Wiebe, Ph.D. Thesis.

(21) H. A. Wiebe, A. R. Knight, O. P. Strausz and H. E. Gunning, J. Am. Chem. Soc., 87, 1443 (1965).

(22) A. R. Knight, O. P. Strausz and H. E. Gunning, J. Am. Chem. Soc., 85, 2349 (1963).

(23) H. E. Gunning and O. P. Strausz, Advances in Photochem., 4, 143 (1966).

(24) W. D. McGrath, J. J. McGarvey and D. N. Dempster, Can. J. Chem., 45, 2451 (1967).

(25) G. S. Forbes, J. E. Cline and B. C. Bradshaw, J. Am. Chem. Soc., 60, 1431 (1938).

(26) W. H. Avery and G. S. Forbes, J. Am. Chem. Soc., 60, 1005 (1938).

(27) G. Porter, Discussions Farad. Soc., 9, 60 (1950).

(28) B. de B. Darwent and R. Roberts, Proc. Roy. Soc., A216, 344 (1953).

(29) B. de B. Darwent and V. J. Krasnansky, "Seventh Symposium (International) on Combustion", Butterworths Scientific Publications, London (1959).

(30) B. de B. Darwent, R. L. Wadlinger and Sr. M. J. Allard, J. Phys. Chem., 71, 2346 (1967).

(31)   D. A. Styles, W. J. R. Tyerman, O. P. Strausz and H. E. Gunning, Can. J. Chem., 44, 2149 (1966).

(32)   E. I. Tiniakova, E. K. Krennikova and B. A. Dolgoplosk, J. Chim. Gen. SSSR., 28, 1689 (1958).

(33)   K. S. Sidhu, Ph.D. Thesis.

(34)   R. G. W. Norrish and G. Oldershaw, Proc. Roy. Soc., A249, 498 (1959).

(35)   A. E. Milton and E. R. V. Douglas, J. Chem. Phys., 41, 357 (1964).

(36)   J. T. Hougen, J. Chem. Phys., 41, 363 (1964).

(37)   Handbook of Preparative Inorganic Chemistry, Vol. 1, Second Edition, Ed. E. Brauer, Academic Press, New York, (1963).

(38)   R. F. Barrow and R. P. du Parq, Elemental Sulfur, C. B. Meyer, Ed., Interscience Publishers Inc., New York, (1965).

(39)   L. W. Bader and E. A. Ogryzlo, Discussions Farad. Soc., 37, 46 (1964).

(40)   A. G. Gaydon, G. H. Kimbell and H. B. Palmer, Proc. Roy. Soc., A279, 313 (1964).

(41)   S. Barton, O. P. Strausz and H. E. Gunning, to be published.

(42)   N. R. Greiner, J. Chem. Phys., 45, 99 (1966).

(43)   H. A. Szwarc, J. Phys. Chem., 66, 255 (1962).

(44)   D. C. Dobson, F. C. James, O. P. Strausz and H. E. Gunning, to be published.

(45)   G. Herzberg, Spectra of Diatomic Molecules, D. Van Nostrand, New York, 1950

(46)   A. B. Callear and W. J. R. Tyerman, Trans. Farad. Soc., 62, 371 (1966)

(47)   H. Mackle and P. A. D. O'Hare, Tetrahedron, $\underline{19}$, 961 (1963).

(48)   B. A. Callear, Disc. Farad. Soc., $\underline{33}$, 28,(1962).

(49)   R. F. Barrow and P. R. DuParcq, Proc. Phys. Soc., London, At. Mol. Phys.[2], $\underline{1}$,(2), 283 (1968).

(50)   S. D. Thompson, D. G. Carroll, F. Watson, M. O'Donnell and S. P. McGlynn, J. Chem. Phys., $\underline{45}$, 1367 (1966).

(51)   P. M. Rao, J. A. Copek and A. R. Knight, Canad. J. Chem., $\underline{45}$, 1369 (1967).

(52)   V. Ramarkrishnan, S. D. Thompson and S. P. McGlynn, Photochem. Photobiol., $\underline{4}$, 907 (1965).

(53)   G. Greig and J. C. J. Thynne, Trans. Farad. Soc., $\underline{62}$, 379 (1966).

(54)   N. R. Greiner, J. Chem. Phys., $\underline{45}$, 99 (1966).

(55)   B. Rosen and M. Desirant, Bull. Soc. Roy. Sci. Liege, $\underline{4}$, 233 (1935).

(56)   J. M. Kettringham and R. F. Barrow, Proc. Phys. Soc., $\underline{84}$, 330, (1964).

(57)   P. V. B. Haranath, Z. Physik, $\underline{173}$, 428 (1963).

(58)   N. A. Narasimham and S. Gopel, Current Sci.(Ind.), $\underline{34}$, 454 (1965).

(59)   O. P. Strausz, R. J. Donovan and M. de Sorgo, Ber. Bunsenges. Phys. Chem., $\underline{72}$, 253 (1968).

VITA

The author was born in Debrecen, Hungary on October 18,
1939.

He attended John Carroll University at Cleveland, Ohio
and received his B.S. in chemistry in 1963.

In the same year he was admitted as provisional
candidate for the degree of Ph.D. at the University of Alberta at
Edmonton. While a graduate student at this institution the author
held a graduate teaching assistantship.